Ground Thermal Regimes in Western Dronning Maud Land, Antarctica in 2016

A thesis submitted in fulfillment of the requirements for the degree of

MASTER OF SCIENCE

of

Rhodes University

By

Consliah Tebogo Masebe

December 2018

Supervisor

Professor K.I. Meiklejohn

Department of Geography, Rhodes University

Abstract

Research shows that the climate of Antarctica is changing and, it is vital that the change is monitored to understand how it will affect global ecosystems. Since the International Polar Year (IPY) 2007-2008, research in permafrost studies has grown. However, there are still existing gaps that impede complete understanding of Antarctic cold environments and landscape processes. Permafrost has been noted as one of the major controlling factors of the terrestrial ecosystem dynamics in Antarctica. However, the understanding of Antarctic permafrost, when compared to other cryospheric components, is limited, especially its thermal and physical properties, evolution, as well as links to pedogenesis, hydrology, geomorphic dynamics, and responses to global change. This project provided an understanding and insight to over-arching research that evaluates the state and status of permafrost and the active layer in Dronning Maud Land (DML) through examining short-term variations on ground thermal regimes. The main focus is on understanding the influence of synoptic, diurnal and seasonal events on the active layer in 2016.

Analysis of available data shows that ground thermal regimes are influenced by variations in air temperature, pressure, wind speed and to some extent, relative humidity. Subsequently, ground thermal regimes also depend on soil physical characteristics including sediment particle size and bulk density. Furthermore, sediment particle size and bulk density have been found to have a great influence on thermal propagation rates as well as active layer depth; the higher the bulk density, the higher the thermal propagation rate and the lower the bulk density, the lower the thermal propagation rate. Conversely, a large proportion of bigger sediment particle size in soil corresponds with a higher thermal propagation rate and a large proportion of smaller sediment particle size in soil corresponds with a lower thermal propagation rate. Also, ground thermal regimes vary according to seasons. Ground temperatures are more variable in summer, while air temperatures are more variable in winter. The variability according to different seasons shows that the active layer responds to seasonal climatic variations. Additionally, the active layer also responds to synoptic and diurnal weather events.

Keywords: ground thermal regimes, meteorological, active layer depth, temperature variability, thermal propagation

Acknowledgements

First and foremost, I would like to dedicate this dissertation to my parents and siblings. I deeply appreciate the support that I received throughout my M.Sc. studies from my family through their encouraging words and their constant prayers. I would like to express my deepest gratitude to Prof. Ian Meiklejohn for his continuous guidance and support. I am very grateful for the assistance received from Mr. Abe Ngoepe in conducting my laboratory analysis. Margot Brooks is thanked for her great assistance in proof-reading my work. I would like to extend my thanks to the National Research Foundation (NRF) and the Ian MacKenzie Scholarship, without which funding the completion of this M.Sc. dissertation would have been very challenging. The South African Weather Service (SAWS) is appreciated for supplying me with the meteorological data used in this study. I would like to thank the South African National Antarctic Programme (SANAP) and the Department of Environmental Affairs (DEA) for their logistical support during the fieldwork season of 2016/17 conducted in Antarctica. Lastly, I would like to extend my deepest gratitude to Rhodes University for their support throughout my M.Sc. studies.

Table of Contents

List of Figures

List of Tables

List of Equations

List of Abbreviations

° – Degree

µm – Micro Metres

ACC – Antarctic Circumpolar Current

ALS – Automated Logging Station

AMPS – Australian Meteorological Division

ANTPAS – Antarctic Permafrost, Periglacial Environments and Soils

C – Celsius

CALM – Circumpolar Active Layer Monitoring

CALM-S – Circumpolar Active Layer Monitoring – Southern Hemisphere

DEA – Department of Environmental Affairs

DJF – Summer

DML – Dronning Maud Land

ENSO – El Ninõ-Southern Oscillation

GTN-P – Global Terrestrial Network for Permafrost

GWC – Gravimetric Water Content

hPa – Hecto Pascal

IPA – International Permafrost Association

IPY – International Polar Year

JJA – Winter

m a.s.l – Metres Above Sea Level

MAAT – Mean Annual Air Temperature

MAGST – Mean Annual Ground Surface Temperature

MAM – Autumn

NRF – National Research Foundation

RSG – Ritscherflya Supergroup

SAM – Southern Annular Mode

SANAP – African National Antarctic Programme

SAO – Semi-Annual Oscillation

SAWS – South African Weather Service

SCAR – Scientific Committee on Antarctic Research

SON – Spring

T – Temperature

TSP – Thermal State of Permafrost

TTOP – Temperature at the Top Of Permafrost

VWC – Volumetric Water Content

WDML – Western Dronning Maud Land

Chapter 1: Introduction

1.1. Background, Context, and Motivation

Antarctica is a continent that has not been greatly affected by human actions, and it, thus, serves as an ideal place to conduct scientific research, particularly in the quest to understand global weather and how the climate of our planet and that of neighbouring planets function (Simmonds *et al.,* 2003; Guglielmin, 2012). It is the continent with the largest extent of continuous permafrost, affecting an area of 14 million km^2, which amounts to about 10 % of the land surface of the Earth (Dobinski, 2011; Convey *et al.,* 2009). Also, Antarctica has trapped in its ice sheet the largest global freshwater reservoir, approximately 30 million km^3 in extent, which serves as an important global climate regulator (Delaygue *et al.,* 2000). In Polar Regions, specifically Antarctica, temperatures can remain below 0 °C for the whole year (Cassano, 2013). Annual air temperatures range from 0 °C in summer to -15 °C in winter in coastal regions, and -30 °C to -65 °C in continental/interior regions through summer and winter respectively (Cassano, 2013). As a continent, it has been subject to cold climatic conditions for approximately 34 million years. If the conditions were to change, as appears to be happening with an apparent global warming trend, the environment would undergo significant changes that might affect the rest of the planet (Turner *et al.,* 2013). It is, therefore, imperative that the environment of Antarctica is explored to determine the rate and nature of change.

Widespread interest exists in the cryospheric environment of Antarctica and how it is affected by climate change (Ingvander *et al.,* 2016). Published research supports the contention that the climate of Antarctica is changing (Convey *et al.,* 2009; Vieira *et al.,* 2010; Turner *et al.,* 2013). Most often studies are conducted at a large scale, focusing on long-term changes/variations in environmental conditions, and while such studies have their merits, short-term variations are often overlooked (Convey *et al.,* 2009; Turner *et al.,* 2013; Williams and Smith, 1989). Short-term variations in environmental conditions may hold the key to understanding large-scale phenomena. Even though Antarctica is a polar continent, the climate varies considerably between continental and maritime areas (Bölter *et al.,* 2002). More attention is given to maritime Antarctica due to its fragility and susceptibility to climate change, as well as ease of access (Michel *et al.,* 2012). However, research on continental Antarctica is just as important, because it can give us a measure of how the continent is changing as a whole.

Continental Antarctica makes up most of the Continent with the largest land mass being East Antarctica (Fig. 1). Antarctica comprises three main morphological zones: the high plateau, inland slopes, and the coast, and is mostly covered by ice. Recently, the continent has been sub-divided

into 16 distinct biogeographical regions (Terauds and Lee, 2016). Mean temperatures in the warmest month are below 0 °C, and annual precipitation is less than 20 cm (Bölter *et al.,* 2002). Most of continental Antarctica is underlain by continuous permafrost, including the snow-free regions (Dobinski, 2011). However, the understanding of Antarctic permafrost compared with that of other cryospheric components is limited because of its remote location (Tsukernik and Lynch, 2013). Permafrost is defined as ground that remains below 0 °C for two consecutive years (Dobinski, 2011). According to Vieira *et al.,* (2010), permafrost is one of the major controlling factors of the terrestrial ecosystem dynamics in Antarctica. The above is highly evident when considering Antarctic thermal and physical properties, evolution and links to pedogenesis, the hydrology, geomorphic dynamics and response to global change (Vieira *et al.,* 2010). As permafrost is coupled to an active layer, the two greatly influence each other (Fig. 2). However, they are also affected by external forces such as atmospheric and topographic factors, which include air temperature, moisture, precipitation, snow cover, aspect, slope angle and altitude, atmospheric pressure and solar radiation (Almeida *et al.,* 2014). In turn, these external forces affect the ecological and biogeographical zones differently.

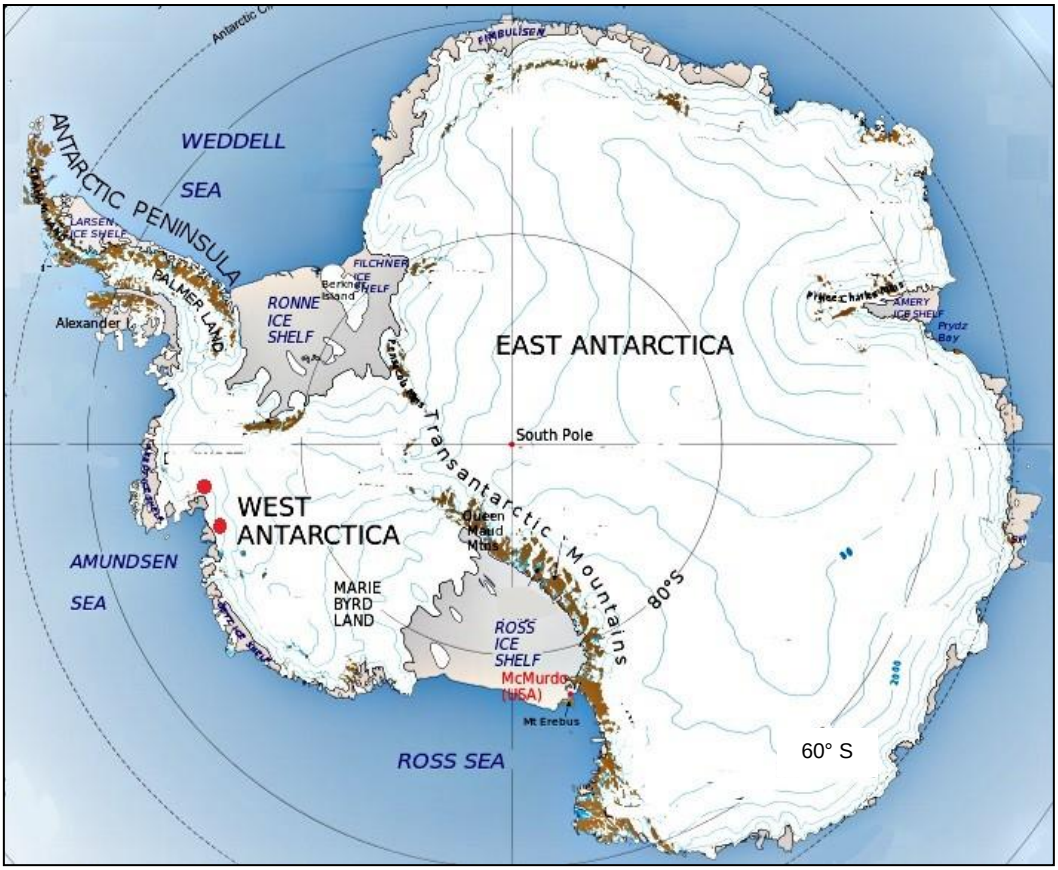

Figure 1. The Antarctic Continent, showing East and West Antarctica (Source: Morano, 2014).

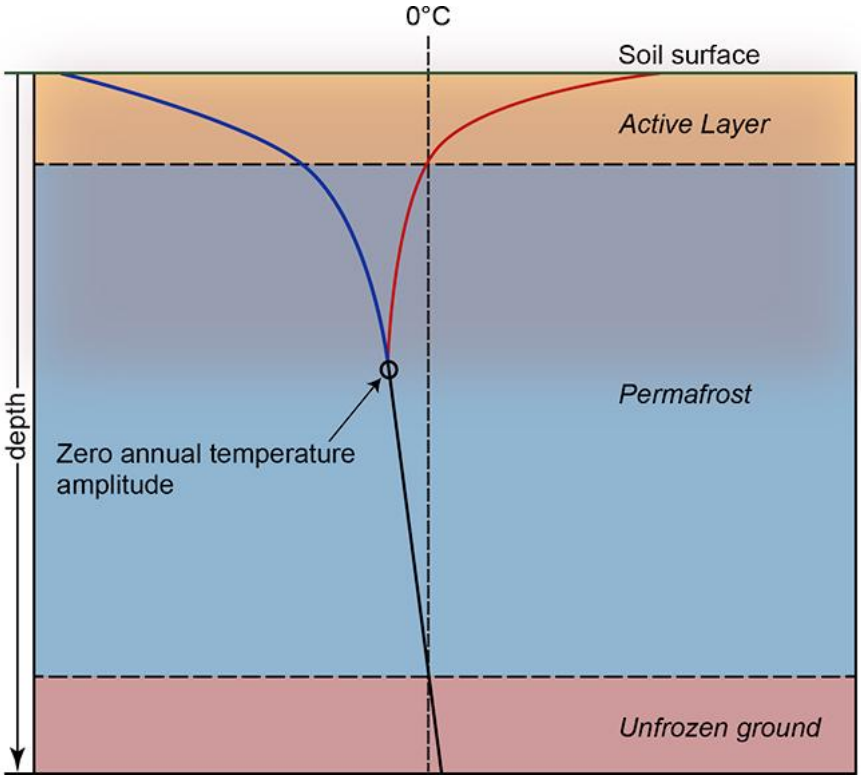

Figure 2. A model defining the active layer and permafrost (Source: ADAPT, 2016)

The International Polar Year (IPY) that took place between 2007 and 2008 saw a growth in the interest in permafrost studies in Antarctica. Historically, permafrost studies were reflected a Northern Hemisphere dominance. The IPY sought to balance the situation by raising awareness and promoting research "to increase the understanding of the environmental dynamics of the ice-free areas of the Antarctic" through the Antarctic Permafrost, Periglacial Environments and Soils Expert Group (ANTPAS) of the Scientific Committee on Antarctic Research (SCAR) and the Working Group of the International Permafrost Association (IPA) (Guglielmin and Vieira, 2014: 1). Following the IPY, specific top priority research questions were developed by the Antarctic and Southern Ocean scientific community (Kennicutt *et al.,* 2014). Vieira *et al.,* (2010) noted that there were still gaps in knowledge and research in permafrost and active layer monitoring efforts in most regions of Antarctica, including Dronning Maud Land (DML).

In response to the envisaged goals of the IPY and Kennicutt *et al.,* (2014), this project aims to provide an understanding and insight into the over-arching question that seeks to evaluate the state and status of permafrost and the active layer in DML through examining short-term variations in ground thermal regimes. The main focus is on evaluating and understanding the influence of synoptic, diurnal and seasonal events on the active layer during 2016.

1.2. Aim and Objectives

The aim of this research project is to use high-frequency data to determine the impact of seasonal, synoptic and diurnal events on ground thermal regimes. Investigations follow the first SCAR Antarctic and Southern Ocean Horizon Scan conducted by Kennicutt *et al.,* (2014). The proposed research creates a platform for answering the 39th and 42nd questions posed by Kennicutt *et al.,* (2014: 7), namely:

39. "*What are and have been the rates of geomorphic change in different Antarctic regions, and what are the ages of preserved landscapes?*" and
42. "*How will permafrost, the active layer and water availability in Antarctic soils [...] change in a warming climate, and what are the effects on ecosystems and biogeochemical cycles?*".

The question most pertinent to this project is Question 42, and the overall aim of the research project will be achieved through the following key objectives:

1. To establish meteorological influences on air and ground thermal regimes.
2. To determine the extent to which meteorological point data measured at Vesleskarvet (SANAE IV base) can be applied regionally to evaluate ground thermal regimes.
3. To determine the extent (depth) of meteorological events on ground thermal regimes.

1.3. Setting

Dronning Maud Land (DML) is on the Atlantic side of Antarctica, extends from 20° W and 45° E, and is bordered by Coats Land in the west and Enderby Land in the east (Schlosser *et al.,* 2008). It is divided into three climatically and topographically different regions: the ice shelves, the escarpment region and the Antarctic plateau (Reijmer and Oerlemans, 2002). DML is covered by an ice-sheet with a small group of rock outcrops called nunataks, and enclosed by four coasts - Princess Martha, Princess Astrid, Princess Ragnhild and Princess Harald (Cooper, 2006; SANAP, 2015). The exposed rock outcrops in DML are part of the approximately 2% of Antarctica's ice-free surface area and they are found on nunataks that form a 1 700 km chain of mountains that extend from "the eastern side of the Weddell Sea to the east of Enderby Land, with an average exposed width of 75 km" (Krynauw, 1986: 5).

The area of focus for this study was in the western part of DML, henceforth referred to as Western Dronning Maud Land (WDML). It spans the region from 5° W to 12° E and 70° S to 75° S (Harris, 1999). WDML is sub-divided into two main geological groups, namely the Grunehogna Province and

the Maud Belt, which are separated by the Pencksökket-Jutulstraumen glacial system (Harris, 1999). The Ahlmannryggen, where most of the study sites were located, is a ridge that is 112 km long, lies on the western side of Jutulstraumen glacier, and is located within Grunehogna Geological Province. Along with Borgmassivet, and its nunataks, the area comprises exposures of the Ritscherflya Supergroup (RSG) (Harris, 1999; Dwight, 2014).

The Ritscherflya Supergroup is a Mesoproterozoic low-grade volcanic and sedimentary sequence that shows little disturbance even though it has been heavily intruded by the mafic Borgmassivet Intrusive Suite, the ultramafic-mafic Robertskollen Suite and the felsic Nils Jörgennutane Suite (Krynauw, 1986; Harris, 1999; Jones *et al.,* 2003). It is a nearly flat-lying litho-stratigraphic unit that dips and is slightly deformed towards the Jutulstraumen glacier, which is 300 km long - the second largest glacier after the Lambert glacier (Krynauw, 1986; Harris, 1999; Jones *et al.,* 2003). Furthermore, the RSG sediments in the Ahlmannryggen Group are described as having been deposited in regressive cycles from shallow marines to braided streams, and finally, meandering rivers that produced alluvial fan deposits (Harris, 1999; Jones *et al.,* 2003).

On the eastern side of the Jutulstraumen glacier lies Jutulsessen in Gjelsvikfjella, which is part of the Maud Belt in central Dronning Maud Land. The exposed geological features belong to the Pan African post-orogenic A-type intrusions that occurred around 500 Ma (Marschall *et al.,* 2013). It is underlain by the Proterozoic high-grade metamorphic rocks (granulite and gneisses) that are polycyclically deformed and are part of the East Antarctic crystalline basement (Krynauw, 1986; Marschall *et al.,* 2013; Kotzé, 2015).

The climate in WDML is characteristic of continental Antarctica, in that it is a cold and dry desert (Hansen, 2013). WDML has low humidity levels due to low temperatures and precipitation, with precipitation falling exclusively as snow (Cooper, 2006). Precipitation in the region is influenced by cyclonic activity along the coast, the influence of which decreases towards the interior (Reijmer and Oerlemans, 2002; Schlosser *et al.,* 2008). WDML receives between 55 - 81 mm annually, while the coastal areas receive between 150 - 200 mm (Schlosser *et al.,* 2008; Hansen, 2013). As the effect of cyclones along the coast decreases towards the interior, katabatic winds gradually dominate and greatly influence the regional climate (Reijmer and Oerlemans, 2002). In DML, the katabatic winds originate from the east-southeast direction (Isaksson and Karlén, 1994). However, in WDML the topography buffers the more northern areas and katabatic winds are relatively weak. Instead, the dominating winds are easterly, which average a speed of 11 m/s (Isaksson and Karlén, 1994; Hansen, 2013).

The passage of low-pressure systems along the coast greatly influences temperature in DML (Kärkäs, 2004). Relatively warm and moist air from the coast from low-pressure systems causes temperatures to be highly variable, especially in winter when meridional and vertical temperature gradients are greatest (Reijmer and Oerlemans, 2002; Kärkäs, 2004). In WDML, temperatures range from an average maximum of 3 ˚C to an average minimum of -35 ˚C and have an average of -17 ˚C annually. In contrast, temperature at Troll (the name given to the station at Nonshøgda in Jutulsessen) has an average of -14.3 ˚C annually (Kotzé, 2015). Temperatures detailed for the Ahlmannryggen area of WDML were sourced from the South African Weather Service (SAWS) data set from the SANAE IV base for a period of ten years from 2006 to 2016. WDML is characterized by an almost equal distribution of solar radiation that changes seasonally and which influences air temperatures. In summer, the region is exposed to roughly three months of sunlight and in winter it receives close to zero radiation, as the sun does not rise (Cooper, 2006). In contrast, in autumn and spring, the region is subject to diurnal cycles (Kotzé, 2015).

The extremely harsh climate of Antarctica allows life on the continent to barely exist at physiological limits of survival (Robinson *et al.,* 2003). Owing to the isolated nature of the mountains and nunataks on the continent, the ecosystems found there are characterized by very basic life forms with minimal ecosystem interactions (Ryan and Watkins, 1989). However, a process of classification based on biogeographic regions was recently applied to Antarctica. A total of 16 biologically distinct ice-free regions, including DML, have been identified as Antarctic Conservation Biogeographic Regions (ACBRs) with the aim to create a biologically protected network area (Terauds and Lee*,* 2016).

Only a few nunataks in WDML have environments that can support biodiversity. Some of these include those at Robertskollen (Steele and Cooper, 2012). In the Ahlmannryggen there are five reported bird species, which include the Antarctic Petrel (*Thalassoica antarctica*), Snow Petrel (*Pagodroma nivea*), Southern Fulmar (*Fulmarus glacialoides*), Wilson's Storm Petrel (*Oceanites oceanicus*) and the South Polar Skua (Steele and Cooper, 2012). Along with the relatively warm and moist environments brought about by free water, the avian species provide the nunataks with the nutrients needed to support the cryptogamic vegetation dominated by lichens (Ryan and Watkins, 1989; Cocks *et al.,* 1998; Cooper, 2006).

Biodiversity in WDML, as well as in the rest of the continent is protected by a treaty that stipulates that the continent is to be used for peaceful exploits, specifically scientific exploration (ATS, 2013). The Antarctic Treaty is a political agreement that was first drafted in 1959 and officially entered into in force in 1961 by a number of countries, including South Africa (ATS, 2013; Dodds *et al.,* 2017). The

Treaty, which followed the establishment of SCAR, and new bodies formed subsequently, declared Antarctica to be a continent for science that no country claims, for as long as the treaty holds and is in effect (ATS, 2013; Elzinga, 2017). As a continent for science, measures have been established to ensure that it remains as pristine as possible. WDML is where South Africa has its base (SANAE IV) and has activities controlled by the South African National Antarctic Programme (SANAP). SANAP ensures that all activities within and around the SANAE IV base comply with the Antarctic Treaty's Committee for Environmental Protection to minimise the impact on the environment (Cooper, 2006). For instance, the SANAE IV base was designed to be aerodynamic so as to minimise its impact on the environment by reducing the accumulation of wind-driven snow around it (Beyers and Harms, 2003). Additionally, environmental audits are done annually around the base and the surrounding researched nunataks to monitor any impacts from human activities (Cooper, 2006).

The study area for this research is in WDML, where a total of 8 sites were chosen from the Ahlmannryggen (7) and the Jutulsessen (1) (see Fig. 3). These sites are well distributed and best represent WDML with regards to active layer dynamics and topography, indicated by their distance from the ice shelf and their altitude (Kotzé, 2015).

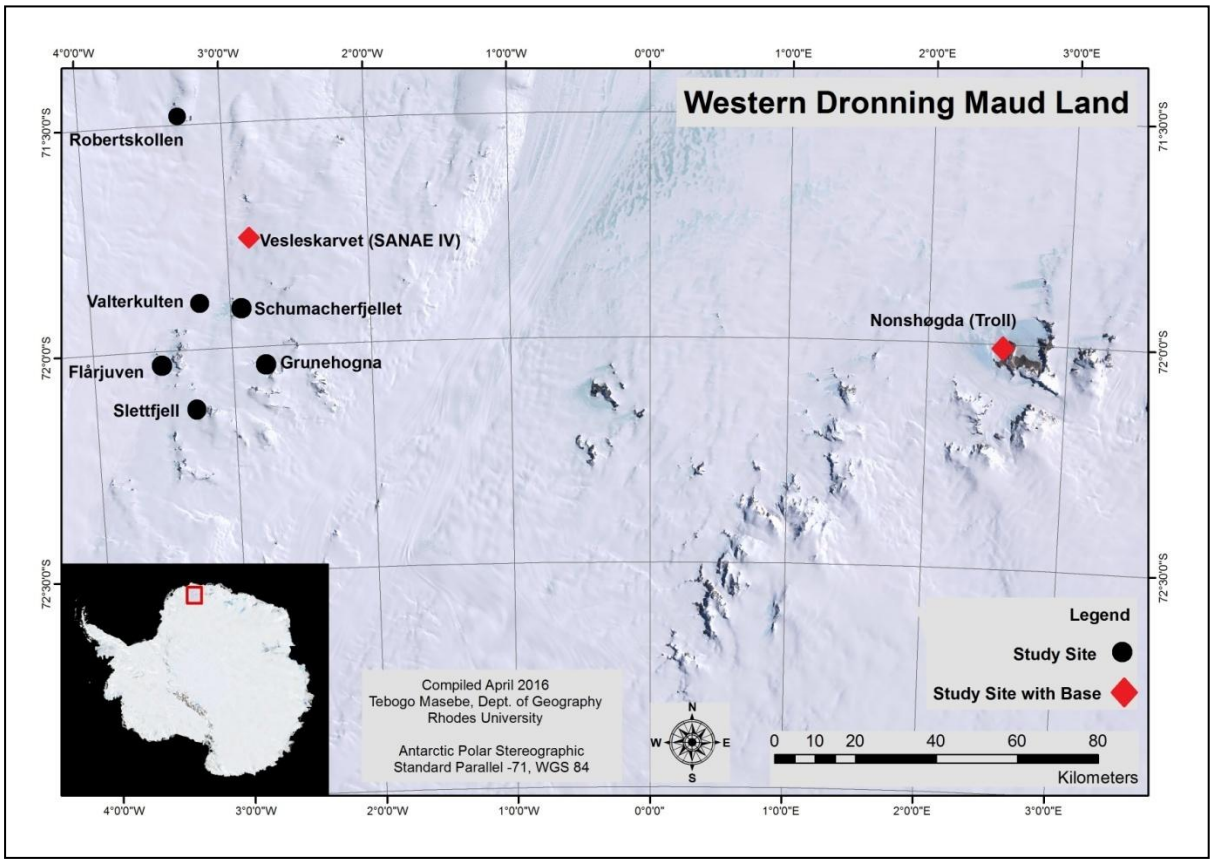

Figure 3. Map of study sites.

Details of the individual study sites are presented below.

1. Vesleskarvet (71°40'S, 2°50'W)

Vesleskarvet served as the main study site due to its proximity to the South African National Antarctic Expedition (SANAE) IV base (Fig. 4). The nunatak is flat-topped with a northern and southern buttress, situated approximately 180 km from the ice shelf, at an altitude of 848 m (Steele and Cooper, 2012; Scott, 2014). Vesleskarvet has approximately 22.5 ha of exposed rock surface (Cooper, 2006). The SANAE IV base is on the Southern Buttress and the logging station is on the Northern Buttress. Due to the presence of the base, the Southern Buttress has only been considered for long-term mass loss monitoring from weathering experiments (Meiklejohn, 2009). The Northern Buttress, on the other hand, was selected as an ideal site for study because it is populated with sorted patterned ground and other active layer features (Meiklejohn, 2009). The Buttress has 200 m high cliffs along the northern and western edges which dip into a wind scoop, whereas on the southern buttress, the eastern and southern edges gently dip into a south-east sloping ice sheet (Cooper, 2006; Dwight, 2014). The rocks of the nunatak on the Northern Buttress are large doleritic and dioritic igneous rocks in the form of large angular boulders (Cooper, 2006; Hansen, 2013).

Figure 4. SANAE IV base. Photo taken from the Northern Buttress.

2. Robertskollen (71°27'S, 3°15'W)

Robertskollen was the most northerly situated study site, located approximately 30 km away from Vesleskarvet to the north-west, and 150 km away from the ice shelf (Steele and Cooper, 2012; Scott, 2014). The study site comprises a number of nunataks that range in altitude from 200 to 500 m a.s.l (Dwight, 2014). It has an abundance of sorted and unsorted

ground, together with tafoni and lobate forms on the slopes (Meiklejohn, 2009). In addition, Robertskollen has a relative abundance of biotic activity in the form of lichens, fungi, and Antarctic Snow Petrel colonies (Scott, 2014). Robertskollen is characterized by lithosols that are made up of gabbronorites, gabbros and dolerites, and it has high cliffs towards the eastern side and gently sloping boulder slopes towards the western side (Dwight, 2014).

3. Valterkulten (71°54'S, 3°14'W)

   Valterkulten is a small nunatak that is situated 28 km away from Vesleskarvet and has a maximum altitude of 1021 m a.s.l (Scott, 2014). It served as an ideal area for investigating geochemistry and chemical weathering because it has a brine lake on top of it, as well as examples of terraces and thermal contraction cracks possibly brought about by active-layer processes (Meiklejohn, 2009).

4. Schumacherfjellet (71°55’S, 2°58’W)

   The study site on Schumarcherfjellet, a nunatak 25 km south of Vesleskarvet, was at an altitude of 960 m a.s.l. It was comprised by a series of mountains that lies approximately 10 km north of Grunehogna (Meiklejohn, 2009). It has flat-topped surfaces of doleritic rocks that are well populated with patterned ground, and the slopes of the north facing aspect of the mountains have examples of solifluction terraces (Meiklejohn 2009).

5. Grunehogna (72°02’S, 2°48’W)

   Grunehogna is a nunatak that is 42 km away from Vesleskarvet, and it has an altitude of 1070 m a.s.l. Along with a wind scoop on its eastern side, it has good examples of both sorted and unsorted patterned ground made up of dolerite rocks (Meiklejohn, 2009).

6. Flårjuven (72°01'S, 3°24'W)

   Flårjuven is a flat-topped mountain that lies approximately 20 km west of Grunehogna and 44 km south-west of Vesleskarvet and is at an altitude of 1380 m a.s.l (Meiklejohn, 2009; Scott, 2014). It has large exposed areas and a great number of patterned ground features that made it one of the preferred locations in all of the Ahlmannryggen to conduct research into active-layer dynamics (Meiklejohn, 2009).

7. Slettfjell (72°08'S, 3°19'W)

Slettfjell is the furthest site south of Vesleskarvet, located 53 km away at an altitude of 1472 m a.s.l. Similar to other sites in the Ahlmannryggen, it has an abundance of sorted and unsorted patterned ground (Meiklejohn, 2009; Scott, 2014).

8. Nonshøgda (72°00’40.6’’S, 2°32’00.2’’E)

Nonshøgda – henceforth referred to as Troll – is where the Norwegian Troll Station is based (see Fig. 5a and 5b). It was the furthest site from Vesleskarvet, located 190 km away to the east at an altitude of 1283 m a.s.l. The location is across the Jutulstraumen glacier in the Jutulsessen, and it is approximately 200 km from the edge of the ice shelf (Scott, 2014; Kotzé, 2015). It has a different geology to that of the Ahlmannryggen, and is part of a chain of coastal mountains that are between approximately 1000 m and 3000 m high (Scott, 2014; Kotzé, 2015). Akin to Vesleskarvet and its surrounding nunataks, it is populated by sorted and non-sorted patterned ground (Scott, 2014; Kotzé, 2015).

Figure 5a. Troll Station and surrounds.

Figure 5b. Troll Station.

Western Dronning Maud Land (WDML) and the selected study sites (nunataks) within it, was identified as an ideal setting to conduct this project because literature and knowledge on the region is limited. This project intends to contribute to the growing literature of WDML with the aim of using high-frequency data to determine the impact of seasonal, synoptic and diurnal events on ground thermal regimes focusing on evaluating and understanding the influence of meteorological events on the active layer during 2016.

The project seeks to evaluate the state and status of permafrost and the active layer by establishing meteorological influences on air and ground thermal regimes; determining the extent to which meteorological point data measured at Vesleskarvet (SANAE IV base) can be applied regionally to evaluate ground thermal regimes and; determining the extent (depth) of synoptic events on ground thermal regimes. The following chapter explores the existing literature on ground thermal regimes and their meteorological influences and seeks to identify a gap that this research will contribute to.

Chapter 2: Literature Review

2.1. Permafrost and the Active Layer Environment

According to Guglielmin (2012), permafrost is present underneath almost all ice-free regions of Antarctica, with the possible exception of the lowest elevations of the sub-Antarctic islands, where microclimatic factors resulted in its absence. The word permafrost is an amalgamation of two words – *permanent frost* – which were originally used to describe land that seemed to be permanently frozen, although this term was replaced with the term *perennially permanent frozen* ground (Dobinski, 2011). There are a number of definitions for the word permafrost (French, 2007). However, in line with geomorphic processes in cryotic areas, it is defined as ground (including soil, rock, ice, and/or organic material) that remains at, or below, 0 °C for a minimum of two consecutive years (Dobinski, 2011). Dobinski (2011) points out that it is important to think of permafrost not as a material phenomenon, but as a physical state of the lithosphere.

Permafrost in continental Antarctica has been identified as dry permafrost; that is, permafrost that contains no liquid water (Dobinski, 2011; Guglielmin, 2012). The reason for an absence of liquid water is that dry atmospheric conditions in continental Antarctica do not allow for liquid water to exist for extended periods of time, due either to sublimation in winter, or its ablation in summer (Hermichen, 1995). The occurrence of permafrost around the globe is reported by Dobinski (2011) to be defined altitudinally as well as latitudinally, *i.e.* it occurs in mountainous, alpine, and polar regions. French (2007) gives a more precise account of the different types of permafrost and the regions where they occur. Permafrost occurring around the globe is categorised into four main types, namely continuous, discontinuous, sporadic and isolated permafrost (French, 2007). A further two sub-types, identified as periglacial and glacial permafrost, are found. These will be expounded further in sections to come.

Discontinuous, sporadic and isolated permafrost are found almost exclusively in the Northern Hemisphere, while continuous permafrost occurs mostly in glacial regions. However, as pointed out by Dobinski (2011), it is difficult to estimate the aerial distribution of permafrost because of its hidden character. Nevertheless, one can infer from available literature that continuous permafrost occurs, to a large extent, mainly in the Southern Hemisphere, because the Antarctic terrain has remained below 0 °C for millions of years and most of it is classified as a glacial zone (French, 2007). To emphasise this point, the largest glacier in the world, the Lambert Glacier, is found in East Antarctica (Krynauw 1986).

Given that permafrost is a physical state of the lithosphere, Marchenko and Etzelmüller (2013) point out, it is defined purely in thermal terms. It, therefore, follows that the distribution of permafrost is controlled by energy exchanges at the atmosphere-land-surface boundary, and in addition, it is governed by climate on a global scale (Marchenko and Etzelmüller, 2013). On a regional and local scale, these energy exchange processes are regulated by snow, vegetation and sediment properties (Marchenko and Etzelmüller, 2013). The development of permafrost is highly dependent on the negative energy budget of the ground surface; *i.e.* the ground needs to experience mean surface temperatures below 0 °C for at least two consecutive years (Marchenko and Etzelmüller, 2013).

The energy budget of the Earth is regulated by the amount of incoming short-wave solar radiation, the transformation of this into long waves, and the absorption of these by the Earth's surface (Marchenko and Etzelmüller, 2013). Net heat being added to or lost by the globe depends on whether the incoming solar radiation is greater than or less than the outgoing radiation (Trenberth *et al.,* 2009). A negative energy budget is a result of the incoming solar energy/radiation from the sun being less than the outgoing energy flux, due to the presence of clouds in the atmosphere (Kato *et al.,* 2008; Trenberth *et al.,* 2009).

The shape of the planet and the position of the planet in its orbit around the sun favour the domination of cold climates in high latitudes, and high mountain regions in mid-latitudes, which in turn support the development and presence of permafrost (French, 2007). This is because the sun's rays travel a greater distance to reach the Earth's surface in high latitudes, and thus get spread out over a greater surface area, when compared to the low latitudes, with the smallest area at the equator (Mlynczak *et al.,* 2011), as shown in Figure 6. As a result, more incoming solar radiation is lost to the atmosphere at high latitudes than at low latitudes. The development and presence of permafrost is further supported and influenced by snow, vegetation, sediment properties, atmospheric and topographic factors (Marchenko and Etzelmüller, 2013; Almeida *et al.,* 2014).

As mentioned earlier, permafrost in continental Antarctica occurs mostly as continuous permafrost, but it also occurs as glacial permafrost (Dobinski, 2011). The latter occurs only in glaciated regions such as continental glaciers, ice caps and ice sheets (Dobinski, 2011). The formation and thermal regimes of the two sub-types of permafrost (periglacial and glacial permafrost) differ greatly (see Fig. 7a and Fig. 7b). Periglacial permafrost has well-defined horizons that exhibit a seasonally active layer of ground and the perennially frozen or inactive layer of ground, termed permafrost. On the other hand, glacial permafrost is defined by a very thin active layer that continually gets removed through sublimation and/or ablation (Dobinski, 2011). The depth of zero annual amplitude shows the point

where the ground temperature remains constant throughout the process of thawing and freezing of the ground (Williams and Smith, 1989).

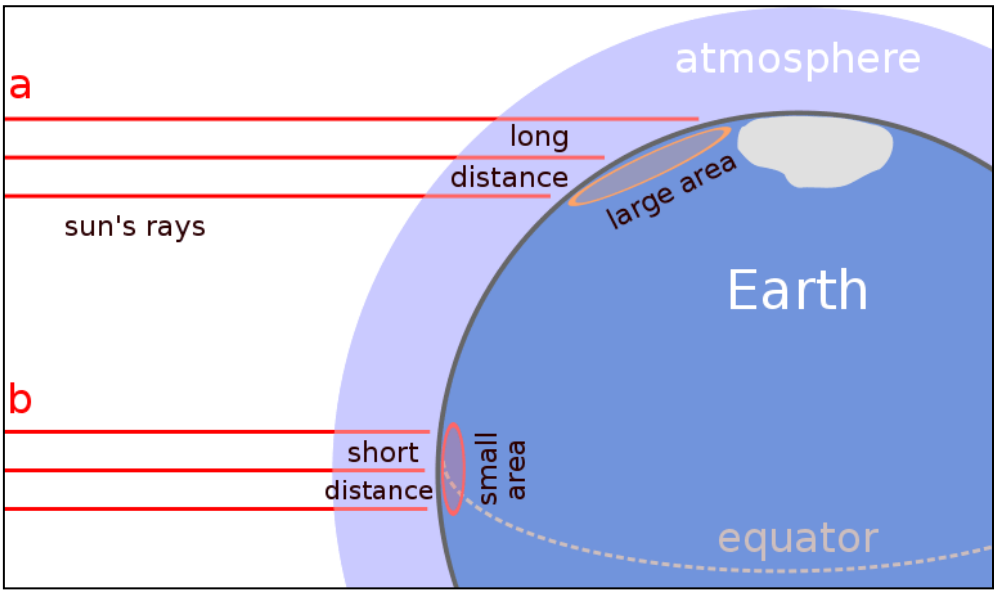

Figure 6. The tilt of the Earth and its atmosphere affect the amount and area of solar radiation that reaches the Earth's surface (Source: National Snow and Ice Data Centre: 2016)

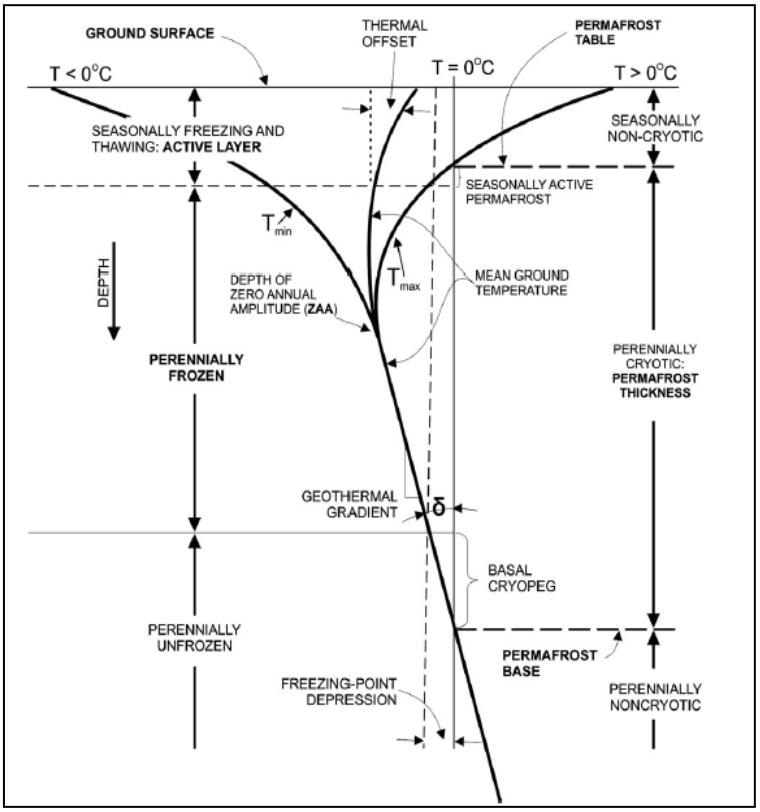

Figure 7a. Thermophysical model of permafrost of a periglacial environment (Source: Dobinski, 2011).

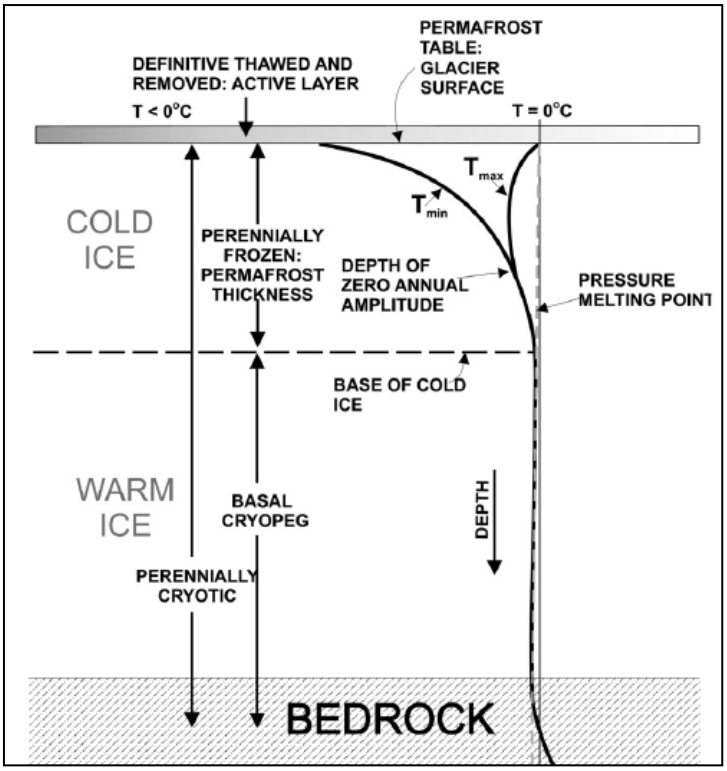

Figure 7b. Thermophysical model of permafrost of a glacial environment (Source: Dobinski, 2011).

Western Dronning Maud Land (WDML) has been identified as having continuous permafrost, with limited areas of glacial permafrost over the Jutulstraumen glacier and areas around the Schirmacher Oasis (Hermichen, 1995). In 1995, it was noted by Hermichen (1995) that thawing had been observed to have occurred at altitudes of up to 1500 m a.s.l. in December/January (the Austral summer), and this was attributed to interglacial conditions prevailing due to the current global climate. However, the thickness of permafrost is not well known.

The state and depth of permafrost (permafrost thickness) and the active layer in continental Antarctica are being monitored by the International Permafrost Association (IPA) (IPA, 2012). The IPA has established a number of monitoring networks to develop a global database of the spatial structure and variability of active layer depth and permafrost temperature, to monitor the long-term thermal state of permafrost in an extensive borehole network, and to monitor the active layer (IPA, 2012). The monitoring networks that oversee the goals of the IPA in the listed order include the Global Terrestrial Network for Permafrost (GTN-P), the Thermal State of Permafrost (TSP) and the Circumpolar Active Layer Monitoring network (CALM) (IPA, 2012).

In the case of Antarctica, the Circumpolar Active Layer Monitoring – Southern Hemisphere (CALM-S) network was established to better monitor ground temperatures, since the CALM network could not

be properly implemented because the rocky terrain prevents the use of 100 m x 100 m grids for mechanical probing (Vieira *et al.,* 2010; Guglielmin and Vieira, 2014). The CALM-S makes use of smaller grids and shallow boreholes to enhance monitoring where probing on the rocky terrain of the ice-free regions is not possible (Vieira *et al.,* 2010). According to Vieira *et al.,* (2010), there are 73 CALM-S sites in Antarctica, one of which is in Dronning Maud Land (DML).

The CALM-S site in DML is situated at Novolazarevskaya. Novolazarevskaya is one of six sites, including one at Versleskarvet, two at Nonshøgda and two at Flårjuven, which have permafrost borehole sites that were established during the IPY (Vieira *et al.,* 2010). These CALM-S sites monitor ground temperatures on the Basen, Flårjuven, Grunehogna, Novolazarevskaya, Robertskollen, Schumacherfjellet, Slettfjell, Nonshøgda, Valterkulten and Vesleskarvet nunataks. Based on the heterogeneous climate, topography and geology of these monitored nunataks, this project will focus on all the above nunataks, excluding Basen and Novolazarevskaya.

2.2. Climatic controls on ground thermal regimes

Although the climate in Antarctica is perceived as being fairly uncomplicated and somewhat well-defined, local(ised) ground thermal regimes are influenced by more than one single factor and are a consequence of interactions between climatic, surface and sub-surface factors (Williams and Smith, 1989; Richter and Bormann, 1995). Focusing on climatic factors, the ground thermal regime is influenced by the seasonal fluctuation of temperature above the mean annual value, including the air, ground surface and near-surface temperatures (Williams and Smith, 1989). As noted by French (2007), air temperatures are a key identifier of periglacial environments.

The ground in periglacial environments is affected by the mean annual temperature immediately above, at, and below, the surface (French, 2007). Immediately above the surface of the ground, air temperature is measured at a standard height above seasonal snow cover, and it is referred to as the Mean Annual Air Temperature (MAAT). The temperature measured at the ground surface is referred to as the Mean Annual Ground Surface Temperature (MAGST), and seasonal fluctuation of this temperature is responsible for periodic thermal stresses in the surface ground layers that give rise to geomorphological phenomena such as ice-wedge development (Williams and Smith, 1989; French, 2007). Temperature below the surface of the ground, at the top of permafrost, is referred to as Temperature at the Top Of Permafrost (TTOP), and fluctuations in this temperature are influenced by the amount of latent heat released from the freezing water within the active layer (Williams and Smith, 1989; French, 2007). In addition, temperature below the ground surface is influenced by sub-

surface factors such as ground/soil properties (including soil particle size, bulk density, thermal conductivity and thermal diffusivity, determined by the minerals making up the soil particles), the microbial life found within the soil and the amount of water/ice available within the soil/ground (Williams and Smith, 1989).

The temperature at the three periglacial zones in Antarctica, above the ground, at the surface, and below the surface of the ground, is influenced by a number of factors, which include the latitude, surface elevation and distance from the ocean (Richter and Bormann, 1995). Antarctica has the highest average surface elevation compared to other continents, and is overlain by an ice sheet of approximately 2 000 m mean thickness; these two factors impose a controlling influence on climate and regional atmospheric circulation. Along with the specific radiation balance in the continent, they have resulted in the formation of three climatic zones, which correspond to the three ecological zones mentioned by Bölter *et al.,* (2002). These encompass the zone of the inner continental plateau and high mountainous terrains, the zone of inland ice slope (near-coastal belt), which is 500-900 km wide and at an elevation of 300-500 m. a.s.l., and the zone of coastal climate, between the latitudinal belt of 60° - 75° S (Richter and Bormann, 1995).

Western Dronning Maud Land (WDML) is located in the second zone, *i.e.* the zone of inland ice slope (Richter and Bormann, 1995). Weather is controlled by varying atmospheric circulation as well as synoptic systems moving across the Weddell Sea. These depend on the position and the behaviour of the central anticyclone over inner Antarctica and the trough of low pressure over the Southern Ocean, respectively (Richter and Bormann, 1995; Kärkäs, 2004). The anticyclone over the inner continent is due to the high-pressure system that brings about predominant downslope katabatic winds (Richter and Bormann, 1995; Bintanja, 2000).

Katabatic winds blow coastward from the high continental interior in a regional counter-clockwise sense of motion (Richter and Bormann, 1995). They are strongest over areas with steep slopes, whereas, over more gentle slopes the Coriolis force turns the downslope winds to a cross-slope direction, which results in geostrophic winds (Bintanja, 2000). Steinhoff *et al.,* (2013) note that even though katabatic winds are traditionally defined as any downslope wind, in Antarctica the term refers to negatively buoyant flow. Katabatic winds occur and/or dominate in winter, due to the stronger surface temperature inversions in winter, while the weaker surface temperature inversions in summer are not sufficient to cause katabatic winds (Steinhoff *et al.,* 2013). In mountainous regions, strong katabatic winds are often referred to in the same category as foëhn winds.

Foëhn winds are defined as winds that warm up and dry out as they descend, generally down the lee side of a mountain (Steinhoff *et al.,* 2013). These winds are the result of the flow of wind changing intensely due to the topography as it flows over the lee side of mountain barriers (Speirs *et al.,* 2010). Foëhn winds can generate wind gusts of over 50 m/s, and in Antarctica, they occur mostly in the McMurdo Dry Valleys (MDVs) (Speirs *et al.,* 2010). In WDML the southern mountains buffer enough for foëhn winds to dominate and therefore their effects are negligible (Meiklejohn, pers. comm., 2016).

It has been observed that in summer, diurnal events dominate temperatures, while in winter, synoptic events (*i.e.,* cyclones) dominate. Diurnal events can be attributed primarily to the passage of the sun over the sky of the continent, and the momentary setting over the horizon. The movement of the sun determines that its rays continuously change direction and position, and this can result in local effects on the air and ground temperatures. Synoptic-scale impacts, on the other hand, are largely due to the movement of the trough of low pressure over the Southern Ocean, and which has been reported by a number of authors to be responsible for cyclones at the coastal region (Noone *et al.,* 1999; Bintanja, 2000; Simmonds *et al.,* 2003; Kärkäs, 2004). The effect of these transient cyclones over inner continental Antarctica is disputed. According to Richter and Bormann (1995), their efficiency is low and restricted to coastal areas, except for the low lying areas of West Antarctica. However, Schlosser *et al.,* (2010) argue that the interior plateau is also affected by synoptic systems in the same way as coastal regions more strongly than previously thought.

Regardless of the level of efficiency of synoptic systems in the interior, they are known to influence the amount of solar radiation reaching the surface, along with air temperatures, precipitation and wind speed and direction (Noone *et al.,*1999; Bintanja, 2000; Richter and Bormann, 1995; Kärkäs, 2004). In the sub-Antarctic, the variation in solar radiation reaching the Earth's surface due to the passage of synoptic systems has been seen to influence soil thermal characteristics (Nel *et al.,* 2009). However, since Vesleskarvet (the main focus of the study region) is on the periphery (*i.e.* it is neither on the coastal plain nor the continental plateau), it seldom experiences strong wind events experienced by other regions such as Casey (an Australian coastal station on Wilkes Land – Antarctica) and Marion Island (in the sub-Antarctic) (Murphy and Simmonds, 1993; Nel *et al.,* 2009). Nevertheless, Bintanja (2000) reports that easterly geostrophic winds caused by the presence of low-pressure systems in the coast, often interact with katabatic winds in the boundary layer to produce strong boundary layer winds that have a significant impact on soil thermal properties.

Climatic variability, especially that caused by synoptic systems in the Southern Ocean, is attributed to the Southern Annular Mode (SAM), which is connected to the El Ninõ-Southern Oscillation (ENSO)

cycle, and to the Semi-Annual Oscillation (SAO) (Noone *et al.,* 1999; Schlosser *et al.,* 2010). The SAM is the regular rotation or circumpolar pattern displacement of atmospheric mass between the mid-latitude (higher pressure) and the Antarctic coast (lower pressure), in which the intensity and location of the air pressure gradient changes in a non-periodic way over a wide range of time scales from days to years (Turner *et al.,* 2013). The SAO consists of the bi-annual "contraction and expansion of the pressure trough around Antarctica, in response to differences in heat storage between Antarctica and the surrounding oceans" (Kärkäs, 2004: 2). The SAM and SAO are integral components to this project because the seasonal and inter-seasonal dynamic between the atmosphere and the ground thermal regime have an effect on climatological variables such as surface air pressure, precipitation, sea ice cover, wind speed and cloudiness, which are all important to active layer research in WDML (Kotzé, 2015).

2.3. Oceanic Influence on continental Antarctica

Research on the heat signature of the ocean shows that Earth is absorbing more energy from the sun than it is radiating back to space as heat (Hansen *et al.,* 2011). This has major effects on Antarctic continental ice and/or ice shelves because the warm sea water continually acts as a lubricant between the ice and the ground surface, thus accelerating the rate of ice shelf loss. This phenomenon is commonly observed in the Antarctic Peninsula (Turner *et al.,* 2013). The warm surface seawater affects synoptic weather in Western Dronning Maud Land (WDML) because of the Antarctic Convergence or the Antarctic Circumpolar Current (ACC) that encircles the whole continent (see Fig. 8) (Richter and Bormann, 1995). According to Toggweiler and Russell (2008), the ACC is a wind-driven current that goes around Antarctica unhindered by any land; it goes through an east-west channel between South America, Australia and Antarctica. Toggweiler and Russell (2008) point out that the ACC is the world's strongest current (by volume of water transported) because the boundary of east wind drift over the channel and the flow of the ACC are aligned for the length of the channel.

Given the fact that water has a high latent heat capacity, the ocean has a slow response to the seasonal cycle of heating when compared to land (Mlynczak *et al.,* 2011). However, water in the ACC does not seem to have warming capabilities, because it is part of the thermohaline circulation of the ocean that transports water around the globe, akin to a large conveyor belt (Toggweiler and Russell, 2008). The thermohaline circulation is an overturning circulation of water in which warm water on the ocean surface and sub-surface flows to the poles, and is subsequently converted into cold water that sinks and flows towards the equator in the interior, or as part of deep water column (Toggweiler

and Key, n.d.). It creates regional density differences within the ocean through heating, cooling, freshening and salinification (Toggweiler and Key, n.d.). According to Toggweiler and Key (n.d.), the thermohaline circulation turns over all the deep water in the ocean every approximately 600 years.

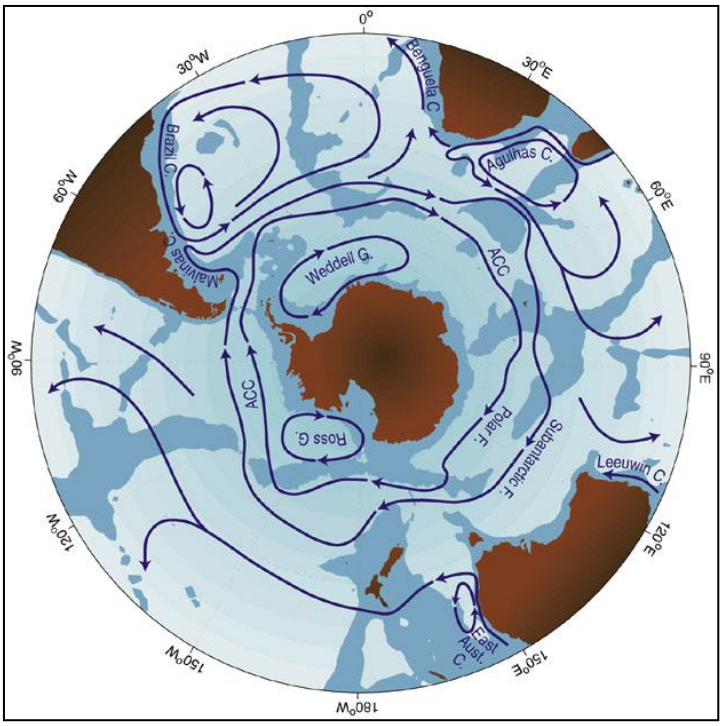

Figure 8. Map of major ocean currents south of 20° S (Adapted from Pidwirny, 2009)

The thermohaline circulation plays a significant role in controlling the Earth's climate. It keeps the poles relatively habitable by transporting approximately 10^{15} W of heat towards the poles into high latitudes, which is about a quarter of the total heat transport of the ocean-atmosphere circulation system (Toggweiler and Key, n.d.). However, the South Pole does not receive the same amount of transported heat as the North Pole, due to heat capture by the upwelled deep water in the Drake Passage. This water flows to the north on account of the Coriolis Force, and when it comes into contact with the atmosphere, it absorbs the solar heat that would have been available to warm up the Southern Ocean and Antarctica (Toggweiler and Key, n.d.; Convey *et al.,* 2009). The resultant state is a situation where the sea surface temperatures at 60° N in the North Atlantic are 6 °C warmer than sea surface temperatures at 60° S (Toggweiler and Key, n.d.). Nevertheless, the Southern Ocean is still home to some of the most intense synoptic cyclones (Kärkäs, 2004).

The Southern Ocean, along with the Antarctic Circumpolar Circulation, synoptic weather systems that originate in the ocean, anticyclonic or katabatic winds in the interior and diurnal fluctuations brought about by air circulation patterns, all have an influence on ground thermal regimes (Richter

and Bormann, 1995). These climatic forces are all governed by the Southern Annular Mode and the Semi-Annular Oscillation that affect active layer processes in WDML.

As Wilhelm and Bockheim (2017) point out, thawing of the permafrost layer points to a long-term warming environment that is evidenced by a warming ground profile. This is shown by an increasing active layer which deepens as seen in Signy Island and Rothera Point (Adelaide Island) due to vegetation cover that helps to raise ground temperatures better than bare and unvegetated ground, and the geology of the region along with air temperature and snow cover (Guglielmin *et al.,* 2012; Guglielmin *et al.,* 2014). In Marion Island, variations in ground temperatures were a direct result of the passage of synoptic scale weather systems. It was noticed that synoptic systems originating in the ocean have a great impact on thermal characteristics and heat fluxes of the ground profile (Nel *et al.,* 2009).

Studies abound of active layer thicknesses and ground thermal regimes in maritime Antarctica such as the ones presented above. However, such studies in continental Antarctica are limited, the closest being research conducted at the McMurdo Dry Valleys (Bockheim, 2004). This chapter has laid the foundation for this project by identifying types of permafrost and the specific type that lies underneath WDML. Along with permafrost, the active layer of WDML is influenced by meteorological factors as well as ground and/or soil properties. The methods in which these will be identified and analysed in great detail are explained in the following chapter.

Chapter 3: Methodology

In order to achieve the aims of this project, an investigative approach was followed, in line with that described by Church (2013). This approach does not focus on one specific area in isolation, unlike the reductionist approach followed in geomorphology in the past. Instead, an attempt is made to consider all factors involved and the extent to which they have an effect on one another. The study conducted feeds into ongoing research into the periglacial landscape in Antarctica, the processes that affect it, and those affected by it. The data for the research was collected over time by permanent, long-term, automated recording stations. Data from these recording stations were downloaded during short field excursions to the sites of interest during summer relief trips to the Antarctic, commencing in 2010. The three objectives identified as necessary to achieve the aim of this project were carried out using a number of instruments and methods, as outlined below.

Objective 1

To establish meteorological influences on air and ground thermal regimes.

The first objective initially involved collecting data from the SANAE IV station (hereinafter referred to as Vesleskarvet), and downloading the data from data loggers that had been left in the field for a year. These data loggers are designed to record ground/soil temperature and moisture data as well as air temperature. The data downloaded were collected using the ACR and XR5 data loggers and a Decagon EC-5 Soil Moisture Sensor. This method of data acquisition has been used by a number of researchers, including Almeida *et al.,* (2014) at King George Island in Maritime Antarctica; Meiklejohn (2009) at the Alhmannryggen and at Troll in Continental Antarctica; and Vieira *et al.,* (2010) in various locations around Antarctica.

The required high-frequency data were measured at different intervals for the different loggers. In the case of the XR5 logger, data were recorded at hourly intervals throughout the collection period from 2009 to the present period. For the ACR logger, data were measured at 3-hour intervals from 2013 to 2015. From 2016 onwards, the logger was reset and adjusted to record data at 10-minute intervals (with the exception of a brief period of a day, where the data were measured at 1-hour intervals, early in 2016). Recording intervals for the ACR logger were reset to enable better detection of small changes in ground conditions brought about by changes in the atmosphere, as well as to enable synchronization with data from the South African Weather Service (SAWS) weather station situated at Vesleskarvet, where measurements were recorded at 5-minute intervals. The

data loggers were installed at the same elevation as the SAWS weather station, which was situated $\pm$ 300m away.

Microsoft Excel® was used as a statistical tool to analyse the collected meteorological point data from the automated logging station (ALS) as well as the SAWS data. This was to find correlations between the two data sets to generate graphs from the statistical variables including averages, maxima and minima in order to make a visual analysis of the seasonal data, synoptic data and diurnal weather events easier. In addition, visual analysis generated by Microsoft Excel® aided in understanding the correlation between the ALS and SAWS data with synoptic charts of the Australian Meteorological Division (AMPS).

Objective 2

To determine the extent to which meteorological point data measured at Vesleskarvet (SANAE IV base) can be used regionally to evaluate ground thermal regimes.

In order to achieve the second objective, data were collected in the same way as that for the first objective, at various selected sites around the Ahlmannryggen. The ALS was set up in a similar way, at the same depths of up to 20 cm for the ACR logger, and up to 60 cm for the XR5 logger, for all sites, to standardise the data collection procedure for future analysis and to allow comparison. Troll Station, however, had a total of four sampling sites around its base; two ACR loggers situated in the centre and at the boundary or crack of a selected polygon, and two XR5 loggers; one old (installed in 2007), and one new (installed in 2013). Both the ACR loggers were buried 20 cm below the ground in the same fashion as those in Ahlmannryggen. The old XR5 logging station recorded temperatures deeper, up to a depth of 2 m due to the deep soil substrate and drilling equipment available, as was the new XR5 logger. However, in 2016 it was found that the new XR5 logger was re-installed too deep below the ground following construction at the Troll Station. The discrepancies meant that the data were not used. At the Alhmannrryggen, the XR5 loggers were buried up to 60 cm below the ground on account of the presence of ice-cemented ground and shallow soils. All the ALS's at the various sites were set to record data at the same (1 hr) intervals, having been reset and adjusted simultaneously with those in Vesleskarvet. The ALS's and their setup will be discussed below.

In a similar manner to the first objective, Microsoft Excel® was used as a statistical and graphing tool to analyse meteorological point data collected from the surrounding sites within the Ahlmannryggen, as well as data from the Troll Station. This was to find

correlations between their data sets and that of Vesleskarvet to create graphs for comparison. The period of comparison was 2016 and emphasis was placed on statistical variables, including averages, maxima and minima, as well as selected strong synoptic events of the year 2016.

Objective 3

To determine the extent (depth) of meteorological events on ground thermal regimes.

The third objective was achieved partly by using data collected for Objective 1 and 2, and partly by collecting and analysing soil samples. The rate at which synoptic scale events are reflected at different depths below the ground surface depends on the soil particle size, bulk density, the specific heat capacity, the thermal conductivity, the thermal properties of minerals present in the soil/ground, the depth of snow cover (since snow acts as an insulator and/or buffer), as well as the time elapsed since change in surface conditions (Williams and Smith, 1989; Schaetzl and Anderson, 2005). Data from the ALS were used to calculate the rate at which selected synoptic events (obtained from synoptic charts of the Australian Meteorological Division (AMPS)) of the year 2016 were transmitted throughout the soil profile, and to determine the maximum depth (as allowed by the ALS) to which transmission of changes occurred.

The rate at which the selected synoptic events were transmitted through the soil profile was calculated using the temperature propagation equation given by Equation 1 (Wilhelm and Bockheim, 2017):

Equation 1: Temperature Propagation

$$\mathrm{T_{prop}} = \frac{Max.monitered\ depth - Transmission\ Start\ Depth}{\sum Hours\ for\ event\ to\ travel\ from\ x\ depth\ to\ max.monitered\ depth}$$

where T_{prop} stands for temperature propagation (in cm/h), and *x* stands for the near surface depth (ground surface = 1cm) (in h).

The physical properties of the soil were determined from soil samples collected at every site, close to the ALS. One soil sample was collected per site, corresponding to the ALS. The grab specimens, as noted by Briggs (1977b), were collected using a bulk density square, a

hammer (to push down the bulk density square), a trowel, sampling bags, a sealing tape and a marker. The method of sampling followed that of Pennock *et al.,* (2008).

3.1. Field Methods

3.1.1. Automated Logging Stations

A setup of the automated logging system is shown in the following schematic diagram (Fig. 9). The ground temperature was and continues to be, measured by loggers which have thermistors (sensors) attached to a rod placed below the surface, in order to record temperatures at different depths. The sensors were placed at 1 cm below the surface for both the PACE XR5 and the ACR data loggers, and at 15 cm intervals up to 60 cm for the PACE XR5 data logger, and at 5 cm intervals up to 20 cm for the ACR data logger. The PACE XR5 data loggers at Troll Station recorded data at 50 cm intervals up to 2 m. Soil moisture was measured at a depth of 1 cm below the surface of the ground by a Decagon EC-5 soil moisture sensor, which was also attached to the PACE XR5 data logger. The air temperature was measured at 1 m above the ground by a sensor protected by a radiation shield. The loggers were set to record temperature in degrees Celsius (˚C).

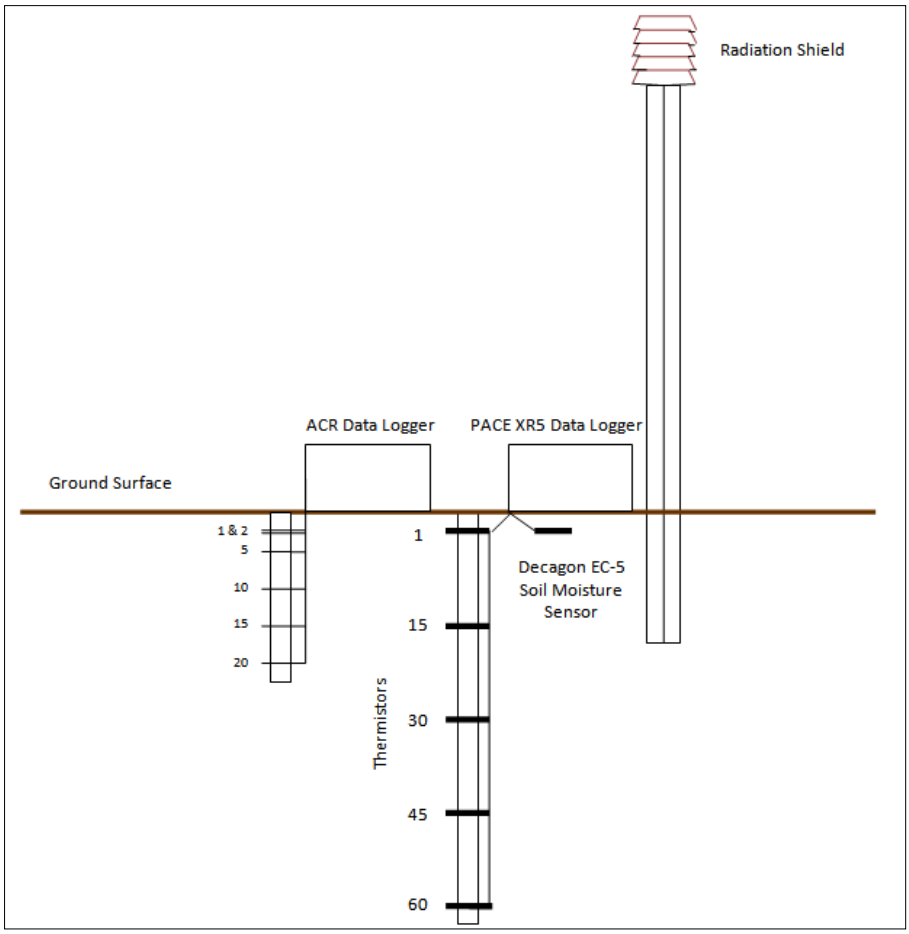

Figure 9. A setup of the automated data logging system (Adapted from Meiklejohn, 2012)

The automated logging stations (ALS's) were installed at various sites around the Ahlmannryggen and Troll Station following the International Polar Year in 2007, with the aim of contributing to the understanding of Antarctic permafrost and the active layer (Vieira *et al.,* 2010). A period of two weeks was allowed to pass after the installation so that the ground around the ALS's could settle before logging could begin. Care was taken when installing the ALS's, and the ground promptly covered, to restore sites to the way they were before being disturbed, thus ensuring that the ALS's recorded the proper conditions of the selected sites (Kotzé, 2015).

3.1.2. Soil Sampling Techniques

Soil sampling at the selected sites was undertaken using a method of judgement sampling (Pennock *et al.,* 2008). According to Pennock *et al*., (2008) judgement sampling is appropriate when soil clearly shows an identified sequence of processes that may have contributed to the soil landscape. In this study, sampling was done as close to the ALS's as possible, to obtain the best possible representation of the soil/ground being monitored for changes in temperature and moisture levels. Given that soils in the selected study sites are poorly developed, there were no clear soil horizons. The soils are classified as gelisols because they have little profile development due to the presence of permafrost (Weil and Brady, 2017). For this reason, only the topsoil was sampled. In order to leave the sites as undisturbed as possible, and in compliance with the Antarctic Treaty and the Rhodes University Ethical Standards, sampling was executed cautiously. The holes left after sampling were promptly covered with surrounding soil, and this also ensured that the ALS's were not disturbed.

3.2. Laboratory Methods

The physical properties of the soil were analysed by calculating the bulk density of each sample, followed by measuring the particle size of soil from each sample. Soil bulk density is defined by Briggs (1977b) as the ratio of the mass of dry soil to its volume. The volume of the soil was calculated from the dimensions of the bulk density square, according to Equation 2:

Equation 2: Volume

$$V = lbh$$

where *l* stands for the length (in cm), *b* the breadth (in cm) and *h* the height (in cm) of the bulk density square.

Bulk density was calculated following Equation 3, highlighted by Hao *et al.,* (2008):

Equation 3: Soil Bulk Density

$$D_b = \frac{m_s}{V_t}$$

where D_b represents soil bulk density (in g/cm^3), m_s represents the mass (in g) of the oven-dried soil and V_t represents the bulk volume (in cm^3) of the soil, including the pore spaces between the soil particles along with the volume of the soil itself (Hao *et al.,* 2008).

Soil samples were weighed before and after drying in order to determine the moisture content within the soils. They were dried in a ProLab oven for 24 hours at 105 ˚C, as advised by Hao *et al.,* (2008). After drying, soils were placed in desiccators overnight to cool down before being weighed again. Thereafter, the samples were disaggregated using a mortar and pestle, following which they were sieved using the Endecott test sieve stack shaker for 10 minutes. The sieves were measured before and after sieving in order to get the mass proportion of the sample in each sediment class size. Thereafter, particles that were less than 1000 µm in diameter were treated with 25 ml of hydrogen peroxide (30%) to remove organic material. Samples were left overnight at room temperature before being heated to allow the hydrogen peroxide to evaporate. This was so that analysis on the Malvern Mastersizer 3000 could be performed on the samples to get a measure of the particles < 63 µm.

The Malvern Mastersizer 3000 utilises Stokes' Law which states that the rate at which a particle falls in a viscous medium (liquid) is directly proportional to its weight (measured from its diameter), *i.e.* the heavier the particle, the faster it falls (Briggs, 1997b). The equation for Stokes' Law is given by Equation 4 (Briggs, 1997b):

Equation 4: Stokes' Law

$$D^2 = \frac{18\,\nu\eta}{(\rho - \rho 0)\boldsymbol{g}}$$

where D is the size of the particle (cm), v is the terminal velocity of the particle (cm/s), η is the viscosity of the liquid, ρ is the density of the particle (g/cm^3), ρ0 is the density of the liquid (g/cm^3) and g is the gravity (cm/s^2).

3.3. Statistical Analysis and Preparation

The first law of geography states that "everything is related to everything else, but near things are more related than distant things" (Tobler, 1970: 236). Tobler's first law of geography is related to the concept of spatial autocorrelation that identifies a connection in data values of spatial measurements (Harris and Jarvis, 2011). Spatial autocorrelation allows for geographical statistical methods to be employed to spatial data analysis. These geographical statistical methods (spatial regression) along with non-geographical, classical forms of statistical analysis (non-spatial regression) were used in analysing the data and interpreting the results generated thereof.

3.3.1. Data Preparation

Prior to analysis, raw field data were captured in Microsoft Excel® for standardization. Standardization was done first by calculating the standard deviations and population means of the data sets. This was done for the calculation of z-values that allow for a data set to be standardized by removing outliers. A z-value is a measure of standard deviation from the population mean and it allows for comparison between data sets whose standard deviations and population means are different (Harris and Jarvis, 2011). It is calculated using the following equation (Harris and Jarvis, 2011):

Equation 5: z-value

$$z = \frac{(x - \mu)}{\sigma}$$

where x represents the value to be standardised, μ represents the population mean and, σ represents the standard deviation. Values greater than 3.5 and less than -3.5 of the z-value were deemed as outliers and therefore removed from the dataset.

3.3.2. Statistical Methods

Statistics allow a data set to be analysed in a descriptive manner, providing a set of summarised measurements of the data that allow for more analysis to be conducted (Harris and Jarvis, 2011). Descriptive statistics are usually the first form of analysis to be performed on a data set following which inferential and relational statistical analysis is conducted. Inferential statistics examine the representativeness of the data set by testing the probability of some data element being true (Harris and Jarvis, 2011). Relational statistics allow for relationships in the variations of data sets to be determined (Harris and Jarvis, 2011). The only statistics used for this project were descriptive and relational statistics and their usage is outlined in the following sections.

3.3.2.1. Descriptive Statistics

Descriptive statistics are centred on two measurements – the average (mean) of the data set and the behaviour of data values around the mean (Harris and Jarvis, 2011). A measurement of summary statistics was calculated to enable the computation of z-values. Amongst other things, summary statistics gave measurements for the mean, the median, the mode, standard deviation, and skewness of the meteorological point data sets for Objectives 1 and 2. The mean, standard deviation and skewness were particularly important for the calculation of z-values. For the z-value equation, refer to Equation 5. The skewness of a data set is important because z-values can only be calculated if the data set has a normal distribution. A normal distribution is given by a skewness value of 0, whereas a skewness value of -1.62 means that the data set is negatively skewed to the left while a skewness value of 1.62 means that the data set is positively skewed to the right (Hansen, 2013). For a full list of skewness values and their descriptions, please refer to Appendix A (pg. 85).

For Objective 1, summary statistics were calculated for data from the ALS measured at Vesleskarvet along with data from SAWS. In addition, monthly averages of the SAWS data set were also calculated. For Objective 2, summary statistics were calculated for daily average temperatures from all the study sites.

3.3.2.2. Relational Statistics

Relational statistics were used to determine the dependency of a set of variables on other variables, for instance, how the bulk density of soil affects the rate of thermal propagation through the ground profile. The statistical tools used were scatter plots and correlation coefficients using the Pearson's product-moment correlation (*r*). A scatter plot is a tool used to determine the relationship between two variables (Harris and Jarvis, 2011). It operates under the assumption that one variable (the X variable plotted on the horizontal axis) is independent of the other variable (the dependent Y variable plotted on the vertical axis) (Harris and Jarvis, 2011).

Pearson's correlation coefficient, *r*, gives a measure of the linear relationship of two variables, assuming that both variables are approximately normal (Harris and Jarvis, 2011). In order to calculate Pearson's correlation coefficient, the mean and standard deviation of each variable are used. A positive relationship is given by positive values, with +1 indicating a perfect positive relationship. On the other hand, a negative relationship is given by negative values, with -1 indicating a perfect negative relationship. Variables that are unrelated are shown by a value of zero (Harris and Jarvis, 2011).

For Objective 1, Pearson's correlation coefficient was used to find a correlation between monthly averages of Vesleskarvet ambient air temperatures, near-surface temperatures and ground temperatures with the SAWS recorded meteorological data. For Objective 2, Pearson's correlation coefficient was used to find a correlation between the SAWS average air temperature with the average ambient air and ground temperatures of all the study sites. For Objective 3, a scatter plot was used to determine the distribution of particle sizes for soils at each study site.

Both the descriptive and the relational statistical methods along with the laboratory methods effectively allow for the analysis and presentation of the collected data. The following section gives an analysis of the results based on the outlined methods described in this section.

Chapter 4: Findings – Analysis of Results

4.1. Objective 1: Influences on temperatures in Vesleskarvet

As discussed earlier in the literature review meteorological phenomena including air temperature, pressure, wind and solar radiation have been noted in various studies to have an impact on ground thermal regimes (Williams and Smith, 1989; Richter and Bormann, 1995). Meteorological data from the South African Weather Service (SAWS) were used to aid the correlation analysis of weather variables with ambient air temperatures from the data logging site and ground temperatures. The weather parameter most influential on ground thermal regimes in Vesleskarvet in 2016 was air temperature, followed by pressure and humidity (see Table 1). Wind speed and wind direction had no influence on ambient and ground temperatures. The influence of solar radiation on ground temperature could not be analysed due to the absence of solar radiation data. Kotzé (2015) provides an in-depth coverage of the effects of solar radiation in Vesleskarvet.

Table 1. Pearson's Correlations (r) for Vesleskarvet 2016 monthly averages of ambient air temperature, near-surface and ground temperature with the SAWS recorded air temperature, pressure, humidity, wind speed and wind direction

SAWS Meteorological Data / ***Temperature Averages***	**Temperature**	**Pressure**	**Humidity**	**Wind Speed**	**Wind Direction**
Ambient Air	0.971	0.190	0.074	-0.089	-0.024
Near-Surface	0.798	0.186	0.211	-0.071	-0.190
15 cm	0.845	0.192	0.161	-0.140	-0.104
30 cm	0.718	0.188	0.145	-0.175	-0.084
60 cm	0.462	0.157	0.062	-0.218	-0.021

Monthly correlations of air temperatures against ground temperatures of different depths throughout the ground profile show that air temperatures have a high positive relationship with ambient and ground temperatures, the highest correlation being with ambient temperatures (average r = 0.971) and the lowest being at a 60 cm depth (average r = 0.462) (see Table 1). A very high correlation of air temperatures with ambient temperatures is not surprising because the SAWS weather station is only +/- 300 m away from the logging site. However, it is intriguing that the correlation between air and ground temperature (near surface temperature) is lower (average r = 0.798) than that between air temperature and temperature at a depth of 15 cm (average r = 0.845).

Pressure had a moderately high and strong positive correlation with ambient air and ground temperatures during the months of January ($r > 0.7$), August ($r > 0.4$), September ($r > 0.4$) and December ($r > 0.5$) (see Appendix B, pg. 87). On the other hand, humidity levels had a weak to moderate positive correlation with ambient air and ground temperatures in February ($r > 0.4$) (excluding ambient air temperatures), April ($r > 0.4$), June ($r > 0.5$) (excluding ambient air temperatures) and August ($r > 0.4$) (excluding 30 cm and 60 cm depths) (see Appendix B, pg. 87). Although it has been noted in literature that wind (speed and direction) can have an influence on ground temperatures (Seppälä, 2004; Adlam *et al.,* 2010; Hansen, 2013), in Vesleskarvet it has been found to have mostly weak negative, to almost no, correlation with ambient air and ground temperatures throughout the year. However, there was a weak positive relationship between wind speed and ambient air and ground temperatures in May ($r > 0.4$ for ambient air temperature, near-surface temperature and temperature at 15 cm depth) (see Appendix B, pg. 87).

The SAWS recorded monthly averages of pressure and wind speed (see Table 2) show varying relationships with ground temperatures in the different months. For instance, the high positive correlations of pressure with ground temperatures during the months of January, August, September and December correspond to the monthly averages of 881.38 hPa, 882.16 hPa, 875.21 hPa, and 891.62 hPa respectively. During these months, near-surface (ground) temperatures corresponded positively to the average pressure values (see Figure 10). Conversely, the negative correlations of wind speed with ground temperatures can also be seen from Table 2 and Figure 10. The highest correlations between wind speed and ground temperatures were during January, May, November and December. The average wind speeds during these months were 8.53 m/s, 13.72 m/s, 9.34 m/s and 5.84 m/s. During these months, ground temperatures corresponded negatively to the average wind speed values, indicating an inversely proportional relationship between wind speeds and ground temperatures.

Table 2. Monthly averages of SAWS meteorological parameters

	Temperature (°C)	*Pressure (hPa)*	*Humidity (%)*	*Wind Speed (m/s)*	*Wind Direction (°)*
Jan	-8.19	881.38	68.22	8.53	100.51
Feb	-10.02	881.65	69.65	10.11	106.54
Mar	-13.46	875.21	70.55	12.00	101.94
Apr	-16.31	879.69	71.18	12.02	107.88
May	-18.71	875.71	78.60	13.72	97.08
Jun	-25.65	874.66	58.37	11.43	115.05
Jul	-24.59	876.60	61.21	12.12	107.37
Aug	-20.81	882.16	66.02	11.84	101.04
Sep	-22.58	875.21	65.38	11.34	103.84
Oct	-16.97	873.95	67.07	11.64	100.84
Nov	-11.77	889.66	65.19	9.34	103.69
Dec	-6.20	891.62	59.03	5.84	104.59

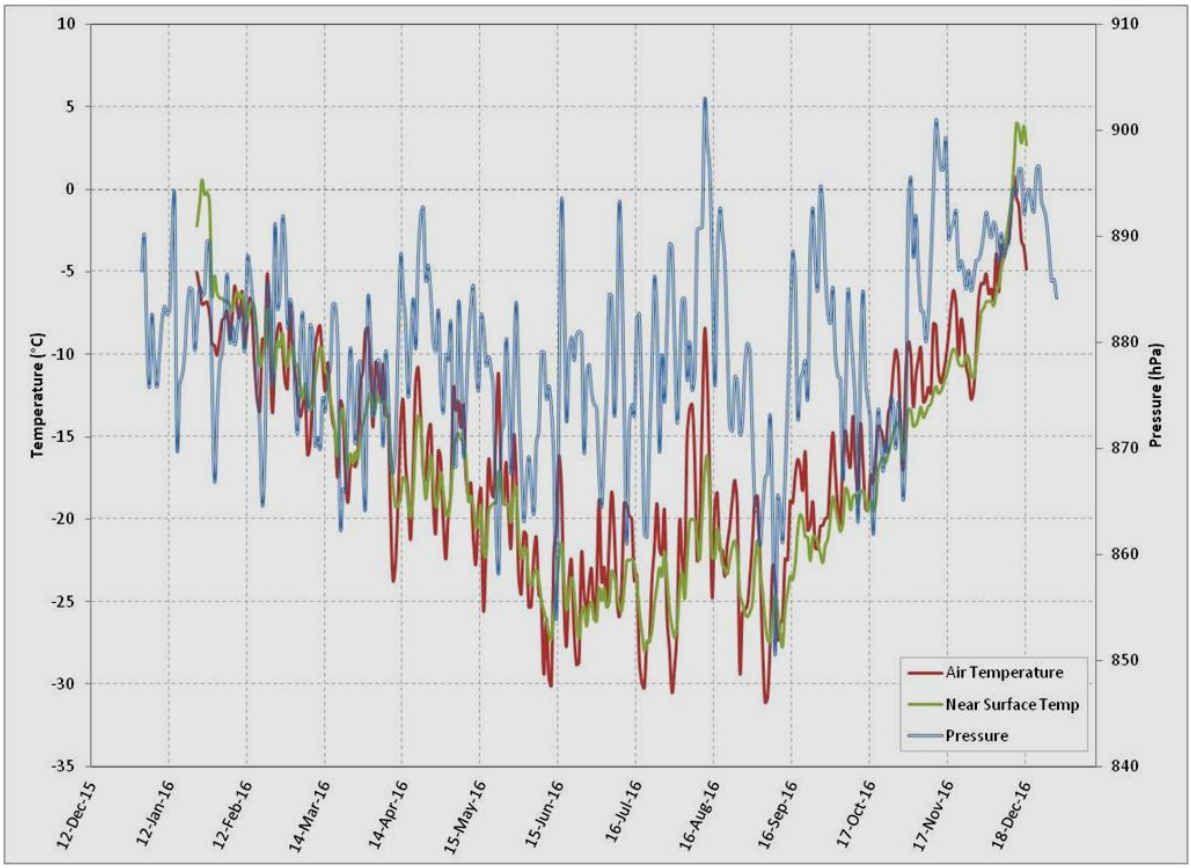

Figure 10. Average ambient air and ground temperature and pressure at Vesleskarvet in 2016

A comparison between seasonal and selected synoptic and diurnal events, as shown in Table 3, shows that the highest recorded average temperature was during the synoptic event in August (-10.42 °C), while the lowest was during the synoptic and diurnal event in June (-27.89 °C). For the selected synoptic and diurnal events, please refer to Section 4.3.3. (pg. 55). The low average temperature in June is synchronous with the low average temperatures recorded in winter. However, the high average temperature in August appears to be anomolous with its season and the following season. On the other hand, the high variance and range of temperatures in spring and winter correspond positively with the high variance of the synoptic and diurnal events of August and June. The same phenomenon is seen between November and summer. Although November has been designated as part of spring, the statistics were recorded at the end of the month, which could qualify as the beginning of summer, given that the divisions of the seasons have been designated arbitrarily for the purposes of this analysis, based on Kotzé (2015).

Table 3. Summary statistics for Temperature for 2016

	Average	*Sample Variance*	*Range*	*Minimum*	*Maximum*
All Year	-16.32	51.12	40.50	-35.70	4.80
June	-27.89	8.75	10.00	-32.20	-22.20
August	-10.42	9.48	10.50	-14.80	-4.30
November	-13.35	2.26	7.60	-17.10	-9.50
Summer (DJF)	-9.09	7.73	18.50	-17.70	0.80
Autumn (MAM)	-16.16	20.74	24.50	-28.50	-4.00
Winter (JJA)	-23.63	23.95	31.40	-35.70	-4.30
Spring (SON)	-17.10	30.81	29.70	-33.70	-4.00

The highest recorded pressure from the selected events, as presented in Table 4, was during an August synoptic event (901.6 hPa), while the lowest (866.1 hPa) was during a June synoptic and diurnal event. Conversely, the highest recorded seasonal pressure (905 hPa) was in winter and the lowest was in spring. Although the difference between the seasonal average pressures is minimal, the variability of pressure differs greatly between seasons.

For instance (see Table 4 and Figure 10), the average pressure in spring (119.26 hPa) is more variable than in all the other seasons throughout the year, while summer has the lowest variability of average pressure (37.63 hPa). In addition, the range of the average pressure in spring was higher than all the other seasons throughout the year, with a minimum pressure of 840.9 hPa and a maximum pressure of 902hPa, while that of summer is the lowest with a minimum pressure of 862 hPa and a maximum of 895.3 hPa).

Table 4. Summary statistics for Pressure for 2016

	Average	*Sample Variance*	*Range*	*Minimum*	*Maximum*
All Year	879.74	85.35	64.10	840.90	905.00
June	870.69	4.72	8.00	866.10	874.10
August	899.22	1.95	5.20	896.40	901.60
November	886.03	2.13	5.80	883.20	889.00
Summer (DJF)	881.51	37.63	33.30	862.00	895.30
Autumn (MAM)	876.84	49.57	43.40	853.10	896.50
Winter (JJA)	877.88	82.97	53.60	851.40	905.00
Spring (SON)	879.55	119.26	61.10	840.90	902.00

The average humidity levels recorded for 2016 (Table 5) show that autumn had the highest average humidity level (73.47 %), while winter, the season directly after autumn, had the lowest average humidity level (61.95 %). These correlate with average pressure values that seem to be inversely proportional to humidity levels of the corresponding seasons. However, an analysis of selected events shows that the highest recorded humidity level was in August (93.50 %) while the lowest was in June at 24.30 %.

Additionally, throughout the seasons, humidity levels were highly variable, with summer presenting maximum variability and winter presenting minimum variability. The highest range of humidity levels was in summer with a minimum humidity level of 11.60 % and a maximum of 92.70%. On the other hand, the lowest range of humidity levels was in spring with a minimum humidity level of 21.50 % and a maximum of 89.20 %. Interestingly, summer displayed the lowest minimum humidity level, while spring showed the highest minimum humidity level. However, winter had the highest maximum humidity level while spring had the lowest minimum humidity level.

Table 5. Summary statistics for Relative Humidity for 2016

	Average	*Sample Variance*	*Range*	*Minimum*	*Maximum*
All Year	66.76	282.78	82.30	11.60	93.90
June	40.17	125.02	32.30	24.30	56.60
August	75.15	174.49	48.30	45.20	93.50
November	72.53	71.61	35.90	48.50	84.40
Summer (DJF)	68.91	310.15	81.10	11.60	92.70
Autumn (MAM)	73.47	289.91	80.10	12.20	92.30
Winter (JJA)	61.95	221.23	73.60	20.30	93.90
Spring (SON)	65.88	233.12	67.70	21.50	89.20

The variability of ambient air and ground temperatures differs throughout the year. In comparison, near surface temperatures are more variable than air temperatures as well as more variable than temperatures at the 15 cm depth, as can be seen from the range and variance values in Table 6. The variability diminishes with increasing depth. However, detailed analysis of seasonal average temperature shows that the variability of air and ground (near surface) temperatures changes and alternates between seasons (see Table 7). Both ambient air and ground temperatures are highly variable in spring. However, ambient air temperatures are less variable in summer while ground temperatures are less variable in winter.

Table 6. Summary statistics of logging station variables at Vesleskarvet

	Air (1m)	*Near Surface*	*15cm*	*30cm*	*45cm*	*60cm*
Mean	-15.91	-16.58	-16.07	-16.23	-16.02	-16.18
Standard Error	0.03	0.03	0.03	0.03	0.03	0.02
Median	-16.25	-18.16	-17.33	-17.55	-17.50	-17.50
Mode	-21.18	-25.50	-21.18	-21.18	-21.18	-20.99
Standard Deviation	7.35	7.55	6.92	6.62	6.24	5.91
Sample Variance	54.03	56.96	47.91	43.84	38.91	34.99
Kurtosis	-0.60	0.39	-0.86	-0.95	-0.98	-0.99
Skewness	0.08	0.78	0.34	0.35	0.39	0.39
Range	47.55	51.98	34.38	31.75	27.52	25.50
Minimum	-40.78	-31.85	-33.96	-31.98	-29.64	-28.56
Maximum	6.77	20.13	0.42	-0.23	-2.12	-3.06
Confidence Level (95.0%)	0.06	0.06	0.05	0.05	0.05	0.04

Table 7. Summary statistics of ambient air and ground seasonal temperatures (°C)

	Summer		*Autumn*		*Winter*		*Spring*	
	Air	NS	Air	NS	Air	NS	Air	NS
Mean	-8.28	-6.29	-15.64	-16.06	-22.66	-23.89	-13.80	-17.57
Sample Variance	9.85	17.22	19.44	10.62	23.20	5.36	51.93	26.72
Range	17.36	23.38	21.8	16.1	28.85	13.3	36.98	24.36
Minimum	-16.67	-13.31	-27.88	-23.24	-33.59	-28.43	-32.39	-28.52
Maximum	0.69	10.07	-6.08	-7.14	-4.74	-15.13	4.59	-4.16

A comparison between summer and winter average temperatures, displayed in Table 7, shows that the maximum near-surface temperatures in summer were higher than the maximum ambient air temperature (10.07 °C and 0.69 °C, respectively). In addition, ambient air temperature recorded the lowest minimum temperature through all seasons. Although minimum near-surface temperatures (-13.31 °C) were higher than the minimum ambient air temperatures (-16.67 °C), summer near-surface temperatures nonetheless had the widest range and were highly variable. In contrast, ambient air temperatures were more variable in winter than near-surface temperatures because they recorded both the highest maximum and lowest minimum temperatures, giving a wide range between the maximum and minimum temperatures.

4.2. Objective 2: Regionality of Ground Thermal Regimes

Objective 2 expands from the first objective in that it considers the regionality/spatiality and synchronicity of ground temperatures using Vesleskarvet as the main site of reference. Air temperature recorded by the weather station in Vesleskarvet was used to analyse the spatial effects of weather influences over a wider region. Of the sites studied, the SAWS recorded average air temperature had the highest correlation with the Schumarcherfjellet average air temperatures (r = 0.990) as presented in Table 8. The correlation magnitude diminished with increasing depth across all sites. Paradoxically, Vesleskarvet had the lowest overall air and ground temperature correlations with air temperature from the weather station, albeit being the reference site. Additionally, while temperature correlations decrease with increasing depths with other sites, Vesleskarvet temperature correlations are irregular. Of great interest is that Troll, even though it is the furthest site from Vesleskarvet in addition to having a deeper borehole (up to 2m), displayed a positive correlation with air and ground temperatures.

Table 8. Pearson's Correlations (r) of the SAWS average air temperature with average ambient air and ground temperatures of all sites for 2016

	Air	Near Surface	15 cm	30 cm	45 cm	60 cm
Vesleskarvet	0.620	0.727	0.715	0.747		0.793
Robertskollen	0.987	0.954	0.933	0.905	0.882	0.869
Valterkulten	0.929	0.914	0.897	0.874	0.862	0.851
Grunehogna	0.984	0.942	0.925	0.916	0.900	0.884
Schumarcherfjellet	0.990	0.984	0.960	0.935	0.916	0.901
Flårjuven	0.984	0.941	0.929	0.911	0.895	0.882
Slettfjell	0.967	0.948	0.875	0.821	0.794	0.774
Troll	0.954	0.927	0.865	0.819	0.763	0.693
Troll Ground Depth			**50 cm**	**100 cm**	**150 cm**	**200 cm**

Daily average temperatures for Vesleskarvet display a highly variable thermal ground near the surface in comparison to the air above the ground and ground at deeper levels. The high variability of the near surface daily average temperatures is confirmed by the large range of temperatures with the minimum average temperature registering -27.98 °C while the maximum average temperature registers 3.98 °C (see Table 9). In fact, the variability of air temperatures, ground temperatures and temperatures down the ground profile correlate perfectly with their temperature ranges with ground temperatures presenting the largest range of daily average temperatures and 60 cm below the ground presenting the lowest range as well as the lowest variability of daily average temperatures. The lowest average temperature was recorded near the ground surface at -16.85 °C while average air temperatures yielded the highest average temperature at -16.17 °C.

Table 9. Vesleskarvet: summary statistics of daily average temperatures for 2016

	Air (1m)	Near Surface	15cm	30cm	60cm
Mean	-16.17	-16.85	-16.39	-16.56	-16.55
Sample Variance	46.56	50.76	42.64	37.46	30.14
Range	31.88	31.96	27.71	24.71	20.50
Minimum	-31.07	-27.98	-28.13	-26.78	-24.97
Maximum	0.82	3.98	-0.42	-2.07	-4.46

In contrast to Vesleskarvet, Robertskollen registered a lower average air temperature compared to ground temperatures, albeit higher average temperatures throughout the ground profile and the air above the ground (see Table 10). Furthermore, average temperatures at the 15 cm depth (-12.97 °C) were lower than near-surface average temperatures (-12.83 °C) while 30 cm deep average temperatures were equal to near surface average temperatures.

Similarly to Vesleskarvet, Robertskollen presents highly variable average near-surface temperatures in comparison to average air temperatures, with a diminishing variability with increasing depth although it displays a different active layer thermal regime. However, in contrast to Vesleskarvet, temperatures at 15 cm below the ground are more variable than air temperatures. This corresponds to the range of the average temperatures as well with average near surface temperatures displaying a minimum of -26.97 °C and a maximum of 4.53 °C while average air temperatures range from a minimum of -28.59 °C to a maximum of 1.25 °C.

Table 10. Robertskollen: summary statistics of daily average temperatures for 2016

	Air (1m)	Near Surface	15cm	30cm	45cm	60cm
Mean	-13.51	-12.83	-12.97	-12.83	-12.76	-12.74
Sample Variance	49.23	85.40	65.43	55.60	49.30	45.75
Range	29.84	38.99	31.50	26.42	23.54	22.01
Minimum	-28.59	-30.33	-26.97	-24.38	-23.24	-22.61
Maximum	1.25	8.66	4.53	2.04	0.30	-0.60

Valterkulten presents average temperatures that are different from both Vesleskarvet and Robertskollen as presented in Table 11. Average air temperatures (-16.41 °C) are lower the average ground temperatures (>-15 °C). Additionally, average temperatures increase with an increasing depth, dropping at 60 cm below the ground. However, similarities between Valterkulten and Vesleskarvet lie in the variability of the average temperatures. Average near surface temperatures are more variable than air temperatures with a higher average maximum temperature recorded at 8.05 °C and a lower average minimum temperature at -33.14 °C giving the largest range of temperatures compared to the air and deeper ground temperatures.

Table 11. Valterkulten: summary statistics of daily average temperatures for 2016

	Air (1m)	Near Surface	15cm	30cm	45cm	60cm
Mean	-16.41	-15.29	-15.25	-15.20	-15.13	-15.19
Sample Variance	50.03	86.57	71.26	56.28	49.13	43.93
Range	32.73	41.19	32.83	26.17	23.25	21.45
Minimum	-32.25	-33.14	-29.21	-26.68	-25.32	-24.77
Maximum	0.48	8.05	3.62	-0.51	-2.07	-3.32

Grunehogna, as presented in Table 12, recorded the lowest average minimum near surface temperatures and as will be seen later, the lowest average near-surface temperature throughout all the sites. However, it recorded the highest average maximum temperature (5.97 °C), significantly overshadowing average maximum air and ground temperatures that were mostly below 0 °C for most of the year.

Additionally, average near-surface temperatures (-33.80 °C) recorded the lowest average minimum temperature after average air temperatures (-34.80 °C). Nevertheless, average near-surface temperatures were the most variable and had the largest temperature range in comparison with average air and ground temperatures similarly to the previously discussed sites. Additionally, near surface average temperatures were higher than both air and ground temperatures at -18.07 °C.

Table 12. Grunehogna: summary statistics of daily average temperatures for 2016

	Air (1m)	Near Surface	15cm	30cm	45cm	60cm
Mean	-18.78	-18.07	-18.32	-18.44	-18.38	-18.45
Sample Variance	51.58	86.91	65.70	58.70	51.46	45.65
Range	33.04	39.77	30.36	27.75	24.65	22.58
Minimum	-34.80	-33.80	-30.46	-29.73	-28.46	-27.84
Maximum	-1.76	5.97	-0.10	-1.98	-3.81	-5.26

Average near-surface temperatures in Schumarcherfjellet, in the same way as Vesleskarvet and the other sites, are more variable and have the largest range of temperatures than air and ground temperatures, with a minimum of -32.19 °C and a maximum of 2.96 °C (see Table 13). Additionally, the degree of the fluctuation is in the same magnitude as Vesleskarvet (sample variance > 50). Average ground temperatures are considerably higher than average air and near surface temperatures. The average temperature trend appears to be increasing from the air above the ground right to 30 cm below the ground before it decreases, noted by -15.86 °C at a depth of 45 cm below the ground.

Table 13. Schumarcherfjellet: summary statistics of daily average temperatures for 2016

	Air (1m)	Near Surface	15cm	30cm	45cm	60cm
Mean	-16.29	-16.27	-15.97	-15.83	-15.86	-15.92
Sample Variance	44.70	55.34	52.09	49.28	46.55	44.15
Range	31.95	35.15	29.26	26.60	24.67	22.99
Minimum	-32.81	-32.19	-29.28	-27.83	-26.99	-26.25
Maximum	-0.87	2.96	-0.03	-1.23	-2.32	-3.26

Flårjuven, as displayed in Table 14, recorded average near-surface temperatures that were more variable than average air temperatures (almost twice the variability). Furthermore, air temperatures are less variable than near surface and ground temperatures except for the 60 cm depth. However, they (air temperatures) had a higher range of temperatures than ground temperatures after near surface temperatures. Near surface temperatures had the highest range with a minimum of -32.58 °C and a maximum of 6.05 °C. Unlike Vesleskarvet and other sites already discussed, near surface average temperatures were higher than both air and ground temperatures at -17.14 °C with temperatures decreasing steadily from near the surface down through the ground profile.

Table 14. Flårjuven: summary statistics of daily average temperatures for 2016

	Air (1m)	Near Surface	15cm	30cm	45cm	60cm
Mean	-18.21	-17.14	-17.29	-17.33	-17.36	-17.44
Sample Variance	49.88	82.89	64.32	56.57	51.33	46.97
Range	32.70	38.63	30.39	26.49	24.04	22.29
Minimum	-34.64	-32.58	-29.83	-28.43	-27.48	-26.90
Maximum	-1.94	6.05	0.57	-1.94	-3.43	-4.61

Slettfjell, even though is the site furthest south of Vesleskarvet, still shares the same characteristics as Vesleskarvet and the other sites. It has averaged near-surface temperatures that are more variable than average air and ground temperatures (see Table 15). Its average temperatures increase from the air above the ground right through to 45 cm below the ground before they start to decrease from 60 cm below the ground.

Unlike all the other sites, Slettfjell recorded average maximum temperatures that were well below 0 °C, with average maximum temperatures near the surface being the highest. However, it is worth mentioning that temperature data logging for Slettfjell continued until 01 May. Therefore, the lack of a full year temperature record means that analysis of the active layer thermal regimes yields inconclusive results in comparison to the other sites.

Table 15. Slettfjell: summary statistics of daily average temperatures for 2016

	Air (1m)	Near Surface	15cm	30cm	45cm	60cm
Mean	-15.77	-15.52	-14.91	-14.61	-14.49	-14.53
Sample Variance	23.32	27.86	22.55	20.76	18.97	16.51
Range	21.90	24.61	19.09	16.73	15.11	13.98
Minimum	-29.29	-27.85	-23.85	-22.35	-21.59	-21.37
Maximum	-7.39	-3.23	-4.76	-5.62	-6.48	-7.39

Troll, similar to Flårjuven, has a higher near-surface average temperature (-16.30 °C) with average air and ground temperatures displaying a decreasing trend with the exception of near-surface average temperatures (see Table 16). In the same way as all the other sites, Troll has a significantly highly variable near surface average temperatures. The variability of temperatures decreases with increasing depth from near the ground surface.

However, air temperatures have the highest range with the minimum being -39.05 °C and the maximum being -1.05 °C. On the other hand, the range of temperatures decreases from the ground surface right through the ground profile with near surface temperatures ranging from a minimum of -33 °C to a maximum of 1.97 °C which is the highest maximum temperature in comparison with air

and ground temperatures. Despite being across the Jutulstraumen glacier, average temperatures are of the same magnitude as those at Vesleskarvet (T > -16 °C for both sites).

Table 16. Troll: summary statistics of daily average temperatures for 2016

	Air (1m)	Near Surface	50cm	100cm	150cm	200cm
Mean	-16.62	-16.30	-16.59	-16.64	-16.81	-17.02
Sample Variance	84.31	107.12	63.25	46.39	34.18	25.30
Range	38.00	34.97	24.55	20.45	16.84	14.02
Minimum	-39.05	-33.00	-28.85	-26.90	-25.28	-23.95
Maximum	-1.05	1.97	-4.30	-6.45	-8.44	-9.93

The regionality and synchronicity of temperatures in Western Dronning Maud Land (WDML), from Robertskollen to Slettfjell and across the province to Troll, can better be represented graphically as shown in Figures 11 – 16. The high synchronicity between average air temperatures recorded by the weather station at Vesleskarvet and Schumarchefjellet average air temperatures is clearly visible in Figure 11.

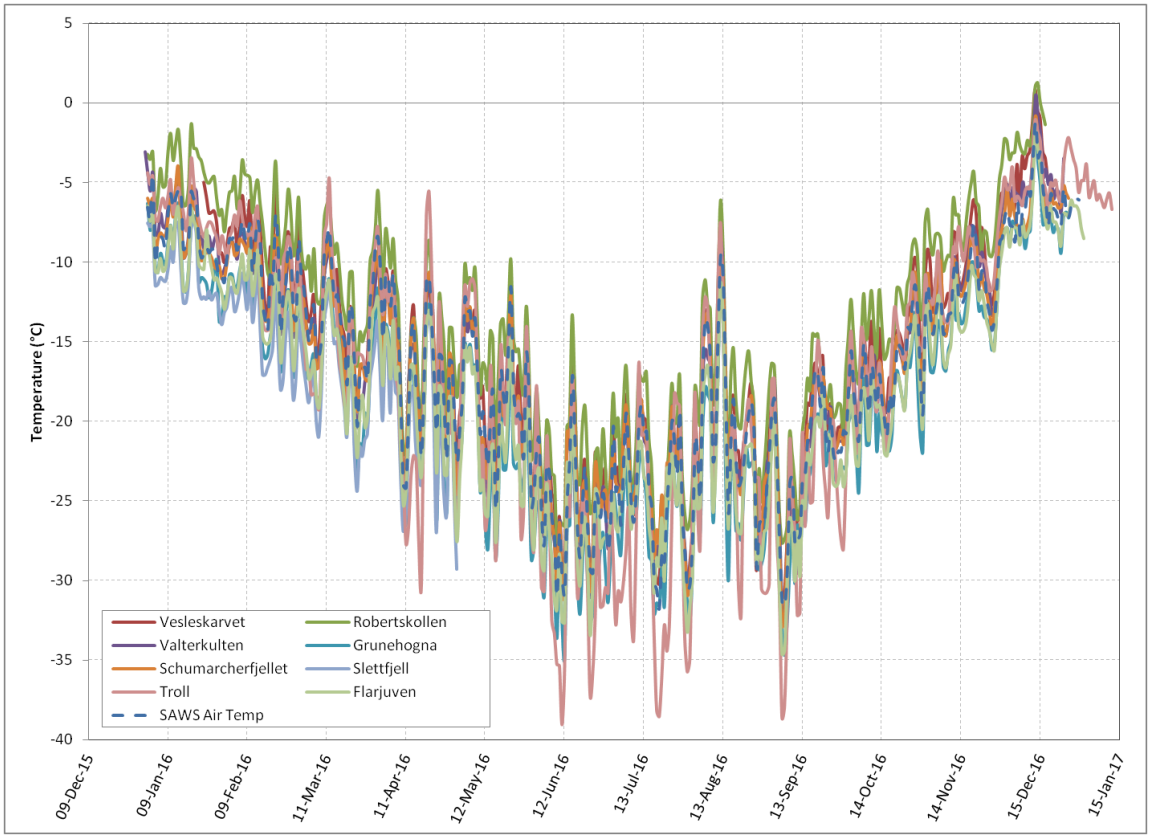

Figure 11. Daily average SAWS air and ambient air temperatures

With exceptions of specific events, the highest average air temperatures throughout the year were recorded at Robertskollen. On the other hand, the lowest average air temperatures varied between

sites with Slettfjell, Grunehogna and Flårjuven dominating during the summer months, while Troll dominated during the winter months. The range of air temperatures between the sites also differs with changing seasons. During the summer months, the range of air temperatures between the sites is minimal. It starts to increase during the autumn months, reaching a maximum during the winter months before it decreases again during the spring months before reaching a minimum again in summer.

In comparison to average air temperatures, the range of near-surface average temperatures between sites is minimal as shown in Figure 12. However, unlike air temperatures, average near-surface temperatures exhibit a large range of inter-site temperatures during summer months. This large range of temperatures shows a diminishing effect around late autumn when temperatures decrease as winter conditions start to dominate. Towards the end of spring, the range in temperatures starts to widen again as summer conditions start to dominate.

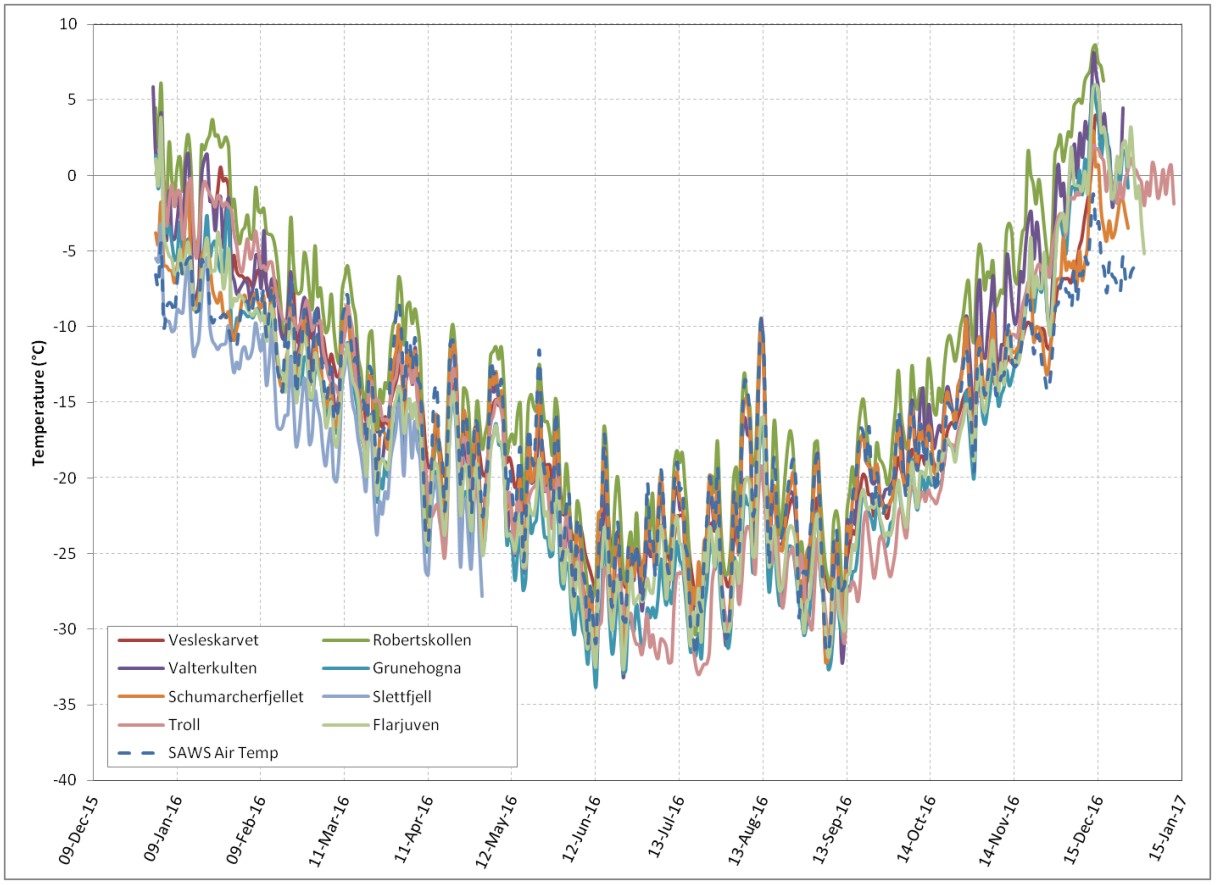

Figure 12. Daily average SAWS air and near-surface temperatures

Once more, Robertskollen average temperatures are the highest throughout the year. Valterkulten has the second highest average near-surface temperatures as can be seen in Figure 12. Conversely, Slettfjell has the lowest average near-surface temperatures during the summer months along with

Schumarcherfjellet. During winter months, Grunehogna and Flårjuven display the lowest average temperatures with Troll occasionally displaying the lowest averages during specific synoptic events. Similar to average air temperatures, Schumarcherfjellet shows a high synchronicity with the SAWS recorded average air temperature. However, this synchronicity varies with seasons, with winter showing the greatest synchronicity while summer presents the lowest synchronicity.

On average, temperatures below the ground exhibit similar patterns as shown by Figures 13 – 16. Additionally, these patterns are similar to trends shown by the near surface average temperature graph (see Figure 12). Robertskollen has the highest average ground temperatures throughout the year. On the other hand, Valterkulten average ground temperatures dominate after Robertskollen during summer months while Vesleskarvet average ground temperatures dominate during the diurnal events in autumn and spring and Schumarcherfjellet average ground temperatures dominate during the winter months.

The range of inter-site temperatures is similar throughout the ground profile. During summer, the ground has a range of temperatures that are higher than during the autumn and winter months. However, unlike air and near-surface temperatures, the range of temperatures starts to increase at the beginning of spring, reaching a maximum in summer.

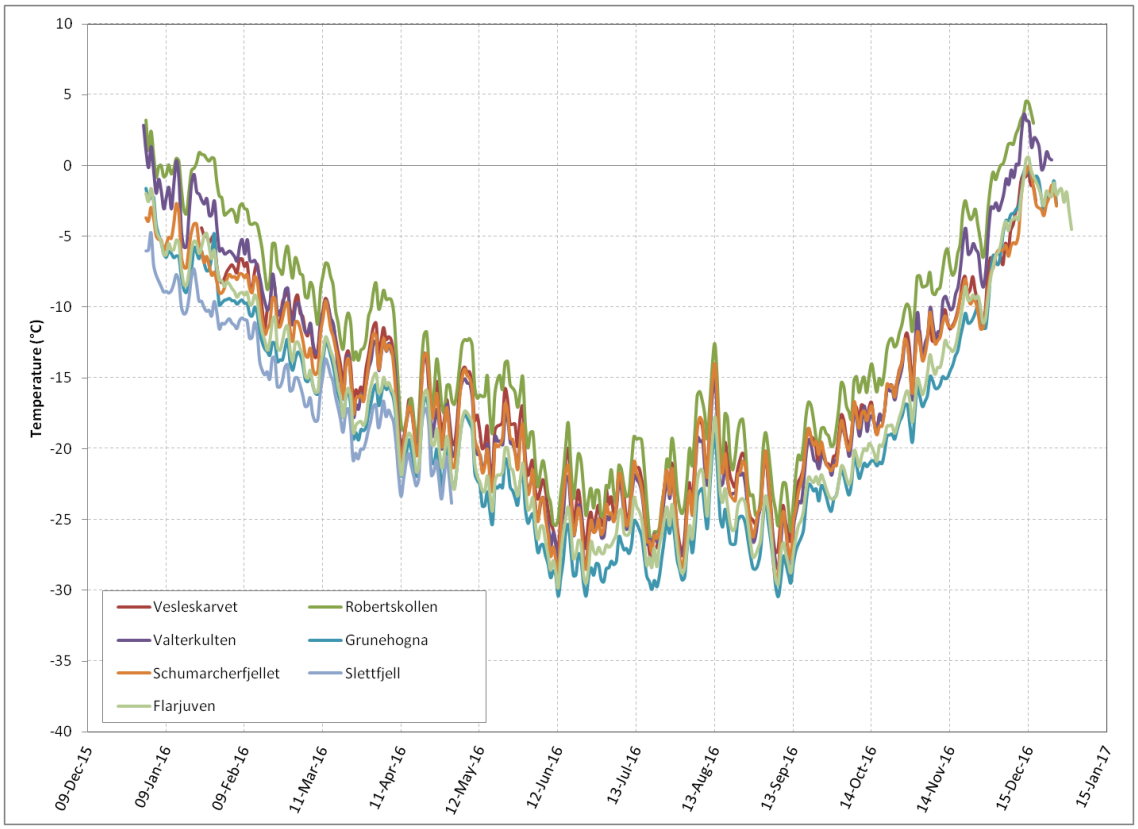

Figure 13. Daily average 15 cm deep temperatures

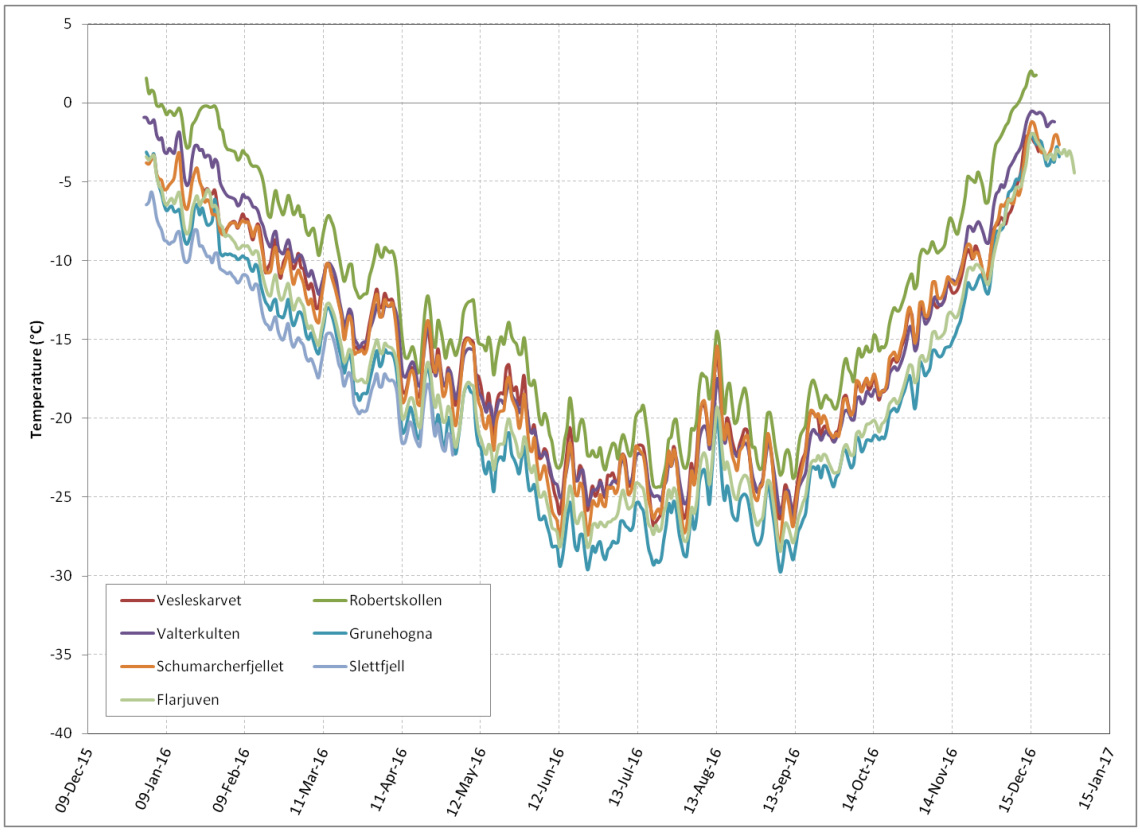

Figure 14. Daily average 30 cm deep temperatures

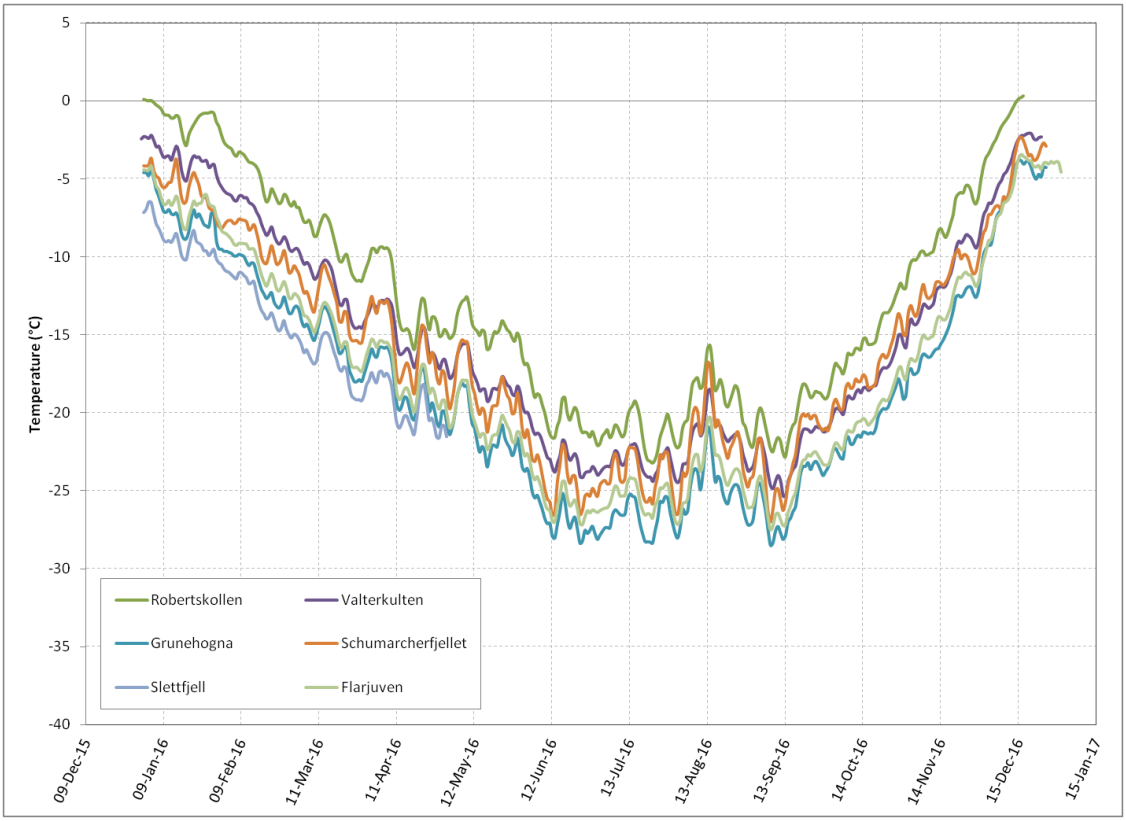

Figure 15. Daily average 45 cm deep temperatures

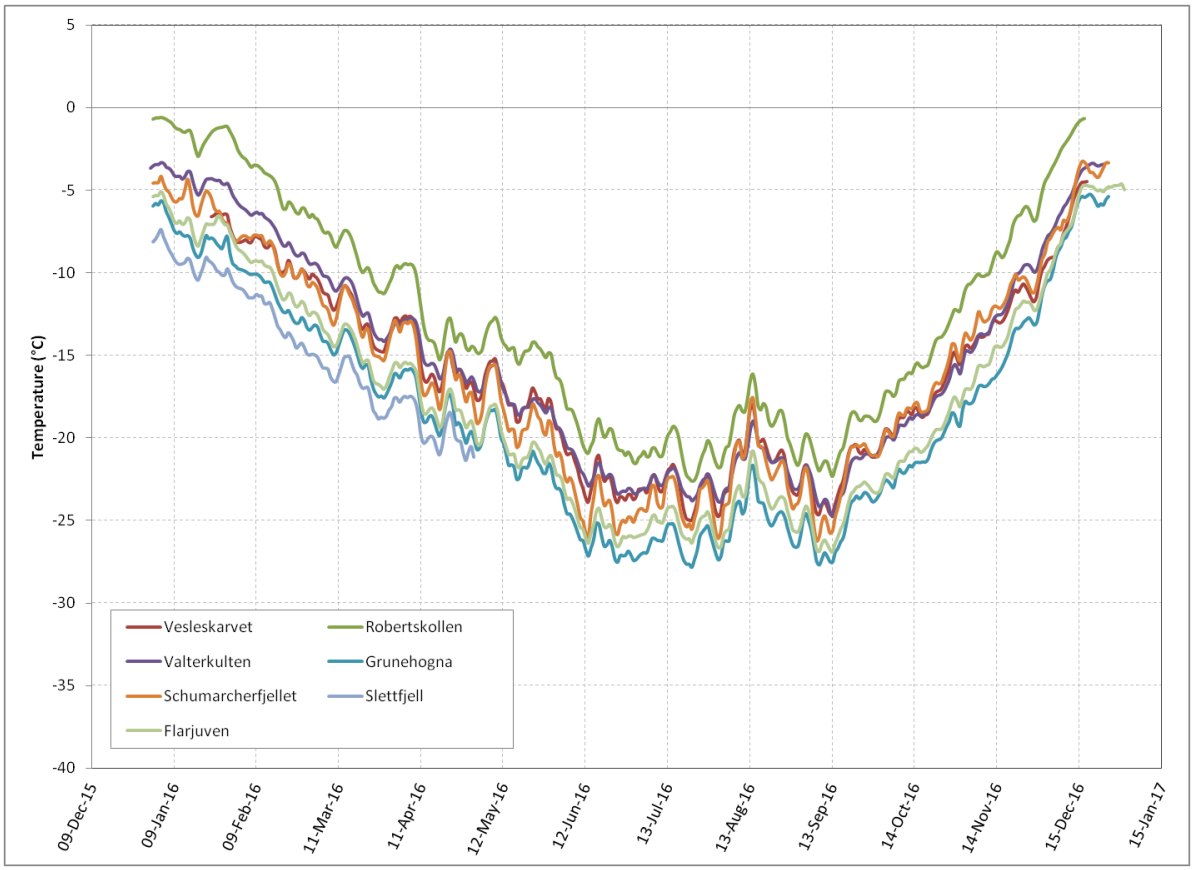

Figure 16. Daily average 60 cm deep temperatures

SAWS and Troll average air temperatures have not been compared with average ground temperatures because they were significantly higher as supported by the decreasing correlation highlighted in Table 8 earlier in the section. Troll, on the other hand, has not been compared because of the differences to the other sites in depths where temperatures were recorded. Ground temperatures at other sites were recorded at 15 cm intervals while temperatures at Troll were recorded at 50 cm intervals. Additionally, at the 45 cm depth, trends in Vesleskarvet temperatures could not be deduced due to incorrect temperature readings resulting from a faulty sensor.

4.3. Objective 3: Active Layer Depth Analysis

4.3.1. Soil Properties

The behaviour of any type of soil is governed by the properties that define it. Three main soil properties – physical, chemical, and/or biological properties – play a role in how soils respond to changes in the environment caused by different climatic and atmospheric factors. Consequently, soil types are classified primarily according to climatic zones (Courtney and Trudgill, 1984). Soils in Antarctica are classified as Gelisols because they have little profile development as a result of the

perennial sub-zero temperatures that inhibit the soil formation process. In addition, they are characterized by the presence of a permafrost layer (Weil and Brady, 2017).

The amount of water, or moisture content, within a soil profile, plays a crucial role in the formation of soil. The very low values for water content in the selected sites, as highlighted by the Gravimetric and the Volumetric Water Content (VWC), strongly correspond to the bulk densities of soil at each site (see Table 17).

Table 17. Soil physical properties at selected study sites

Soil Sample Site	Wet Soil Sample (g)	Dry Soil Sample (g)	Mass & Volume of water (cm^3)	Gravimetric Water Content (%)	Volumetric Water Content (cm^3/cm^3)	Bulk Density (g/cm^3)
Slettfjell	349.44	349.34	0.1	0.0286	0.00042	1.456
Troll	405.66	405.38	0.28	0.0691	0.00117	1.689
Schumarcherfjellet	383.59	382.58	1.01	0.2640	0.00421	1.594
Grunehogna	380.34	379	1.34	0.3536	0.00558	1.579
Robertskollen	441	439.64	1.36	0.3093	0.00567	1.832
Valterkalten	425.67	421.73	3.94	0.9343	0.01642	1.757
Flårjuven	383.7	376.92	6.78	1.7988	0.02825	1.571
Vesleskarvet	525.2	499.86	25.34	5.0694	0.10558	2.083

Of all the study sites, soil at Vesleskarvet has the highest bulk density, followed by Robertskollen, Valterkulten and Troll, and the highest water content (refer to Table 17). However, soil at Flårjuven has the second highest water content followed by Valterkulten and then Robertskollen. Soil at Slettfjell has the lowest bulk density, followed by Flårjuven, Grunehogna and Schumarcherfjellet. Soil at Troll has the lowest water content after Slettfjell. However, although it has a higher bulk density compared to Schumarcherfjellet and Grunehogna, it has the lowest water content in relation to the two sites.

Soil particles of ≤ 63 µm describe particles ranging from coarse silt to clay particles (see Appendix A. for sedimentary particles size grades, pg. 85). Depending on the soil type, soil particles of ≤ 63 µm have the capacity to hold and retain moisture within soil due to a widespread distribution of pore size and a larger particle surface area (Bilskie, 2001). Flårjuven has the highest proportion of soil particles of ≤ 63 µm (13.57 %) followed by Vesleskarvet (7.46 %) and Valterkulten (3.55 %) (refer to Fig. 17). These percentages directly correspond with the water content within the respective soils. In contrast, the proportion of soil particles of ≤ 63 µm at Schumarcherfjellet (1.19 %), Troll (0.85 %),

Slettfjell (0.39 %), Robertskollen (0.31 %) and Grunehogna (0.05 %) seem to be inversely proportional to the water content available within the soil.

Overall, the soils of all sites, with the exception of Slettfjell and Schumarcherfjellet, have the bulk of their particles distributed between coarse sand and clay (see Fig. 18). Slettfjell and Schumarcherfjellet have the highest proportion of medium gravel (Phi size -3.0 ø). Flårjuven and Vesleskarvet appear to have similar distributions of their particles – they have the lowest distribution between fine gravel and medium gravel (Phi size -1.0 ø to -3.0 ø). Conversely, Slettfjell and Grunehogna have the highest distributions of particles between coarse sand and fine gravel (Phi size 0.0 ø to -3.0 ø).

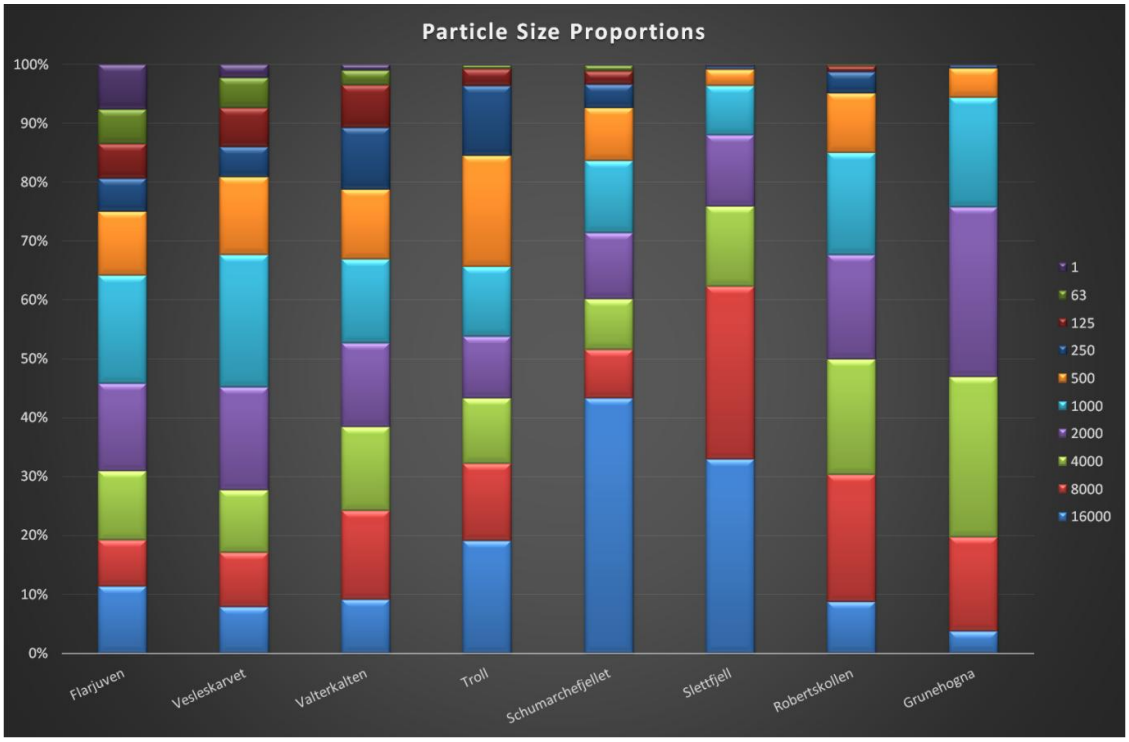

Figure 17. Proportions of particle sizes at each study site

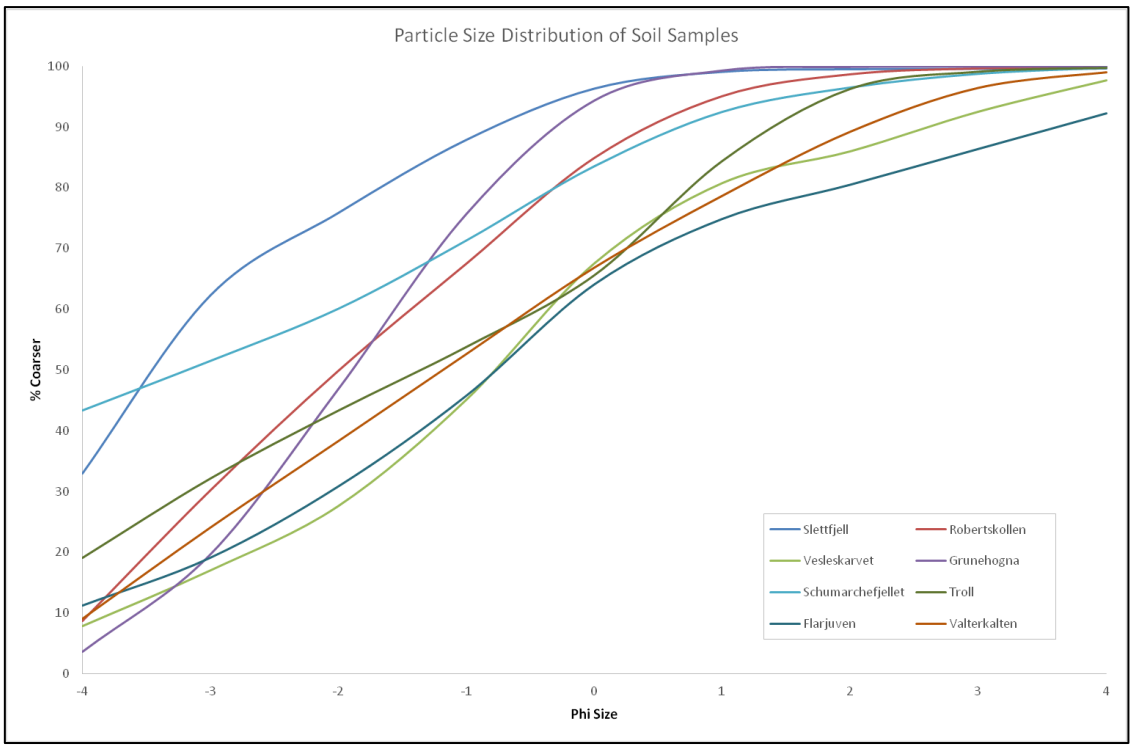

Figure 18. Cumulative distribution of particles sizes at each site

4.3.2. Active Layer Depth

The depths of the active layers were determined by observing the cryofront, which is the boundary between the seasonally non-cryotic ground (the active layer) and the perennially cryotic layer (permafrost). The cryofront is seen when the maximum ground temperature intercepts the 0 ˚C isotherm (Dobinski, 2011). The depth profiles of the 8 sites shown in Figures 19-26 illustrate the active layers of the year 2016, as well as the mean active layer depth averaged over the total monitoring years of the individual borehole sites.

The active layer depth at Vesleskarvet in 2016 measured 24 cm, while the average annual active layer depth for a period of seven years from 2009-2016 was also 24 cm (see Fig. 19). Maximum ground temperatures exhibit a smaller inter-annual variability when compared to minimum ground temperatures.

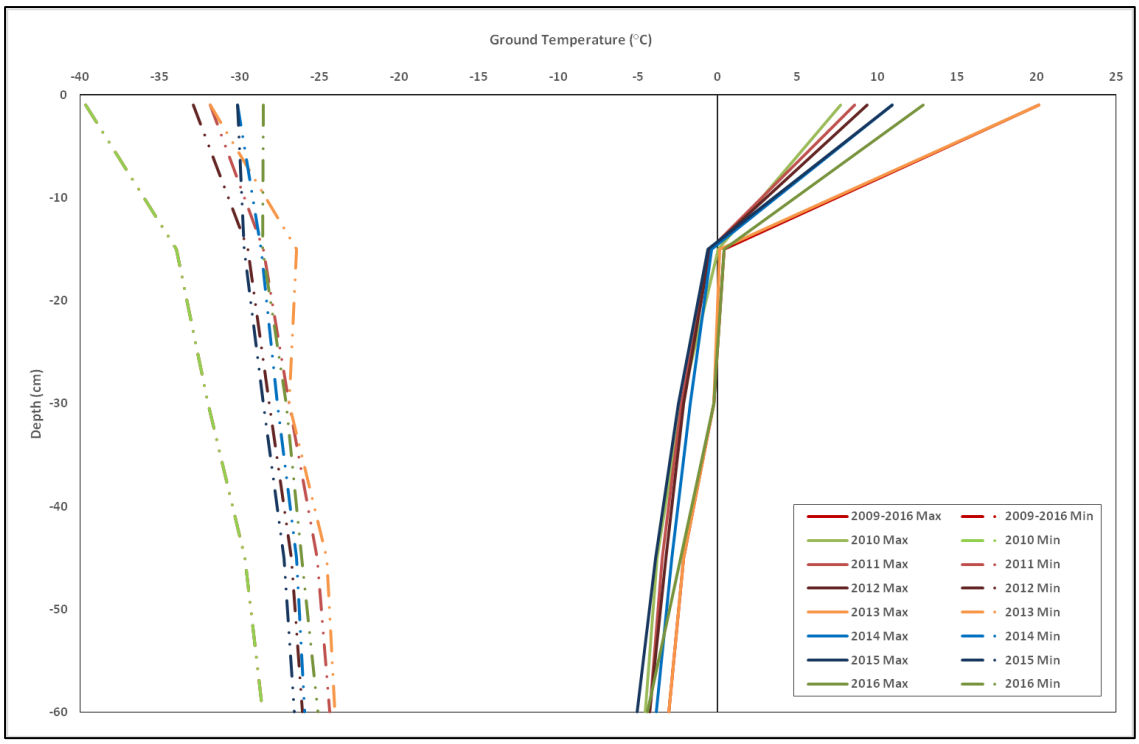

Figure 19. Soil thermal profiles with depth at Vesleskarvet from 2009 to 2016

Robertskollen, on the other hand, had a deeper active layer at a depth of 51 cm in 2016 (see Fig. 20). The average annual active layer depth averaged over 4 years from 2013-2016 was also much deeper than that at Vesleskarvet, exceeding the measured borehole length at 60 cm. The inter-annual variability exhibited by the maximum ground temperatures seem to be slightly smaller than that of the minimum ground temperatures in comparison to Vesleskarvet.

The active layer depth at Valterkulten in 2016 was 29 cm (see Fig. 21), which was also deeper than that at Vesleskarvet. The mean active layer depth averaged over a period of 4 years from 2013-2016 was 4 cm deeper than that at Vesleskarvet, at 29 cm. Disregarding the depth profile of 2015, there appears to be no difference in the inter-annual variability exhibited by both maximum and minimum temperatures, as they both exhibit a smaller inter-annual variability. The higher minimum temperatures of 2015 are a result of an incomplete data set. Data logging in 2015 for Valterkulten persisted just until 12-February, therefore giving readings for only the summer period

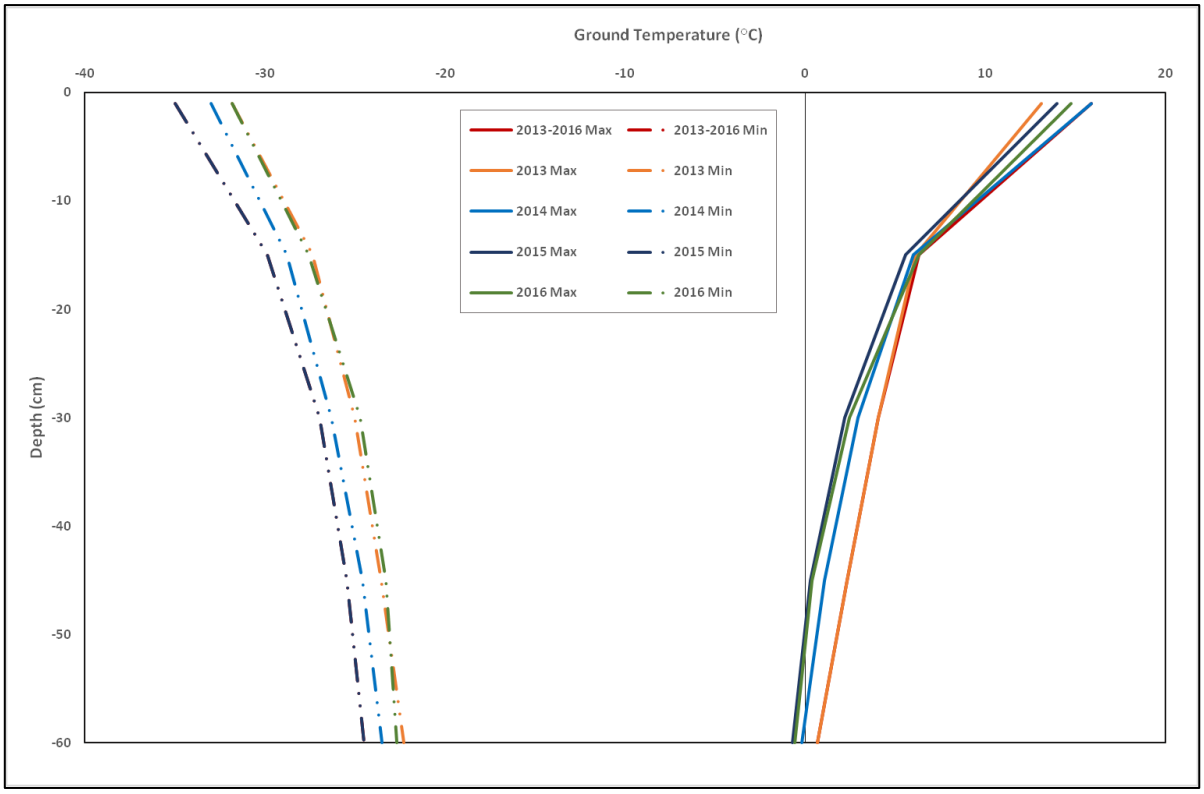

Figure 20. Active layer depths at Robertskollen

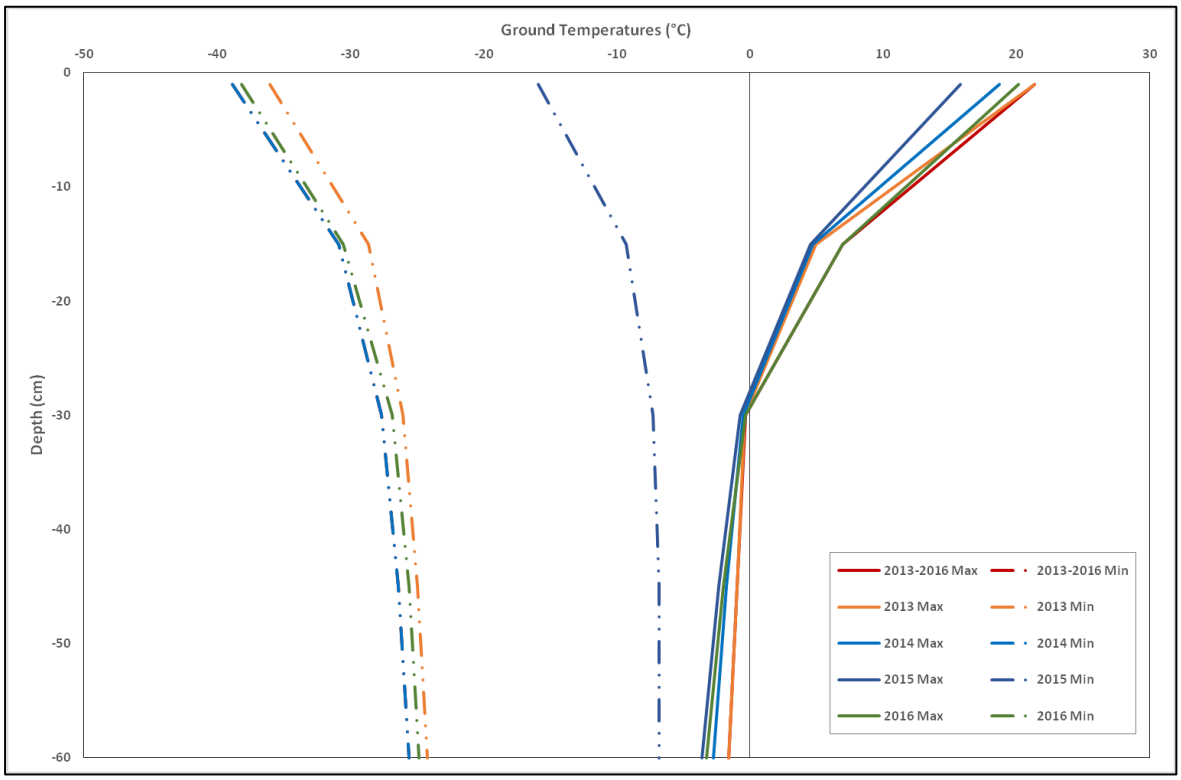

Figure 21. Active layer depths at Valterkulten

The active layer depth at Schumacherfjellet in 2016 was measured at 16 cm, 8 cm shallower than the active layer at Vesleskarvet (see Fig. 22). However, the mean active layer depth averaged over 4 years from 2013-2016 was deeper than that at Vesleskarvet, at 30 cm. Akin to Vesleskarvet, the minimum ground temperatures exhibit a larger inter-annual variability than maximum ground temperatures.

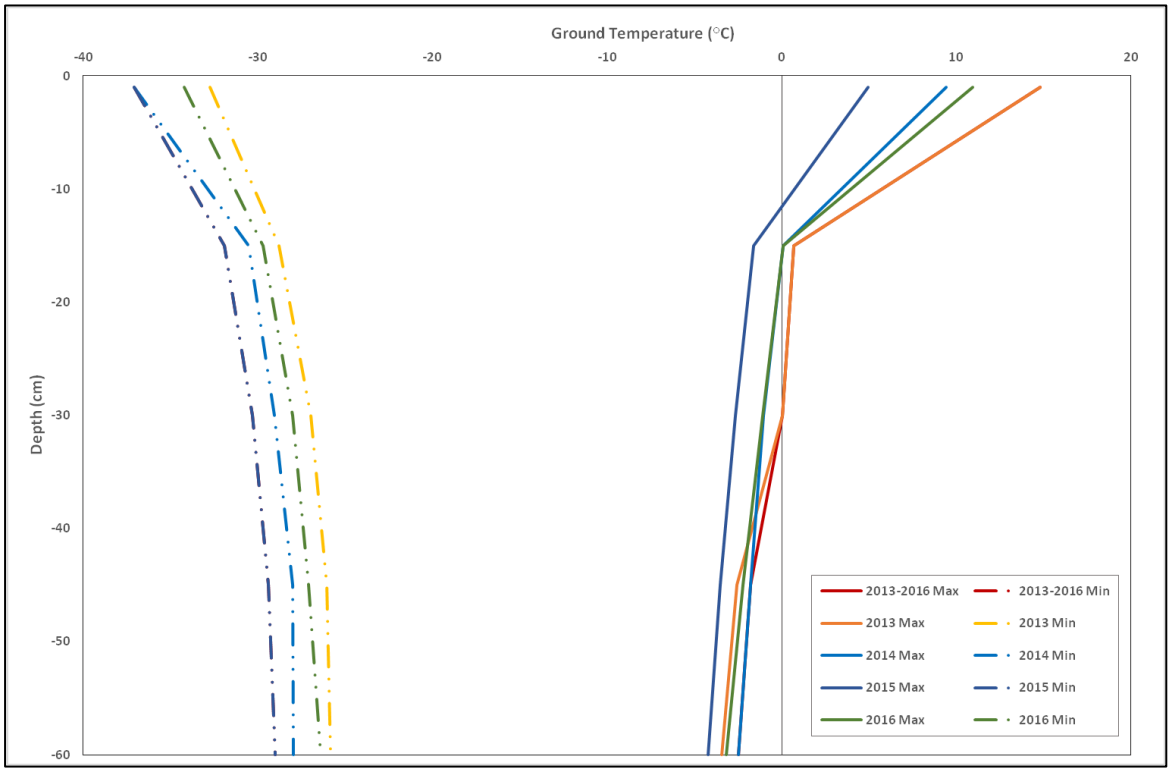

Figure 22. Active layer depths at Schumarcherfjellet

Grunehogna had a shallower active layer compared to Vesleskarvet in 2016. Its active layer had a depth of 21.5 cm (see Fig. 23). On the other hand, the mean active layer depth averaged over 4 years from 2013-2016, was deeper, at a depth of 29 cm. However, unlike Vesleskarvet, the maximum ground temperatures exhibit a larger inter-annual variability than the minimum ground temperatures.

The active layer depth at Flårjuven in 2016 was 25 cm as shown by Figure 24. It was slightly deeper than the 2016 active layer at Vesleskarvet. However, the mean active layer depth averaged over a period of 4 years was significantly deeper than the average active layer depth at Vesleskarvet, at 30 cm. Disregarding the depth profile of 2014, maximum ground temperatures exhibited a larger inter-annual variability than minimum ground temperatures. Data logging in 2014 was part of the 2013 data logging season that ended on 10-January-2014.

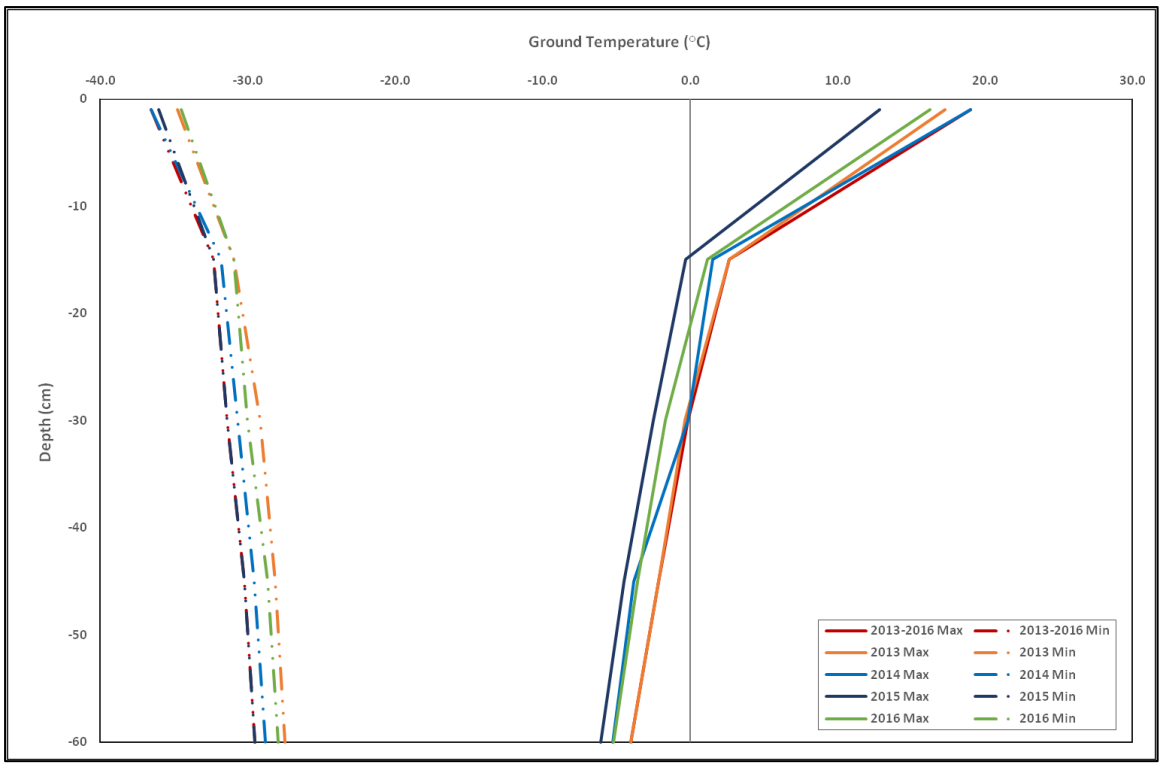

Figure 23. Active layer depths at Grunehogna

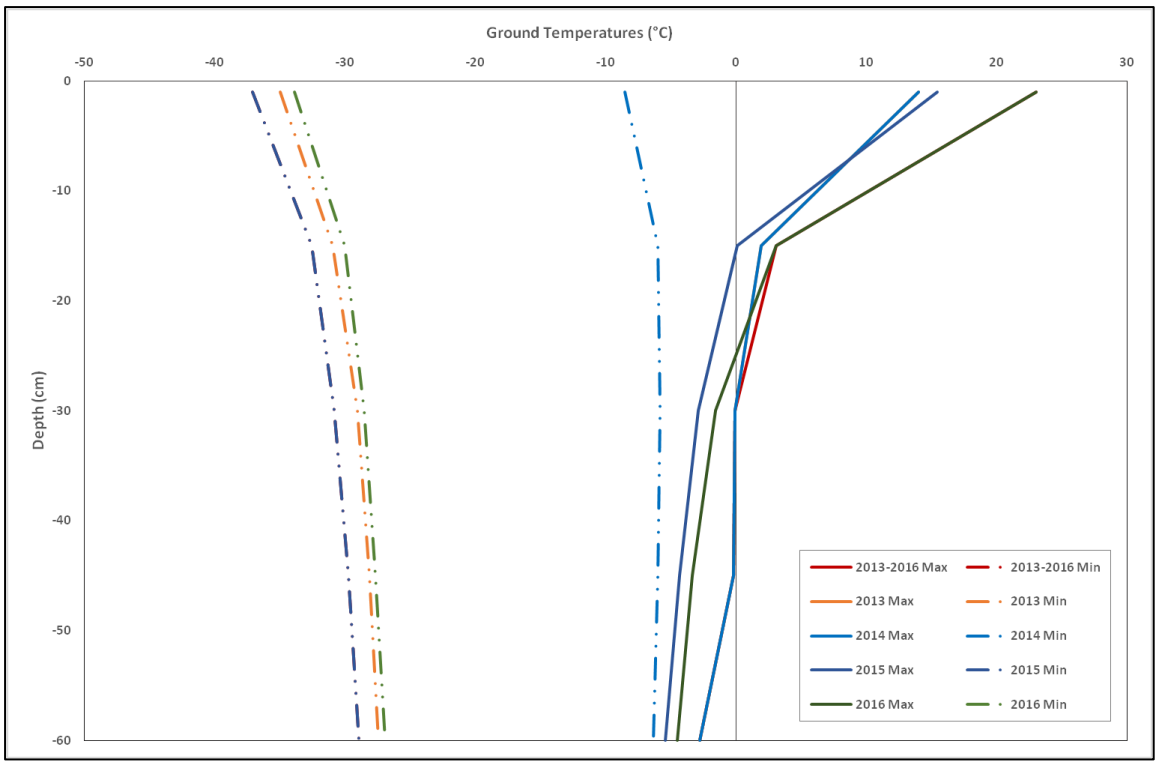

Figure 24. Active layer depths at Flårjuven

The active layer depth at Slettfjell was significantly shallower than that at Vesleskarvet and all the other sites, at 10 cm (see Fig. 25). However, it should be noted that the Slettfjell 2016 data were incomplete, and data were recorded only until 01-May. A more representative depiction of the active layer could be inferred from the mean annual active layer depth averaged from 2013 to the first quarter of 2016. Nevertheless, the mean active layer depth is still significantly shallower than all the other sites, at 11.8 cm. Similarly to Flårjuven, disregarding the depth profile of 2016, maximum ground temperatures exhibit a larger inter-annual variability compared to Vesleskarvet.

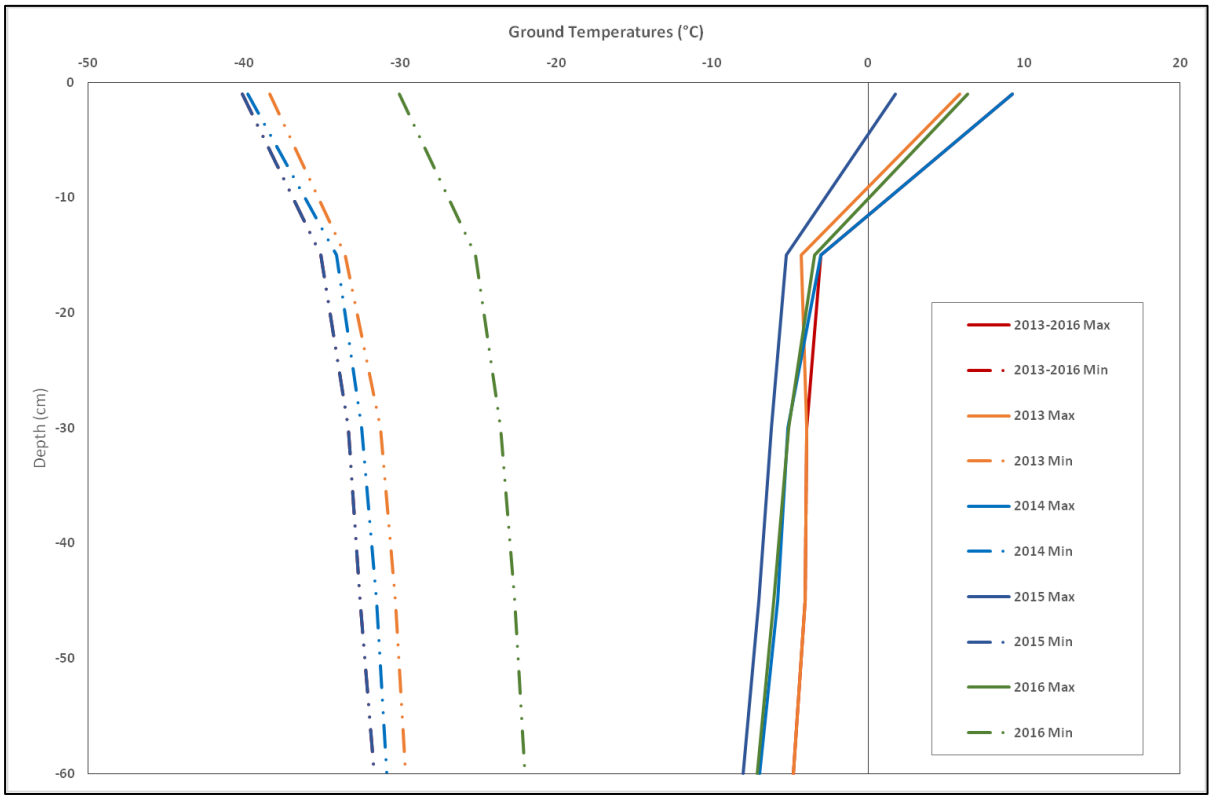

Figure 25. Active layer depths at Slettfjell

Troll, being the site furthest from Vesleskarvet, has the second deepest active layer. In 2016, the active layer depth was 36 cm, while the mean annual depth averaged from 2007-2016 was 40 cm (see Fig. 26). Disregarding the depth profile of 2009, the inter-annual variability is the same for both the maximum and the minimum ground temperatures, as they are both large. Data logging in 2009 persisted only until 25-May.

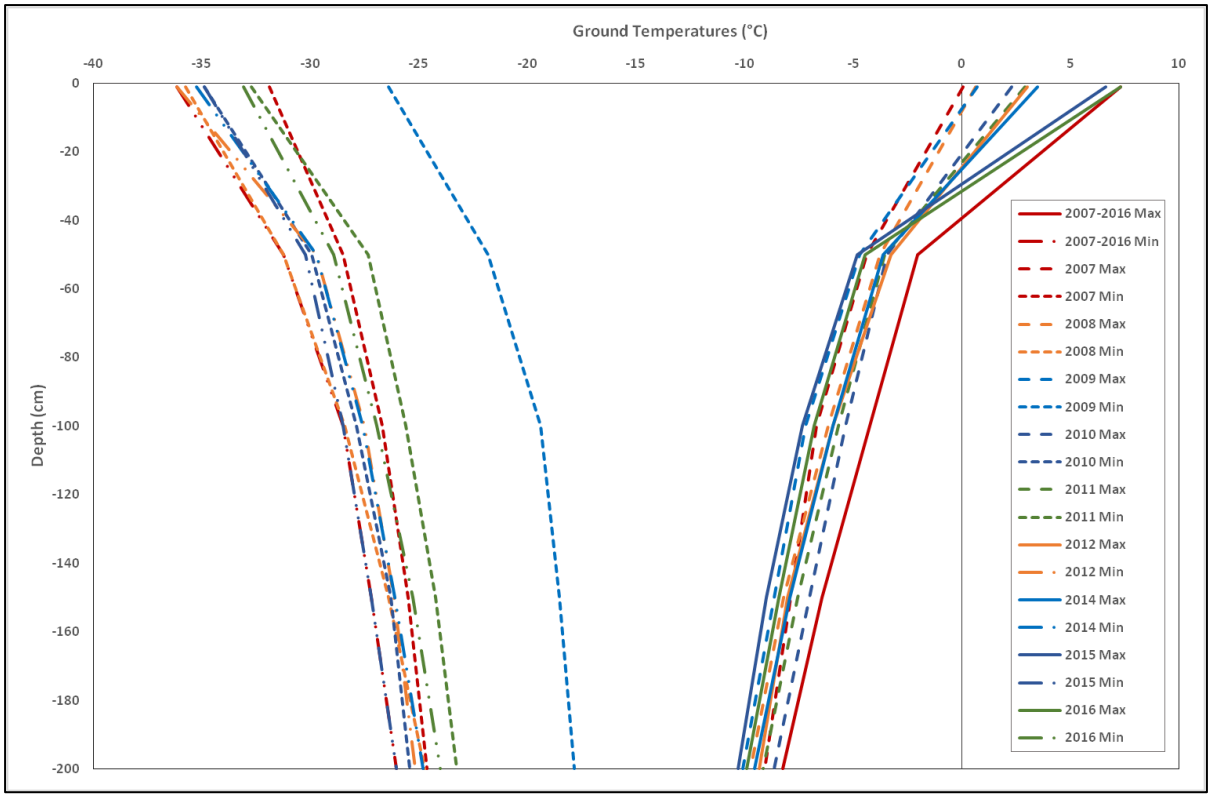

Figure 26. Active layer depths at Troll

4.3.3. Thermal Propagation

The ground thermal profile is dependent on the transport processes of heat within the ground as well as the exchange of heat between the soil and the atmosphere (Koorevaar *et al.,* 1983). Thermal propagation through the soil profile relies on the soil particle size, bulk density, the specific heat capacity, and the thermal conductivity, and it can happen via three processes; through conduction, convection and diffusion (Schaetzl and Anderson, 2005). The rate at which temperature propagates through the ground represents thermal lag, which is the time required for the temperature (heat) to be transferred to, or from, a certain depth (Schaetzl and Anderson, 2005).

Determining the thermal lag of soil accurately can be challenging. Instead, two methods commonly used to produce results that are as close to reality as possible are the heat transfer method and an observational method where the thermal propagation rate is calculated by tracking temperature events through the ground profile (Wilhelm and Bockheim, 2017). The observational method was used over the heat transfer method because it factors in the varying delay time through the ground profile based on the soil texture, water content, depth and the magnitude of temperature change (Wilhelm and Bockheim, 2017). The heat transfer method, on the other hand, is a theoretical method that assumes steady-state conditions where the water content remains unchanged through the soil profile (Wilhelm and Bockheim, 2017).

The thermal propagation rate was calculated using three observed events, and the time taken for the events to be reflected at the maximum monitored depth at the sites. The transmission start depth for all sites was 1 cm and the maximum monitored depth was 60 cm, with the exception of Troll where the maximum depth was 200 cm. The events chosen for most sites were two low-pressure systems recorded by the Australian Meteorological Division (AMPS) that brought about a noticeable drop in temperatures (see Figures 27-34). One was on 02-June and one was on 17-November.

A further event was the substantial increase in temperatures in August. It is important to point out that for Slettfjell, calculations for thermal propagation were done on an event that occurred in April during which there was a rise in temperatures. Analysis for the June, August and November events could not be performed for Slettfjell because there is no recorded data from May to December. Similarly, analysis for Troll involved only one event, in August, when it was easier to determine changes through the ground profile. The other events exhibited a dampening effect through the ground profile from 50 cm downwards.

The thermal propagation rate was calculated when the passage of the cyclones was first reflected on the ground surface. For the June event, the cyclone passed along the coast on the 2nd of June and was consequently reflected inland on 10-June for Robertskollen and 12-June for the other sites. For the November event, the cyclone passed along the coast on 17-November and was first reflected on 26-November for Vesleskarvet, Valterkulten, Grunehogna, and Schumarcherfjellet; and on 27-November for Robertskollen and Flårjuven. The August event was calculated from 12-August for all sites excluding Flårjuven and Slettfjell. For Slettfjell, the April event was calculated from 20-April.

The number of hours starting from when the event was reflected on the ground surface all the way to the maximum observed depth varied for all sites. For the April event for Slettfjell, the number of hours was 17 hrs. For the June event, the number of hours for each site excluding Slettfjell and Troll were 13.17 hrs (Vesleskarvet), 3 hrs (Robertskollen), 3 hrs (Valterkulten), 1 hr (Grunehogna), 20 hrs (Schumarchefjellet), and 16 hrs (Flårjuven). For the August event, the number of hours for each site excluding Slettfjell were 20.67 hrs (Vesleskarvet), 7 hrs (Robertskollen), 6 hrs (Valterkulten), 4 hrs (Grunehogna), 6 hrs (Schumarcherfjellet), 7 hrs (Flårjuven), and 15 hrs (Troll). Lastly, for the November event, the number of hours for each site excluding both Slettfjell and Troll were 7.67 hrs (Vesleskarvet), 13 hrs (Robertskollen), 12 hrs (Valterkulten), 11 hrs (Grunehogna), 12 hrs (Schumarcherfjellet), and 11 hrs (Flårjuven).

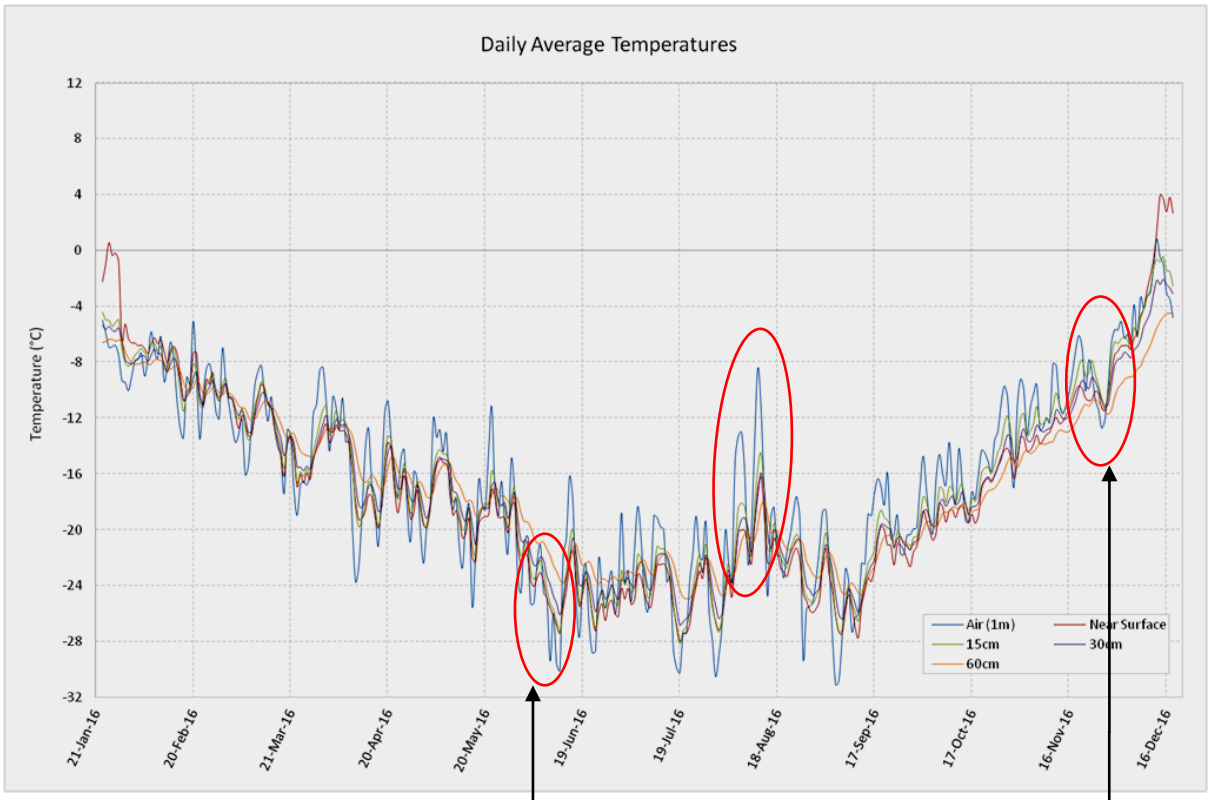

Figure 27a. Vesleskarvet

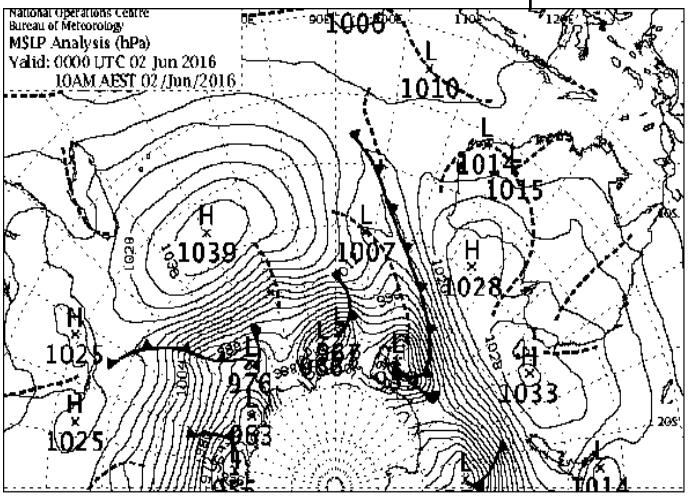

Figure 27b. Synoptic Low Pressure Cell – June

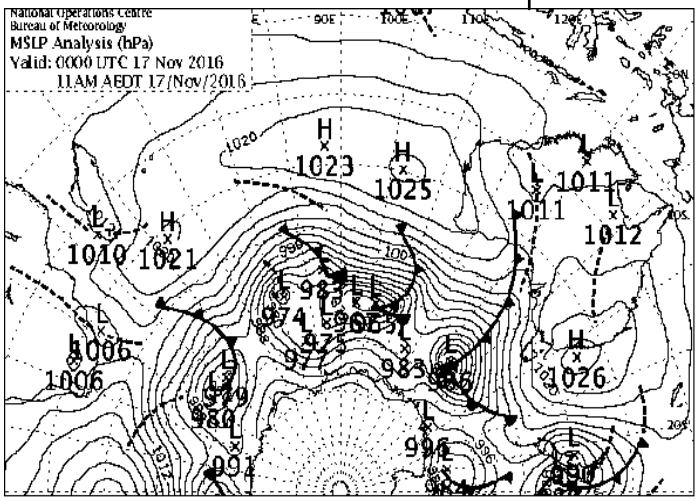

Figure 27c. Synoptic Low Pressure Cell - November

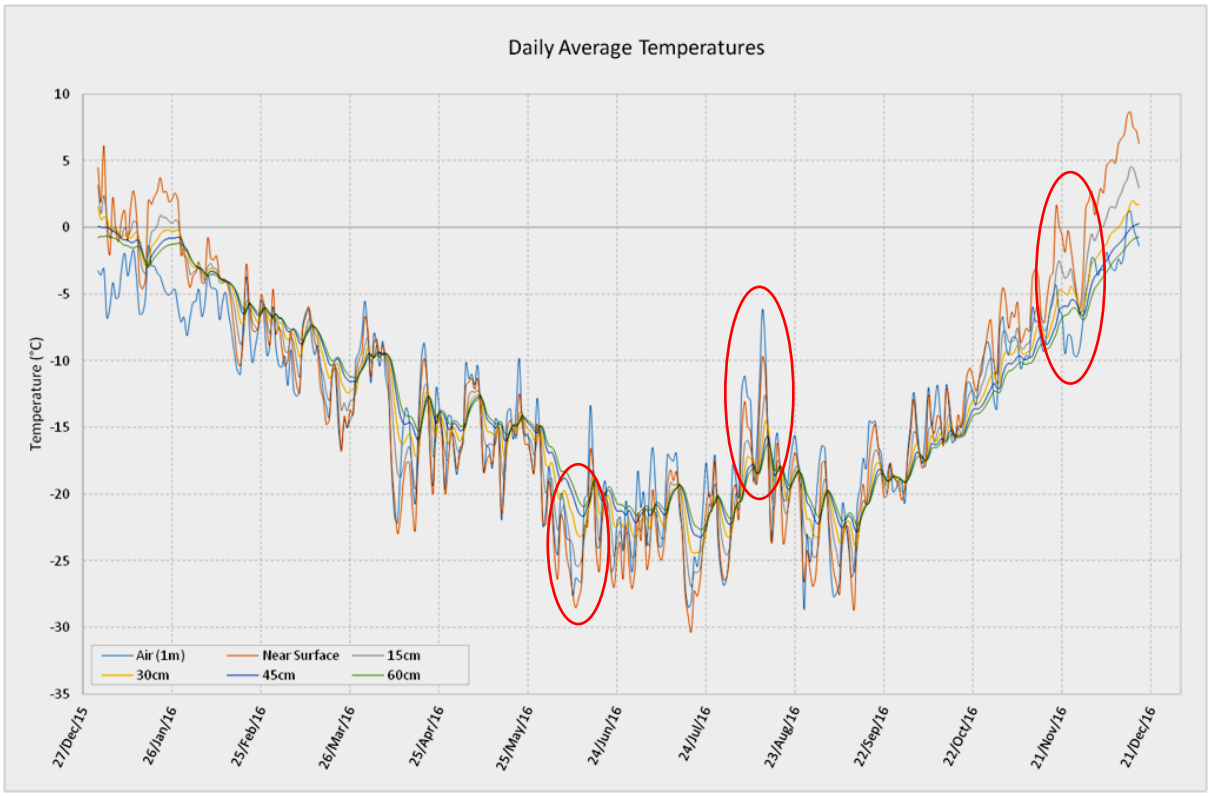

Figure 28. Robertskollen

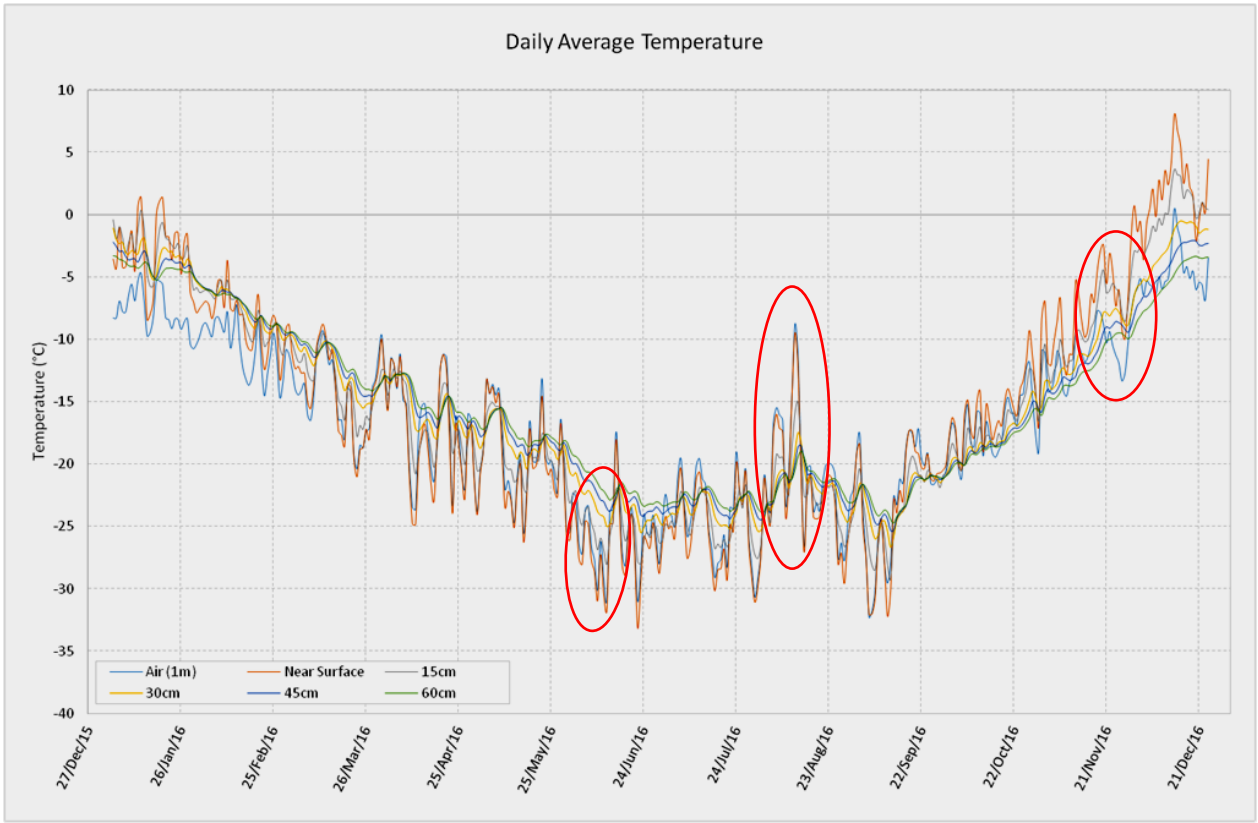

Figure 29. Valterkulten

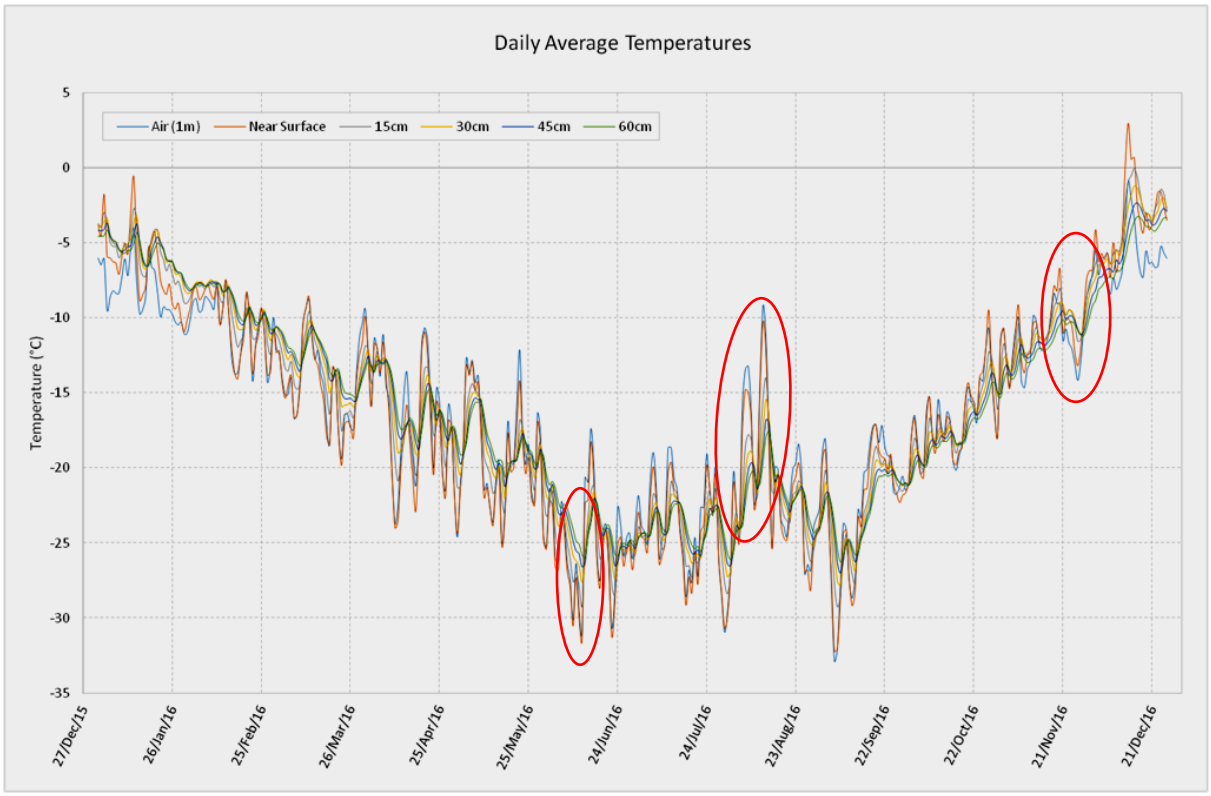

Figure 30. Schumarcherfjellet

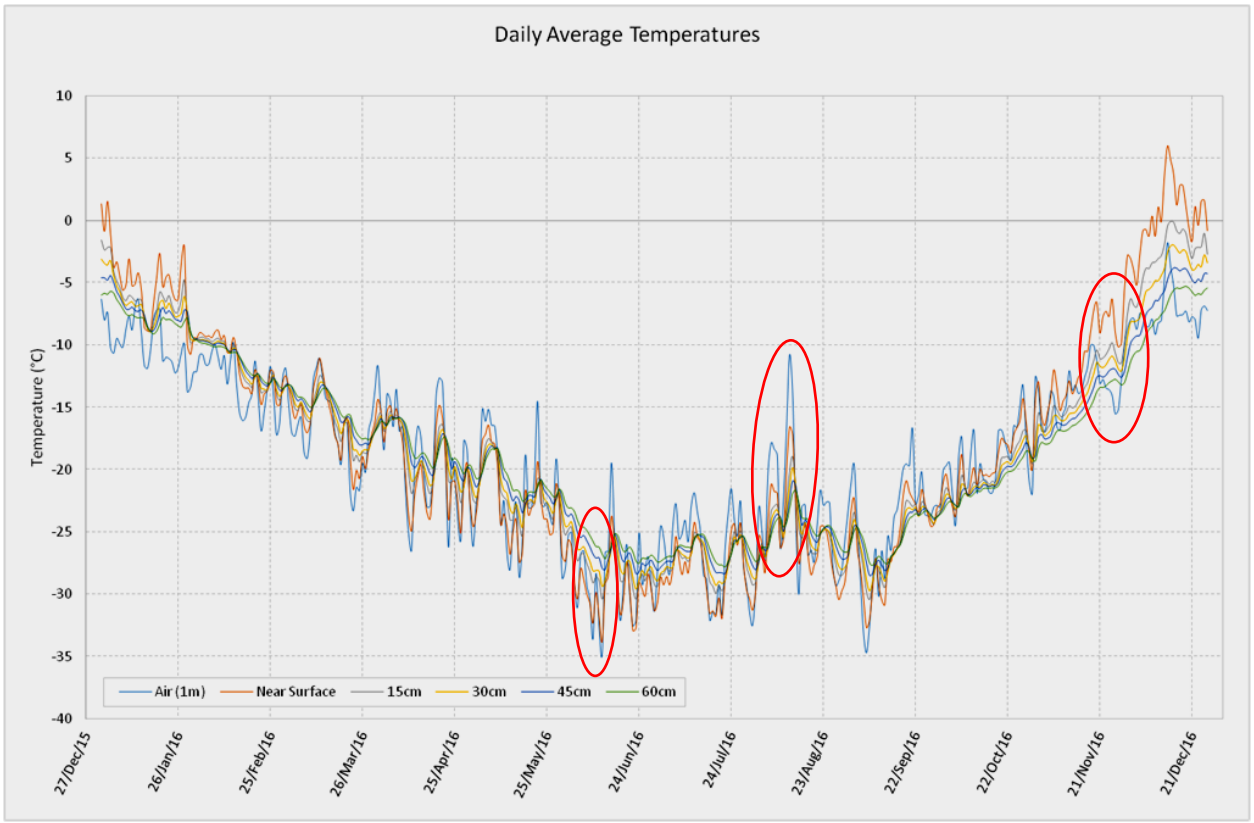

Figure 31. Grunehogna

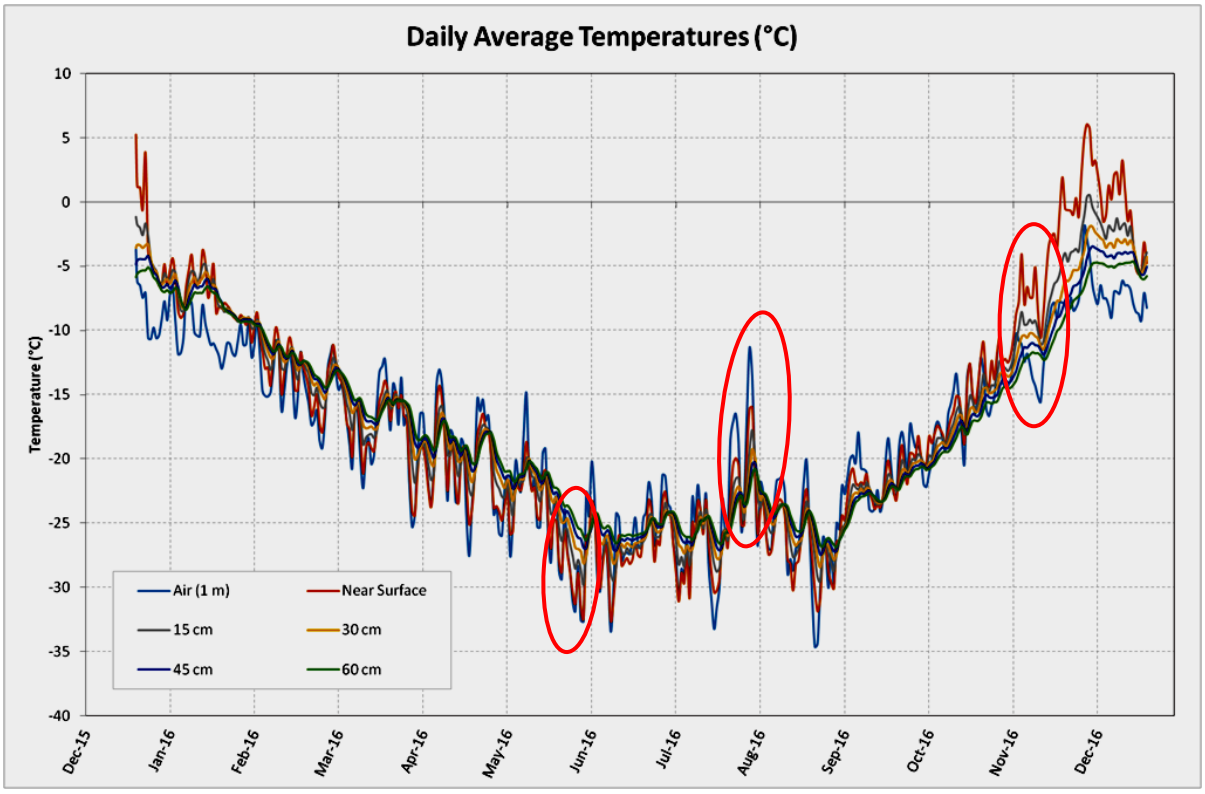

Figure 32. Flårjuven

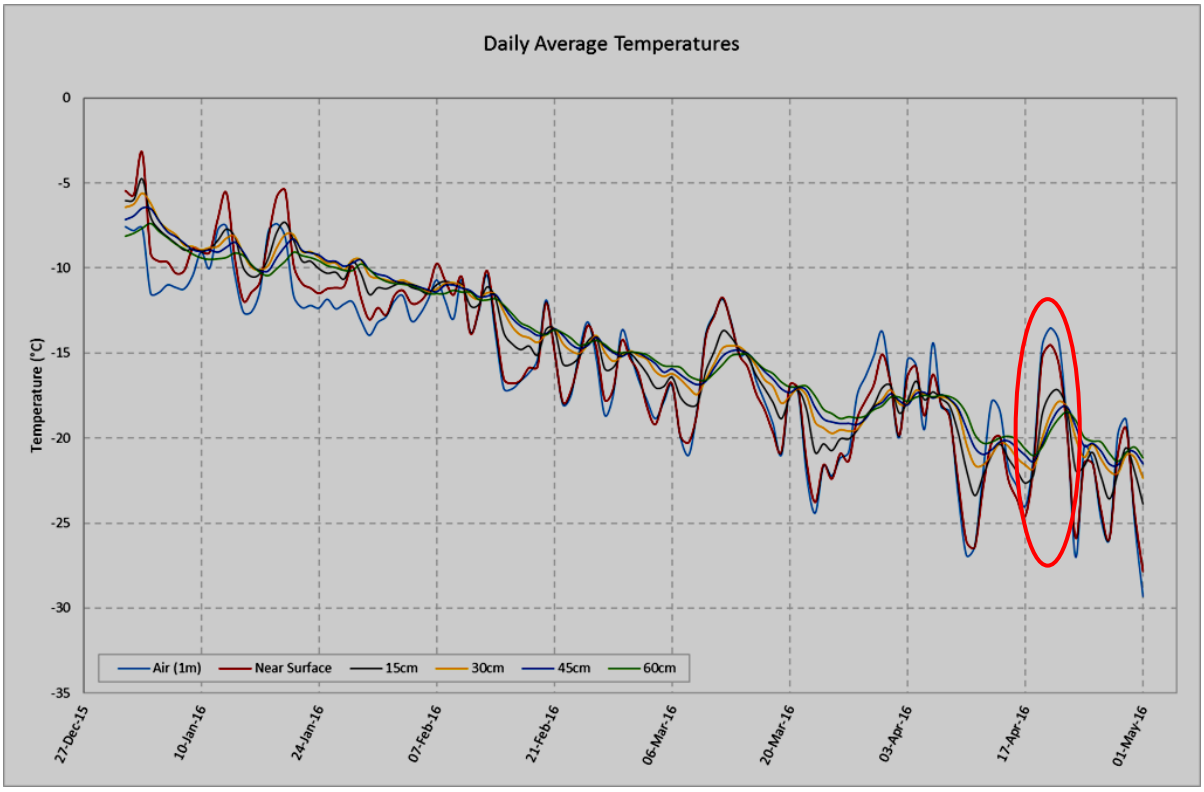

Figure 33. Slettfjell

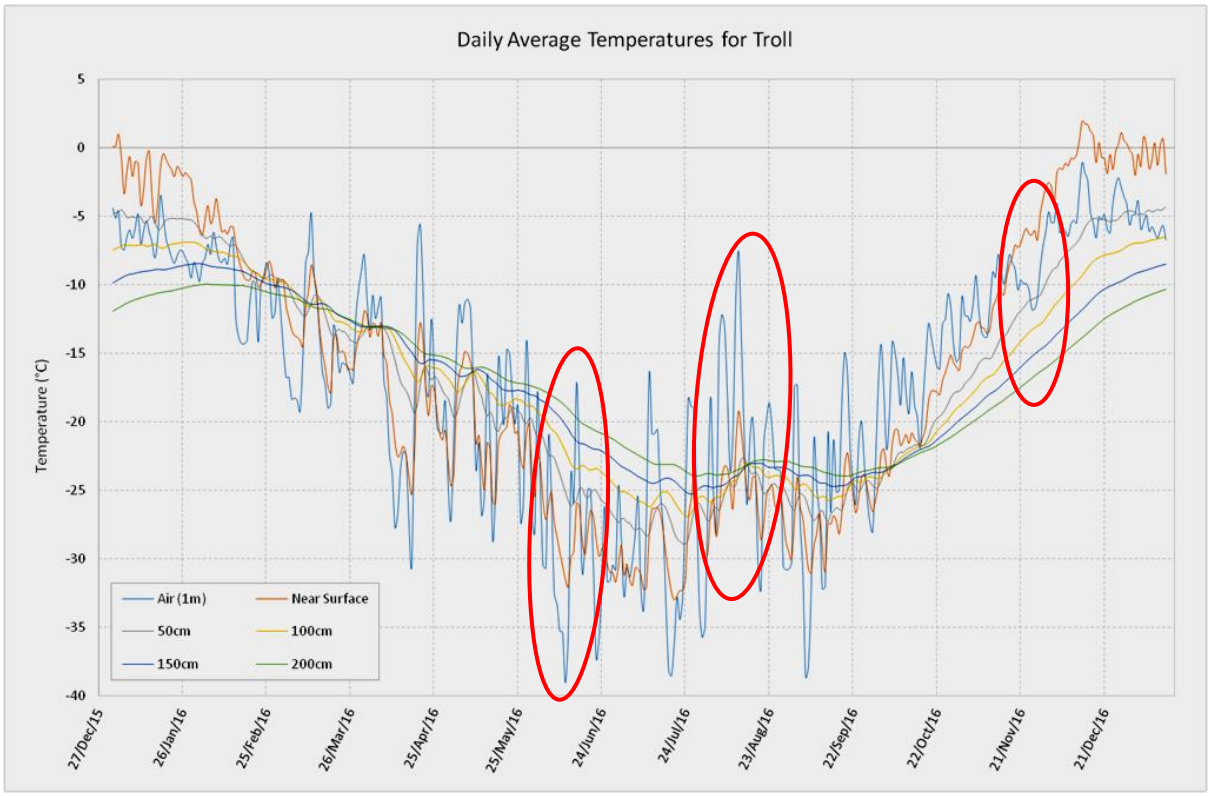

Figure 34. Troll

If Slettfjell and Troll are excluded from the average thermal propagation rate analysis, it can be seen from Table 18 that Vesleskarvet had the lowest average thermal propagation rate of 5.05 cm/h while Grunehogna had the highest average thermal propagation rate of 26.37 cm/h. Valterkulten had the second highest average rate (11.47 cm/h), followed by Robertskollen (10.88 cm/h), Schumarcherfjellet (5.90 cm/h) and Flårjuven (5.83 cm/h).

Table 18. Thermal lag times at each study site

	Thermal propagation (cm/h)				
	April	*June*	*August*	*November*	*Average*
Vesleskarvet		4.60	2.85	7.69	5.05
Robertskollen		19.67	8.43	4.54	10.88
Valterkulten		19.67	9.83	4.92	11.47
Grunehogna		59.00	14.75	5.36	26.37
Schumarcherfjellet		2.95	9.83	4.92	5.90
Flårjuven		3.69	8.43	5.36	5.83
Slettfjell	3.47				3.47
Troll			3.93		3.93

In June, the highest thermal propagation rate was in Grunehogna (59 cm/h), followed by Robertskollen and Valterkulten (19.67 cm/h), Vesleskarvet (4.6 cm/h), Flårjuven (3.69 cm/h) and, Schumarcherfjellet (2.95 cm/h). In August, the highest thermal propagation rate was still in Grunehogna (14.75 cm/h) followed by Valterkulten and Schumarcherfjellet (9.83 cm/h), Robertskollen and Flårjuven (8.43 cm/h), Troll (3.93 cm/h) and Vesleskarvet (2.85 cm/h). In November, the highest thermal propagation rate was in Vesleskarvet (7.69 cm/h), followed by Grunehogna and Flårjuven (5.36 cm/h), Valterkulten and Schumarcherfjellet (4.92 cm/h) and Robertskollen (4.54 cm/h). Slettfjell had the lowest overall thermal propagation rate of 3.47 cm/h.

Site specific characteristics influence how the soil and ground respond to different climatic and meteorological variables. As presented in this chapter, the variability of meteorological phenomena has a spatial effect both laterally and temporally. Following is a discussion on the presented results and what they mean for the periglacial environment of Western Dronning Maud Land.

Chapter 5: Discussion

5.1. The influence of weather variables on Vesleskarvet thermal regimes

An analysis of the weather variables, temperature, pressure, humidity, wind speed and wind direction at Vesleskarvet shows that only temperature, pressure and humidity have a strong influence on ground thermal regimes in Vesleskarvet with temperature showing the highest influence.

The variability of ambient air and ground temperatures differs throughout the year. In comparison, near surface temperatures are more variable than ambient air temperatures (see Table 6) which suggests that ground (near surface) temperatures are influenced by more than variations in air temperatures, while air temperatures have a greater influence at depths near the ground surface with a diminishing effect with greater depths (Ishikawa, 2003). To further elucidate this phenomenon, near surface temperatures throughout the year are more variable than temperatures at the 15 cm depth, as can be seen from the range and variance values in Table 6. However, detailed analysis of seasonal average temperature shows that the variability of air and ground (near surface) temperatures changes and alternates between seasons. Both ambient air and ground temperatures are highly variable in spring. However, ambient air temperatures are less variable in summer while ground temperatures are less variable in winter.

Temperature variability in spring can be compared to the autumn temperature variability given that in spring, Western Dronning Maud Land (WDML) experiences day and night cycles just as in autumn. Similarly, the summer temperature variability can be compared to the winter temperature variability since WDML experiences 24-hour sunlight in summer while in winter, the amount of shortwave solar radiation reaching the ground surface is minimal because of the approximately 3-month long night time.

The high variability of ambient air temperatures in winter is possibly indicative of large synoptic events that have a greater effect in the absence of warming due to an extremely reduced shortwave solar radiation. According to Bintanja (2000), the passage of cyclones along the coast in winter have an influence on ground thermal regimes because they produce easterly geostrophic winds that interact with katabatic winds in the boundary layer to produce strong boundary layer winds. To elucidate this point, wind speed was found to have some influence on ambient air and ground temperatures in May.

On the other hand, winter ambient air temperatures could be highly variable due to the moderately low average relative humidity of winter. Even though humidity is variable throughout the year, with summer being the most variable, winter was the least variable in addition to presenting the lowest average humidity level. Conversely, the high average pressure of winter supports the relatively low humidity levels and low precipitation events. It is worth noting that the difference between the average seasonal pressures is relatively minimal and they are all relatively high. Given the reported conditions, lack of solar radiation coupled with low average relative humidity and the persistence or low variability of the high-pressure system, result in air that cannot retain heat, hence the highly variable ambient air temperatures in winter (Keys, n.d).

Near-surface temperatures are less variable in winter because of the occasional intense storms along the coast that bring snow into the interior. Since snow has properties of an insulator, the minimum radiation from the sun during winter is trapped within the ground causing temperatures within the ground to rise and fall at a slow rate (Brown, 2012). Interestingly, there was a significant increase in both pressure and air and near-surface temperatures in August. This significant increase positively coincides with the expansion of the sea ice in winter. While no documentation exists, it may be that the expansion of the sea ice releases latent heat in the atmosphere along the coast which in turn might have a delayed reaction on temperatures in the interior (Meiklejohn, 2017).

Vesleskarvet is situated in a region that experiences solar radiation that is almost symmetrical. During summer, it experiences nearly 3 months of sunlight, when near surface temperatures show the greatest changes and have the highest maximum values. The opposite of this trend occurs in winter where for 3 months it receives next to zero solar radiation as it is plunged into a perpetual night time. Alternatively, for approximately 6 months, 3 months in autumn and 3 months in spring, Vesleskarvet experiences a diurnal (roughly 12-hour day and 12-hour night) cycle.

Air temperatures observed during the winter period show the highest variability, followed by near surface temperatures. The air temperatures have the highest maximum values and temperatures near the surface have the lowest minimum values. Autumn and spring seasons display a mirror effect because of the day and night cycles giving rise to diurnal influences during these seasons (see Figure 10). In the autumn months, as the season changes to winter, the decreasing temperatures are caused by the decrease in solar radiation, whereas in spring going into summer, the rise in temperature is a result of increased solar radiation. Although ambient air and ground temperatures exhibit a mirror effect during autumn and spring, it is worth noting that temperatures in spring are more variable showing higher maximums and lower temperature minimums.

The behaviour of air and ground temperatures throughout the different seasons can further be explained by greater synoptic events that operate globally and have far-reaching effects. The Southern Annular Mode (SAM) and the Semi-Annual Oscillation (SAO) are great synoptic systems that have a significant impact on pressure systems in the Southern Ocean. The SAM, which is linked to the El Niño-Southern Oscillation cycle, is responsible for the long wave atmospheric amplification which results in a reduced pressure gradient in the Southern Ocean (Schlösser *et al.,* 2010). The reduced pressure gradient brings about weaker westerlies which occur when the SAM is in its negative phase (Schlösser *et al.,* 2010).

It has been reported that the strength of the westerly winds has continuously increased during summer and autumn due to the SAM becoming positive over the last 5 decades (Turner *et al.,* 2013). The loss of the ozone layer, particularly during spring, has aided the change to a positive phase of the SAM, which has resulted in the occurrence of more intense cyclones that have an impact in the interior (Pezza and Simmonds, 2008; Turner *et al.,* 2013). Regardless of the effects of the SAM, the regularity of its linked cycle to the ENSO is ambiguous, which means that its influence on ground thermal regimes can only be deduced when it is in the positive or the negative phase.

As has been pointed out, the SAM is increasingly becoming positive during summer and autumn, and this leads to the conclusion that the behaviour of ground temperatures in summer and autumn can be attributed to the strengthening of the SAM during these seasons. Moreover, it can be inferred from the literature that the loss of the ozone layer around spring that eventually affects the behaviour of the SAM, affects the variability of both air and ground temperatures to some extent. Lastly, assuming that the SAM becomes weaker during winter, it can be deduced that air temperatures, to some degree, fluctuate as they do because the storms brought about by the resultantly weaker westerlies are less intense and dissipate as early as they occur.

Unlike the ambiguity resulting from the cycle of the SAM, the cycle of the SAO and its effects are well understood. The effects of the semi-annual contraction and expansion of the pressure low around Antarctica on ground thermal regimes in WDML have been expounded greatly by Kotzé (2015). Nevertheless, it is important to note that both the SAM and the SAO are great atmospheric pressure systems, the cycles of which have an influence on active layer temperatures through varying pressure gradients.

5.2. Site Characteristics

5.2.1. Spatial and Regional Analysis

Comparisons between sites to determine the regional influence of meteorological variables, using air temperatures recorded from the South African Weather Service (SAWS) weather station at Vesleskarvet, has shown that the thermal regimes at the selected sites behave more similarly than differently. Site specific characteristics including the geology, geomorphology, distance and altitude of the site, contribute both to the regional similarities and differences of ground thermal behaviour.

An evaluation of the SAWS air temperatures and site ambient air temperatures shows a synchronicity between sites with Vesleskarvet and Schumarcherfjellet being highly synchronous with each other. The highest average air temperatures at Robertskollen throughout the year are due its location and altitude. At a distance of 150 km away from the ice shelf, it is the least continental site which means that warm coastal air advected by passing cyclones contributes to the relatively warm air temperatures that characterise the site. Additionally, the presence of liquid water at the site also regulates temperatures by contributing to a relatively high humidity level that ensures that air temperature variability is controlled.

On the other hand, Slettfjell, Grunehogna and Flårjuven had the lowest average air temperatures in summer while Troll had the lowest average air temperatures in winter. Slettfjell, Grunehogna and Flårjuven are all located further away from the ice shelf. Additionally they are at very high altitudes which could be a factor in the variability of the air temperatures. Similarly, the same could be said about Troll as well. The high range of temperatures could account for the temperature variability. Katabatic winds during winter may also have an influence on the persistently low air temperatures. The range of air temperatures during the summer months between sites is minimal which points to similar meteorological influences while in winter, the range of temperatures between sites is large which point to different influences including snow precipitation and the presence of winds along with the geology of the sites.

Ground temperatures have shown great synchronicity between the sites and between the SAWS air temperatures with the greatest synchronicity being between Schumacherfjellet and the SAWS air temperatures and the lowest being between Vesleskarvet and the SAWS air temperatures. The weak relationship between Vesleskarvet air and ground temperatures is intriguing because the SAWS weather station is +/- 300 m away from the logging station. The reason there is a weak relationship between the variables could be because of the presence of the blockfield at Vesleskarvet which promotes the accumulation of snowmelt water from the periodic snow cover (Kotzé. 2015). This leads to the suggestion that ground thermal regimes in Vesleskarvet are influenced by more than

variations in air temperatures as discussed in the previous section. On the other hand, the strong relationship between air temperatures recorded by the SAWS weather station and the ground thermal regimes in Schumarcherfjellet could point to the geology and the geomorphology of the site. Even though it is 25 km away from Vesleskarvet, it has flat-topped surfaces of doleritic rocks that comprise of patterned ground. Variations in temperature have been seen to influence ground behaviour (Kotzé, 2015).

Close analysis of the different sites shows that as synchronous as the temperatures across the sites are, site characteristics such as location and altitude as well as geomorphology, have a direct influence on temperature variations. For instance, in Vesleskarvet, a comparison of the near surface with deeper layers in the ground shows that the ground near the surface seems to be colder than at greater depths indicating that on average, temperatures near the ground surface are colder than the air above the ground and ground at greater depths. This can be attributed to the thermal properties of the large field of boulders that characterise the ground in Vesleskarvet. For Robertskollen however, on average, at greater depths (>30 cm) temperatures increase indicating a warmer and subsequently, a deeper active layer. This can be ascribed to the geomorphology and location of the site. Robertskollen has a higher altitude than Vesleskarvet and most sites. Morever, the presence of water on the site due to its high average maximum temperatures resulting from its close proximity to the ice shelf has a great effect on how the thermal regime of the active layer at Robertskollen greatly differs from Vesleskarvet.

Conversely, for Valterkulten, the increasing average temperatures with increasing depth suggest that Valterkulten, similar to Robertskollen, has a warmer and deeper active layer than Vesleskarvet. Similar to Robertskollen, Valterkulten has liquid water on its surface. The site of the logger was close to a brine lake in a depression. In addition to the longer heat retention properties of water, the presence of salts within the lake ensure that the active layer at Valterkulten remains warmer and deeper for longer with little change in temperature with increasing depth. Although Grunehogna and Schumarchefjellet are in close proximity, they do not exhibit similar ground thermal regimes which points to the different geomorphology that characterises each site.

For Flårjuven, the recorded average maximum temperatures above 0 °C near the surface and a depth of 15 cm below the ground (6.05 °C and 0.57 °C respectively) indicate that thawing of the active layer was at most up to 15 cm deep. For Slettfjell, average minimum temperatures exhibit an increasing trend of temperatures that might be attributed to the geology of the site. However, it is worth mentioning that temperature data logging for Slettfjell continued until 01 May. Therefore, the lack of a full year temperature record means that analysis of the active layer thermal regimes yields

inconclusive results in comparison to the other sites. Lastly, for Troll, despite being across the Jutulstraumen glacier, average ground temperatures are of the same magnitude as those at Vesleskarvet (T > -16 °C for both sites). This points to the climatic factors that influence both thermal regimes at Troll and at Vesleskarvet.

5.2.2. Inter-site Active Layer and Ground Thermal Properties

The characteristics of soils within continental Antarctica are dominated by physical properties. The physical properties of soils at the selected sites show that the soils are relatively dry, which corresponds to the atmospheric factors that influence the climatic conditions. The Gravimetric Water Content (GWC) of an active layer relates to the age of the soil (Kotzé, 2015). The GWC of all sites apart from Vesleskarvet, Valterkulten and, Flårjuven was less than 5%, which suggests that the soils beneath the active layer at these sites are less than 18 000 years old (Kotzé, 2015). This briefly satisfies the second part of the 39th question posed by Kennicutt *et al.,* (2014) that asks what the rates of geomorphic change in different Antarctic regions are and have been, and what the ages of the preserved landscapes are.

According to Briggs (1977b), soils that have an average bulk density of 1.25 g/cm^3 are identified as mineral soils, and those with an average bulk density of 0.5 g/cm^3 are identified as organic soils. Following the bulk density classification of soils, it can be seen that soils at the Ahlmannryggen are mineral soils. This is supported by visual evidence showing the absence of organic matter (see Appendix C, Figures 35 - 36, pg. 90). The bulk density values of soils at Vesleskarvet, Robertskollen and Flårjuven closely correspond with those found by Hansen (2013) at Vesleskarvet of 1.84 – 1.99 g/cm^3, and by Kotzé (2015) at Vesleskarvet, Robertskollen and Flårjuven of 1.97 g/cm^3, 1.83 g/cm^3 and 1.69 g/cm^3, respectively. The bulk density value of soil at Troll is significantly lower than that found by Kotzé (2015) of 2.04 g/cm^3.

The fact that soil at Vesleskarvet has the highest bulk density and water content when compared to all the other sites is most likely because of its location. The local climate for Veslekarvet, along with the combination of a high proportion of silt and clay particles ($\leq$ 63 µm) and the presence of a blockfield, promotes the accumulation of snowmelt water from periodic snow cover (Kotzé, 2015). Soil at Flårjuven and Valterkulten has relatively high water content compared to Robertskollen because both of these sites have a high proportion of silt and clay ($\leq$ 63 µm) and, moreover, Valterkulten has a depression where a brine lake is located. Robertskollen, on the other hand, has the highest proportion of medium to fine gravel (8 000 µm to 2 000 µm) after Grunehogna. In addition, the sampling site was on elevated ground, therefore any meltwater from accumulated snowfall easily drained downwards towards low lying meltwater pools. This is verified by the fact

that during the 2016/17 field season, streams and pools of meltwater from accumulated snow were present at the site (pers. obs, 2016).

Grunehogna has the lowest proportion of silt and clay (0.05 %) but greater water content than Schumarcherfjellet, Troll, and Slettfjell. The fact that its soil has a higher bulk density than that of Troll and Slettfjell means that, even though it has a low proportion of silt and clay, it can store more water within its soil. This can be attributed to the location of Grunehogna in relation to Troll and Slettfjell, as well as to the local climate. Even though the bulk density of soil at Schumarcherfjellet is greater than that of Grunehogna, the difference is very minimal, and the higher water content at Grunehogna could be attributed to other factors.

Given the ground (soil) properties of the sites, all sites with the exception of Vesleskarvet and Valterkulten, have shallower active layer depths compared to the long-term average active layer depth. The active layer depth at Schumarcherfjellet in 2016 was significantly shallower in comparison to the long-term average. Vesleskarvet and Valterkulten exhibited the same active layer depths both in 2016 and over the long-term average.

The deeper active layer of Robertskollen is attributed to spatial factors. At an altitude of approximately 350 m a.s.l. and a distance of 150 km away from the ice shelf, it is the least continental site, which means that its close proximity to the ice shelf allows for an influence of maritime climate conditions. On the other hand, the deep active layer at Troll could be due to geological properties of the ground. Compared to sites at Ahlmannryggen, Troll has a different geology, comprising of metamorphic granulites and gneisses. Vesleskarvet and all the sites in Ahlmannryggen consist mainly of doleritic igneous rocks. In contrast, Slettfjell has the least deep active layer depth and similarly to Robertskollen, it could be attributed to spatial factors. Slettfjell is the furthest site inland, at a distance of 233 km away from the ice shelf and an altitude of 1472 m a.s.l. Along with the low soil moisture content, the location of Slettfjell results in extremely dry conditions that do not encourage the formation of or the deepening of the active layer.

The inter-annual variability of the depth profiles was evenly balanced. For three sites, Vesleskarvet, Robertskollen, and Schumarcherfjellet, the minimum ground temperatures exhibited a larger inter-annual variability. In contrast, for Grunehogna, Flårjuven, and Slettfjell, the maximum ground thermal regimes exhibited a larger inter-annual variability. The inter-annual variability for Valterkulten and Troll was the same for both the minimum and the maximum ground thermal regimes, with that of Valterkulten being smaller and that of Troll being larger.

Furthermore, the long-term average active layer depth of all sites except Valterkulten and Troll was deeper than the 2016 active layer depth. This suggests a negative effect where various studies report on the warming conditions of the climate over Antarctica. It has been noted that global warming and climate change is evident in the loss of ice mass over West Antarctica (Vaughan and Arthern, 2007). However, east Antarctica has been reported to be gaining an additional ice mass annually (Vaughan and Arthern, 2007). However the above trends are difficult to predict with certainty (Vaughan and Arthern, 2007). The continuous addition of ice mass from increased snowfall over east Antarctica could explain the seemingly diminishing depth over the Ahlmannryggen sites.

However, since snow acts as an insulator, thus assisting in warming or increasing ground temperatures, it can be argued that as temperatures decrease along the ground profile, there is limited heat available to increase temperatures down the ground profile, thus resulting in shallower active layer depths and by inference, accruing permafrost. Therefore, in responding to part of the 42nd question asked by Kennicutt *et al.,* (2014) that asks how permafrost, the active layer and water availability in Antarctic soils [...] will change in a warming climate, and what the effects on ecosystems and biogeochemical cycles are; in a warming climate, it appears that the active layer depth of most sites in the Ahlmannryggen grows shallower and permafrost grows deeper.

According to Kotzé (2015), a larger inter-annual variability of minimum ground thermal regimes is due to an increased fluctuation of air temperatures in winter, caused by large meridional and vertical temperature gradients in winter as compared to summer. This means that low-pressure systems passing along the coast advect the relatively warm and moist air from the ocean towards the continent, which results in large changes in air temperature and wind speed. A larger inter-annual variability of maximum ground thermal regimes is due to a change in thermal diffusivity of the ground. Minimum and maximum ground thermal regimes that exhibit the same inter-annual variability mean that there is little variation in the temperatures and as a result they are synchronous with each other.

The properties of the active layer influence the transmission of thermal events from meteorological events. Three meteorological events were selected to determine the thermal propagation rate of the active layer at the study sites. Two of the events were low pressure systems that passed along the coast on 02-June and 17-November (see Figures 27b-c). These synoptic systems moved in a clockwise rotational motion with pressures well above 900 hPa. The other event was chosen in April for Slettfjell and August for Troll. The passage of the warm sector of the cyclone is accompanied by a drop in pressure and an increase in temperatures while the passage of the cold front is accompanied by a drop in temperatures as pressure rises again (Nel *et al.,* 2009). The rise and fall of temperatures

can clearly be seen in Figures 27-34 and the rate at which these events were first observed on the ground surface right down to the last monitored depth was analysed.

According to Schaetzl and Anderson (2005), the thermal propagation of soil is linked to the thermal conductivity of the specific soil, which is linked to the bulk density and the texture or the particle size of the soil. Thermal conductivity increases with an increase in bulk density and soil particle size. Following this point, the high thermal propagation rate of Grunehogna can be linked with the high proportion of medium to fine gravel particles of its soil (see Figure 17, pg 48). The high thermal propagation rates of Valterkulten and Robertskollen are linked to the large bulk densities of their soils (see Table 17, pg 47). The relatively high thermal propagation rate for Schumarcherfjellet can be linked to its soil bulk density as well, whereas the low thermal propagation rate for Slettfjell can be linked to the low bulk density of its soil. On the other hand, the relatively low thermal propagation rates for Flårjuven, Vesleskarvet and Troll can be linked to their high proportions of silt and clay particles (see Figure 17, pg 48).

It is clear and evident that in a warming climate, the periglacial environment of Western Dronning Maud Land (WDML) responds by decreasing the active layer depth and increasing the permafrost layer. Owing to different site characteristics such as geology, geomorphology, site location and altitude, and soil physical properties, ground thermal regimes respond variably to meteorological influences that differ seasonally and diurnally and per event. This chapter has succinctly shown how sites in WDML react to meteorological influences. The following chapter draws on final conclusions to this project by giving remarks, limitations on the current project and recommendations for future research.

Chapter 6: Conclusion

6.1. Remarks

This chapter focuses on linking the objectives discussed in the previous chapter to the aim of the project. The aim of this study was formulated to add to the growing contribution to research on permafrost and active layer dynamics of Antarctica, notably phrased by the 42nd question put forward by Kennicutt *et al.,* (2014). In order to fulfil the aim of using high-frequency data to determine the impact of seasonal, synoptic and diurnal events on ground thermal regimes, three objectives were devised as thus:

1. To establish meteorological influences on air and ground thermal regimes.
2. To determine the extent to which meteorological point data measured at Vesleskarvet (SANAE IV base) can be applied regionally to evaluate ground thermal regimes.
3. To determine the extent (depth) of meteorological events on ground thermal regimes.

The main crux of the first objective was to understand climatic and weather influences on ground temperatures in Vesleskarvet. Five meteorological parameters (air temperature, pressure, relative humidity, wind speed and wind direction) were explored and it was revealed that the active layer thermal regime is influenced by air temperature, relative humidity, pressure, and to some degree, wind speed. The influence of air temperatures, pressure, relative humidity and wind speed on the behaviour of ground temperatures differs according to seasons.

Air temperatures and near-surface temperatures were inversely related. During summer, near surface temperatures had the highest maximums and the lowest minimums, thus resulting in a high variability. During winter, air temperatures had the highest maximums and the lowest minimums resulting in a high variability therefore, indicating a more thermally active ground in summer in comparison to winter. The selected synoptic and diurnal events further attest to the varying thermal behaviour of the ground seasonally.

Pressure and relative humidity had an indirect relationship whose relationship with ground temperatures was dependent on the variability (instead of average values) of pressure and relative humidity. Pressure had a greater influence on ambient air and ground temperatures in summer than in winter even though on average, the mean pressure was high in summer and less variable than in winter. The behaviour of pressure is linked to the SAM and SAO in the Southern Ocean as well as low pressure cell over the interior of Antarctica. Together, the two pressure systems affect variability of pressure in Vesleskarvet whose impact on ground thermal regimes can be seen mainly in summer.

On average, whilst wind direction has been found to have no influence on ground temperatures, wind speed had a very limited influence on the active layer thermal regimes, showing a weak positive correlation in May and a strongly negative correlation with ground temperatures in January, November and December. The positive correlation corresponded with low ground temperatures in May and the negative correlations corresponded with high ground temperatures in January, November and December, as can be seen in Figure 10 (pg. 34). However, as Table 3 showed, the average wind speed in May was the highest average speed in 2016 at 13.72 $m.s^{-1}$ and the lowest average speeds that correspond with January, November and December were 8.53 $m.s^{-1}$, 9.34 $m.s^{-1}$ and 5.84 $m.s^{-1}$. These results suggest that wind speed is inversely proportional to ground temperatures. It is worth mentioning however, that the predominant direction of the wind is south-easterly as highlighted by numerous authors.

The second objective focused on using air temperature data from the SAWS weather station situated in Vesleskarvet to determine the linkages between Vesleskarvet and other sites (Robertskollen, Valterkulten, Grunehogna, Schumarcherfjellet, Flårjuven, Slettfjell, and Troll) in WDML. As presented in Table 8, Figure 11 and Figure 12, air and ground temperatures in Schumarcherfjellet had the highest correlation with SAWS air temperatures and, air and ground temperatures in Vesleskarvet had the lowest correlation with the SAWS air temperatures in comparison to other sites. However, the synchronicity between SAWS air temperatures and Schumarcherfjellet near-surface ground temperatures differs seasonally, with summer showing the greatest synchronicity and winter showing the least synchronicity. Temperature ranges and fluctuations also differed according to seasons, with air temperatures showing the lowest range between sites in summer and the largest range in winter. Conversely, near surface and ground temperatures showed the largest range of temperatures between sites in summer and the lowest range of temperatures in winter.

Close analysis of each site showed that on average, Vesleskarvet near surface temperatures were colder than both the air above the ground and deeper depths down the ground. In contrast, all the other sites had colder average air temperatures in comparison to the ground. However, Grunehogna had the coldest near surface temperatures at -18.07 °C and Robertskollen had the warmest (relatively speaking) near surface temperatures at -12.83 °C.

Furthermore, Robertskollen had the highest average air and ground temperatures throughout the year. Grunehogna, Flårjuven and Slettfjell had the lowest average air temperatures in summer while Troll had the lowest average air temperatures in winter. Conversely, Valterkulten had the highest average near-surface temperatures throughout the year after Robertskollen. Schumarcherfjellet and Slettfjell had the lowest average near-surface temperatures in summer and Grunehogna, Flårjuven

and on occasion, Troll had the lowest near-surface temperatures in winter. With increasing depths below the ground (after Robertskollen), Valterkulten had the highest average ground temperatures in summer and Schumarcherfjellet had the highest average ground temperatures in winter. Vesleskarvet had the highest average ground temperatures in autumn and spring.

The focal point of the third objective was to determine the degree of influence that selected weather events exert on the active layer depth. In as much as meteorological parameters have an effect on ground thermal regimes; their influence relies on soil properties of the site affected. Due to their bulk density, soils in the Ahlmannryggen are classified as mineral soils, which means that they lack considerable organic matter. This suggests that thermal activity within the soils is governed mainly by physical properties including bulk density and sediment particle size of soils.

Of all the sites studied, Vesleskarvet had the highest bulk density, followed by Robertskollen, Valterkulten, and Troll. Equally, Slettfjell had the lowest bulk density, followed by Flårjuven, Grunehogna, and Schumarcherfjellet. It is worth mentioning that although Vesleskarvet had a high proportion of silt and clay sediment particles after Flårjuven and the highest bulk density, sediment particle size does not necessarily correspond with bulk density. Instead, sediment particle size strongly corresponds with the amount of water that can be stored within the soil seen from Table 17. However, sediment particle size along with soil bulk density has been found to influence the propagation of temperature through the ground profile. As such, thermal propagation rates of sites varied according to the different sediment particle sizes and bulk densities of soils at each site.

Grunehogna had the highest average thermal propagation rate, followed by Valterkulten, Robertskollen and Schumarcherfjellet. Conversely, Troll had the lowest average thermal propagation rate, followed by Slettfjell, Flårjuven and Vesleskarvet. The thermal propagation rate of Grunehogna was due to the high proportion of medium to fine gravel particles of its soils, while those of Valterkulten, Robertskollen, Schumarcherfjellet as well as Slettfjell were due to the bulk densities of their soils. In contrast, the thermal propagation rate of Troll, Flårjuven and, Vesleskarvet were due to the high proportion of silt and clay particles of their soils.

The varying thermal propagation rates of each site could have an influence on the yearly active layer depth of each site. The active layer depths for 2016 in each site differed from the site long-term average active layer depths. All sites, with the exception of Vesleskarvet and Valterkulten, had on average, a deeper active layer compared to the 2016 depth. On close analysis, in 2016, Robertskollen had a deeper active layer, followed by Troll, Valterkulten, Flårjuven and Vesleskarvet. Equally, Slettfjell had a shallower active layer, followed by Schumarfjellet and Grunehogna. The

active layer depths are, in addition to the thermal propagation rates, dependent on site characteristics. Robertskollen and Valterkulten have deep active layers because of the presence of liquid water during summer. As has been pointed out, the presence of water aids in heat retention in the ground. Furthermore, distance from the ice shelf along with altitude has a great influence on the maximum depth of an active layer for each site. This is highly evident with Robertskollen and Slettfjell.

6.2. Recommendations and Limitations

The monitoring of the active layer and subsequently permafrost layer in Western Dronning Maud Land (WMDL) has great advantages in advancing Antarctic science research. In order to ensure that progressive research in WDML continues, certain limitations encountered in this project need to be considered for future research on the subject.

To get a full measure of the active layer depth and the behaviour of the regimes thereof, the boreholes of the sites need to be increased to at least 2 m or more. Additionally, long-term monitoring needs to continue so as to get the long-term changes in the active layer regimes. Meteorological variables have been noted to have an impact on ground thermal regimes. In WDML, there are no recorded precipitation and solar radiation values. Solar radiation analysis was based on Kotzé (2015) whose results were based on averaged interpolated readings from nearby stations. The absence of the meteorological variables impedes proper analysis of the active layer thermal regimes. Instead, it is suggested that for precipitation (in order to get snow depth at each site) iButtons need to be installed along with the temperature data loggers along the pole that supports the air temperature sensor at fixed heights (Lewkowicz, 2008; Kotzé, 2015). For solar radiation values, each borehole needs to have a pyronometer installed in order to get site-specific solar radiation readings.

Soil moisture values that were available from the soil moisture sensor could not be used due to faulty readings. This is due to fact that the soil moisture sensors were installed horizontally instead of vertically. The horizontal installation was so that a more representative reading of the site soil moisture could be obtained since only one soil moisture sensor was used per site. However, due to the dry conditions of WDML, the soil moisture sensors recorded static electricity generated by the friction between the wind and the low relative humidity of the region (Meiklejohn, pers. comm., 2017). Therefore, in order to get usable readings, the soil moisture sensors need to be installed vertically (Cobos and Chambers, 2009; Kotzé, 2015).

Finally, each site needs to have more loggers installed to avoid faulty loggers that capture incomplete data as in Slettfjell and Vesleskarvet. Moreover, more data loggers per site would ensure a more holistic analysis of the active layer thermal regimes because more loggers would provide a good representation of the site, instead of only one logger that does not capture the whole thermal regime of the site.

In conclusion, this research has contributed to the growing research on Antarctic science, focusing particularly on ground thermal regimes. It has shown that active layer thermal regimes depend on atmospherical phenomena as well as site-specific soil and geomorphological characteristics. Overall, the study has shown that climate change indeed does have an impact on the localised Antarctic interior as much as it does on coastal regions. Further research needs to be conducted in other nunataks in addition to the ones studied in the Ahlmannryggen, in order to get a broader understanding of the long-term responses of the active layer and the permafrost layer to climate change. Such research could focus on the presence of human activity in the Ahlmannryggen and the influence that it has on the local ecosystems and biogeochemical cycles. Although care is taken by researchers in the Ahlmannryggen (and Antarctica as a whole), some form of impact is exerted on the environment and effects of this are still yet to fully manifested.

References

Adlam, L.S., Balks, M.R., Seybold, C.A. and Campbell, D.I. 2010. Temporal and spatial variation in active layer depth in the McMurdo Sound Region, Antarctica. *Antarctic Science*, 22: 45-52.

Almeida, I.C.C., Schaefer, C.E.G.R., Fernandes, R.B.A., Pereira, T.T.C., Nieuwendam, A. and Pereira, A.B. 2014. Active layer thermal regime at different vegetation covers at Lions Rump, King George Island, Maritime Antarctica. *Geomorphology,* 225: 36-46.

ATS, 2013. *Antarctic treaty*. Center for Nonproliferation Studies: Inventory of International Nonproliferation Organizations and Regimes, June 1961.

Beyers, J.H.M. and Harms, T.M. 2003. Outdoors modelling of snowdrift at SANAE IV Research Station, Antarctica. *Journal of Wind Engineering and Industrial Aerodynamics,* 91: 551-569.

Bilskie, J. 2001. Soil water status: content and potential. *Campbell Scientific, Inc.,* 432: 753-2342.

Bintanja, R. 2000. Mesoscale Meteorological Conditions in Dronning Maud Land, Antarctica, during Summer: A Qualitative Analysis of Forcing Mechanisms. *Journal of Applied Meteorology,* 39(12): 2348-2370.

Bockheim, J.G. 2005. *International Workshop on Antarctic Permafrost and Soils.* Office of Polar Programs, Antarctic Section: National Science Foundation, Project OPP-0425692.

Bölter, M., Beyer, L. and Stonehouse, B., 2002. Geoecology of Antarctic Ice-Free Coastal Landscapes. *Ecological Studies,* 154: 1-6.

Briggs, D.J. 1977a. *Sources and methods in Geography – Sediments.* London: Butterworth & Co. Ltd.

Briggs, D.J. 1977b. *Sources and methods in Geography – Soils.* London: Butterworth & Co. Ltd.

Brown, A. 2012. Accounting for Snow Types. *Nature Climate Change*, 2, 394.

Bunting, B.T. 1967. *The Geography of Soil.* London: Hutchinson & Co. Ltd.

Cassano, J.J. 2013. Climate of extremes. *In* Walton, D.W.H. (ed.). *Global Science From a Frozen Continent.* New York: Cambridge University Press. p. 102-136.

Church, M. 2013. Refocusing geomorphology: Field work in four acts. *Geomorphology,* 200: 184-192.

Cobos, D. and Chambers, C. 2009. Calibrating ECH2O soil moisture sensors. Application note, *Decagon Devices, Inc*., Pullman, Wash. p. 1-4.

Cocks, M.P., Newton, I.P. and Stock, W.D. 1998. Bird effects on organic processes in soils from five microhabitats on a nunatak with and without breeding snow petrels in Dronning Maud Land, Antarctica. *Polar Biology,* 20: 112-120.

Convey, P., Bindschadler, R., di Prisco, G., Fahrbach, E., Gutt, J., Hodgson, D.A., Mayewski, P.A., Summerhayes, C.P., Turner, J. and The ACCE Consortium. 2009. Antarctic climate change and the environment. *Antarctic Science,* 21(6): 541-563.

Cooper, J. Department of Environmental Affairs and Tourism. 2006. *Antarctica and Islands.* Cape Town: University of Cape Town.

Courtney, F.M. and Trudgill, S.T. 1984. *The soil – An introduction to Soil Study* (2ed). London: Edward Arnold Ltd.

Delaygue, G., Masson, V., Jouzel, J., Koster, R.D. and Healy, R.J. 2000. The origin of Antarctic precipitation: a modelling approach. *Tellus,* 52B: 19-36.

Dobinski, W. 2011. Permafrost. *Earth-Science Reviews,* 108(3-4): 158-169.

Dodds, K., Hemmings, A.D. and Roberts, P. 2017. Introduction – the politics of Antarctica. *In* Dodds, K., Hemmings, A.D. and Roberts, P. (eds), *Handbook on the Politics of Antarctica.* Cheltenham: Edward Elgar Ltd.

Dwight, R.A. 2014. *Geomorphic and ambient environmental impacts on lichen distribution on two inland nunataks in Western Dronning Maud Land, Antarctica.* Grahamstown: Rhodes University (MSc thesis) [pdf].

Elzinga, A. 2017. The continent for science. *In* Dodds, K., Hemmings, A.D. and Roberts, P. (eds), *Handbook on the Politics of Antarctica.* Cheltenham: Edward Elgar Ltd.

French, H. 2007. *The periglacial environment (3ed.).* Sussex, England: John Wiley & Sons Ltd.

Guglielmin, M. 2012. Advances in permafrost and periglacial research in Antarctica: A review. *Geomorphology,* 155-156: 1-6.

Guglielmin, M. and Vieira, G. 2014. Permafrost and periglacial research in Antarctica: New results and perspectives. *Geomorphology,* 225: 1-3.

Guglielmin, M., Worland, M.R., Baio, F. and Convey, P. 2014. Permafrost and snow monitoring at Rothera Point (Adelaide Island, Maritime Antarctica): Implications for rock weathering in cryotic conditions. *Geomorphology,* 225: 47-56.

Gugliemin, M., Worland, M.R. and Cannone, N. 2012. Spatial and temporal variability of ground surface temperature and active layer thickness at the margin of maritime Antarctica, Signy Island. *Geomorphology,* 155-156: 20-23.

Hansen, C.D. 2013. *The Characterisation of an openwork block deposit, Northern Buttress, Vesleskarvet, Dronning Maud Land, Antarctica.* Grahamstown: Rhodes University (MSc thesis) [pdf].

Hansen, J., Sato, M., Kharecha, P. and von Schuckmann, K. 2011. Earth's energy imbalance and implications. *Atmospheric Chemistry and Physics,* 11(24): 421-449.

Hao, X., Ball, B.C., Culley, J.L.B., Carter, M.R. and Parkin, G.W. 2008. Soil Density and Porosity. *In* Carter, M. R. and Gregorich, E. G. (eds.), *Soil Sampling and Methods of Analysis* (2ed). Boca Raton: CRS Press.

Harris, P.D. 1999. *The Geological evolution of Neumayerskarvet in the northen Kirwanveggen; Western Dronning Maud Land, Antarctica.* Johannesburg: Rand Afrikaans University (PhD thesis) [pdf].

Harris, R. and Jarvis, C. 2011. *Statistics in Geography and Environmental Science.* Harlow: Pearson Education Ltd.

Hermichen. W.D. 1995. The continental ice cover in the surroundings of the Schirmacher Oasis. *In* Bormann, P. and Fritzsche, D. (eds.*). The Schirmacher Oasis, Queen Maud Land, East Antarctica, and its surroundings.* Germany: Justus Perthes Verlag Gotha, 221-242.

Huggett, R.J. 2011. *Fundamentals of Geomorphology (3ed.).* USA: Routledge.

Ingvander, S., Jansson, P., Brown, I.A., Fujita, S., Sugyama, S., Surdyk, S., Enomoto, H., Hansson, M. and Holmund, P. 2016. Snow particle sizes and their distributions in Dronning Maud Land, Antarctica, at sample, local and regional scales. *Antarctic Science,* 1-13.

IPA. 2012. *Global terrestrial network on permafrost (GTN-P): Strategy and implementation plan*. 2012-2016.

Isaksson, E. and Karlen, W. 1994. Spatial and temporal patterns in snow accumulation, western Dronning Maud Land, Antarctica. *Journal of Glaciology,* 40(135): 399-409.

Ishikawa, M. 2003. Thermal regimes at the snow-ground interface and their implications for permafrost investigation. *Geomorphology*, 52: 105-120.

Jones, D.L., Bates, M.P., Li, Z.X., Corner, B. and Hodgkinson, G. 2003. Palaeomagnetic results from the ca. 1130 Ma Borgmassivet intrusions in the Ahlmannryggen region of Dronning Maud Land, Antarctica, and tectonic implications. *Tectonophysics,* 375: 247-260.

Kärkäs, E., 2004. Meteorological conditions of the Basen nunatak in western Dronning Maud Land, Antarctica, during the years 1989-2001. *Geophysica,* 40(1-2): 39-52.

Kato, S., Rose, F.G. and Rutan, D.A., 2008. Cloud effects on the meridional atmospheric energy budget estimated from clouds and the earth's radiant energy system (CERES) data. *Journal of Climate,* 21(17): 23-41.

Kennicutt II, M.C., Chown, S.L., Cassano, J.J., Liggett, D., Peck, L.S., Massom, R., Rintoul, S.R., Storey, J., Vaughan, D.G., Wilson, T.J., Allison, I., Ayton, J., Badhe, J., Baeseman, Barrett, P.J., Bell, R.E., Bertler, N., Bo, S., Brandt, A., Bronmwich, D., Cary, S.C., Clark, M.S., Convey, P., Costa, E.S., Cowan, D., Deconto, R., Dunbar, R., Elfring, C., Esctia, C., Francis, J., Fricker, H.A., Fukuchi, M., Gilbert, N., Gutt, J., Havermans, C., Hik, D., Hosie, G., Jones, C, Kim, Y.D., Le Maho, Y., Lee, S.H., Leppe, M., Leitchenkov, G., Li, X., Lipenkov, V., Lochte, K., López-Martínez, J., Lüdecke, C., Lyons, W., Marenssi, S., Miller, H., Morozova, P., Naish, T., Nayak, S., Ranindra, R., Retamales, J., Ricci, C.A., Rogan-Finnemore, M., Ropert-Coudert, Y., Samah, A.A., Sanson,L., Scambos, T., Schloss, I. R., Shiraishi, K., Siegert, M.J., Simões, J.C., Storey, B., Sparrow, M.D., Wall, D.H., Walsh, J.C., Wilson, G., Winther, J.G., Xaveir, J.C., Yang, H. and Sutherland, W. J. 2014. A roadmap for Antarctic and Southern Ocean science for the next two decades and beyond. *Antarctic Science*, 27: 3-18.

Keys, H.J.R. n.d. *Air temperature, wind, precipitation and atmospheric humidity in the McMurdo region, Antarctica.* Wellington: Victoria University of Wellington.

Koorevaar, P., Menelik, G. and Dirksen, C. 1983. *Elements of soil physics.* Amsterdam: Elsevier.

Kotzé, C. 2015. *Active Layer Dynamics at Four Borehole Sites in Western Dronning Maud Land, Antarctica.* Grahamstown: Rhodes University (MSc thesis) [pdf].

Krynauw, J.R. 1986. *The petrology and geochemistry of intrusions at selected nunataks in the Ahlmannryggen and Giaverryggen, Western Dronning Maud Land, Antarctica.* Pietermaritzburg: University of Natal (PhD thesis) [pdf].

Lewkowicz, A.G. 2008. Evaluation of miniature temperature-loggers to monitor snowpack evolution at mountain permafrost sites, North Western Canada. *Permafrost and Periglacial Processes*, 19: 323-331.

Marchenko, S. and Etzelmüller, B. 2013. Permafrost: Formation and distribution, thermal and mechanical properties. *In* Giardino, R. and Harbor, J (eds.). *Treatise on Geomorphology*. London: Elsevier Inc., 202-222.

Marshall, H.R., Hawkesworth, C.J. and Leat, P.T. 2013. Mesoproterozoic subduction under the eastern edge of the Kalahari-Grunehogna Craton preceding Rodinia assembly: The Ritscherflya detrital zircon record, Ahlmannryggen (Dronning Maud Land, Antarctica). *Precambrian Research,* 236: 31-45.

Meiklejohn, K.I. 2009. Initial Environmental Evaluation - Geomorphology and Climate Change. Pretoria: Department of Environmental Affairs.

Meiklejohn, K.I. 2017. Professor and Researcher, Geography Department: Rhodes University. Personal Communication. 2016 – 2017.

Michel, R.F.M., Schaefer, C.E.G.R., Poelking, E.L., Simas, F.N.B., Fernandes Filho, E.I. and Bockheim, J.G. 2012. Active layer temperature in two cryosols from King George Island, Maritime Antarctica. *Geomorphology,* 155-156: 12-19.

Mlynczak, P.E., Smith, G.L. and Doelling, D.R., 2011. The annual cycle of earth radiation budget from clouds and the Earth's Radiant Energy System (CERES) data. *Journal of Applied Meteorology and Climatology,* 50(12): 2490-2503.

Murphy, B.F. and Simmonds, I., 1993. An Analysis of Strong Wind Events Simulated in a GCM Near Casey in the Antarctic. *Monthly Weather Review,* 121: 522-534.

Nel, W., van der Merwe, B. and Meiklejohn, K.I. 2009. Rethinking climate change impacts on subsurface temperatures in a sub-Antarctic mire affected by synoptic scale processes. *Earth Surface Processes and Landforms,* 34: 1446-1449.

Noone, D., Turner, J. and Mulvaney, R., 1999. Atmospheric signals and characteristics of accumulation in Dronning Maud Land, Antarctica. *Journal of Geophysical Research,* 104(D16): 191-211.

Pennock, D., Yates, T. and Braidek, J. 2008. Soil sampling designs. *In* Carter, M. R. and Gregorich, E. G. (eds.), *Soil Sampling and Methods of Analysis* (2ed). Boca Raton: CRS Press.

Pezza, A.B. and Simmonds, I. 2008. Large-scale factors in tropical and extratropical cyclone transition and extreme weather events. *Annals of the New York Academy of Sciences,* 1146: 189-211.

Reijmer, C.H. and Oerlemans, J. 2002. Temporal and spatial variability of the surface energy balance in Dronning Maud Land, East Antarctica. Journal of Geophysical Research, 107(D24): 4759-4770.

Richter, W. and Bormann. P. 1995. Weather and climate. *In* Bormann, P. and Fritzsche, D. (eds.*). The Schirmacher Oasis, Queen Maud Land, East Antarctica, and its surroundings.* Germany: Justus Perthes Verlag Gotha, 207-220.

Robinson, S.A., Wasley, J. and Tobin, A.K. 2003. Living on the edge-plants and global change in continental and maritime Antarctica. *Global Change Biology,* 9(12): 1681-1717.

Ryan, P.G. and Watkins, B.P., 1989. Snow petrel breeding biology at an inland site in continental Antarctica. *Colonial Waterbirds,* 12(2): 176-184.

SANAP. 2015. *SANAE – History.* [Online]. Available: http://www.sanap.ac.za/sanap_sanae/sanae_history.html [10/04/2015].

Schaetzl, R. J. and Anderson, S. 2005. *Soils – Genesis and Geomorphology.* New York: Cambridge University Press.

Schlosser, E., Duda, M.G., Powers, J.G. and Manning, K.W. 2008. Precipitation regime of Dronning Maud Land, Antarctica, derived from Antarctic mesoscale prediction System (AMPS) archive data. *Journal of Geophysical Research*. 113: 1-9.

Schlosser, E., Manning, K.W., Powers, J.G., Duda, MG., Birnbaum, G. and Fujita, K. 2010. Characteristics of high-precipitation events in Dronning Maud Land, Antarctica. *Journal of Geophysical Research Atmospheres,* 115(D14107): 1-14.

Schlosser, E., Powers, J.G., Duda, M.G., Manning, K.W., Reijmer, C.H., van den Broeke, M.R. 2010. An extreme precipitation event in Dronning Maud Land, Antarctica: A case study with the antarctic mesoscale prediction system. *Polar Research,* 29(3): 330-344.

Scott, D.A. 2014. *On active layer processes and landforms in Western Dronning Maud Land, Antarctica.* Grahamstown: Rhodes University (MSc thesis) [pdf].

Seppälä, M. 2004. *Wind as a Geomorphic Agent in Cold Climates.* Cambridge: Cambridge University Press.

Simmonds, I., Keay, K. and Lim, E.-P., 2003. Synoptic Activity in the Seas around Antarctica. *Monthly Weather Review,* 131(2): 272-288.

Speirs, J.C., Steinhoff, D.F., McGowan, H.A., Bromwich, D.H. and Monaghan, A.J. 2010. Foehn winds in the McMurco Dry Valleys, Antarctica: The origin of extreme warming events. *Journal of Climate*, 23: 3577-3598.

Steele, W.K. and Copper, J. 2012. Some food items of the South Polar Skua *Stercorarius Maccormicki* at inland sites in the Ahlmannryggen, Dronning Maud Land, Antarctica. *Marine Ornithology,* 40: 63-66.

Steinhoff, D.F., Bromwich, D.H. and Monaghan, A.2013. Dynamics of the foehn mechanis, in the McMurdo Dry Valleys of Antarctica from Polar WRF. *Quarterly Journal of the Royal Meteorological Society,* 139: 1616-1631.

Terauds, A. and Lee, J.R. 2016. Antarctic Biogeography Revisited: Updating the Antarctic Conservation Biogeographic Regions. *Diversity and Distributions*, 22, 836-840.

Tobler, W.R. 1970. A computer movie simulating urban growth in the Detroit region. Economic Geography 46: 234–40.

Toggweiler, J.R. and Key, R.M. n.d. *Ocean Circulation-Thermohaline Circulation*. 1-9.

Toggweiler, J.R. and Russell, J., 2008. Ocean circulation in a warming climate. *Nature,* 451(7176): 286-288.

Trenberth, K.E., Fasullo, J.T. and Kiehl, J., 2009. Earth's global energy budget. *Bulletin of the American Meteorological Society,* 90(3): 311-323.

Tsukernik, M. and Lynch, A.H. 2013. Atmospheric meridional moisture flux over the Southern Ocean: a story of the Amundsen Sea. *Journal of Climate,* 26: 8055-8064.

Turner, J., Barrand, N.E., Bracegirdle, T.J., Convey, P., Hodgson, D.A., Jarvis, M., Jenkins, A., Marshall, G., Meredith, M.P., Roscoe, H., Shanklin, J., French, J., Goosse, H., Guglielmin, M., Gutt, J., Jacobs, S., Kennicutt, M.C., Masson-Delmotte, V., Mayewski, P., Navarro, F., Robinson, S.,

Scambos, T., Sparrow, M., Summerhayes, C., Speer, K. and Klepikov, A. 2013. Antarctic Climate Change and the Environment: An Update. *Polar Record,* 50: 1-23.

Vaughan, D.G. and Arthern, R. 2007. Why Is It Hard to Predict the Future of Ice Sheets? *Science*, 315: 1503-1504.

Vieira, G., Bockheim, J., Guglielmin, M., Balks, M., Abramov, A.A., Boelhouwers, J., Cannone, N., Ganzert, L., Gilichinsky, D.A., Goryachkin, S., López-Martínez, J., Meiklejohn, I., Raffi, R., Ramos, M., Schaefer, C., Serrano, E., Simas, F., Sletten, R. and Wagner, D. 2010. Thermal state of permafrost and active-layer monitoring in the Antarctic: Advances during the International Polar Year 2007-2009. *Permafrost and Periglacial Processes,* 21: 182-197.

Weil, R.R. and Brady, N.C. 2017. *The nature and properties of soils* (15ed). Harlow: Pearson Education.

Wilhelm, K.R. and Bockheim, J.G. 2017. Climatic controls on active layer dynamics: Amsler Island, Antarctica. *Antarctic Science,* 29(2): 173-182.

Williams, P.J. and Smith, M.W. 1989. *The frozen earth: Fundamentals of Geocryology*. Cambridge: Cambridge University Press.

Appendices

Appendix A. Statistical Descriptions, Ranges, and Classes

Table 19. Skewness classes descriptive terms and ranges (Kotzé, 2015)

Description	Range
Highly negatively skewed	< -1.62
Negatively skewed	-1.0 – -1.62
Moderately skewed	-0.3 – -0.1
Finely negatively skewed	-0.1 – 0.1
Positively skewed	0.1 – 0.3
Finely negatively skewed	0.3 – 1.0
Very positively skewed	1.0 – 1.62
Highly positively skewed	> 1.62

Table 20. Pearson's Correlation descriptive terms and ranges (Hansen, 2013)

Description	Range
Perfect downhill linear relationship	-1
Strong downhill linear relationship	-0.70
Moderate downhill linear relationship	-0.50
Weak downhill linear relationship	-0.30
No linear relationship	0
Weak uphill relationship	0.30
Moderate uphill linear relationship	0.50
Strong uphill linear relationship	0.70
Perfect uphill linear relationship	1

Table 21. Sedimentary Particle Size Grades (Briggs, 1977a)

Phi Size (ø)	Millimetres (mm)	Micrometres (µ)	Wentworth Grade
-6.0	64	64000	*Cobbles*
			60.0 mm
-5.5	44.8	44800	*Coarse Gravel*
-5.0	32	32000	
-4.5	22.4	22400	
			20.0 mm
-4.0	16	16000	*Medium Gravel*
-3.5	11.2	11200	
-3.0	8	8000	
			6.0 mm
-2.5	5.6	5600	*Fine Gravel*
-2.0	4	4000	
-1.5	2.8	2800	
-1.0	2	2000	2.0 mm
-0.5	1.4	1400	*Coarse Sand*
0.0	1	1000	
0.5	0.71	710	
			0.6 mm
1.0	0.5	500	*Medium Sand*
1.5	0.355	355	
2.0	0.25	250	
			0.2 mm
2.5	0.18	180	*Fine Sand*
3.0	0.125	125	
3.5	0.090	90	
4.0	0.063	63	
			0.06 mm
4.5	0.045	45	*Coarse Silt*
5.0	0.032	32	
5.5	0.023	23	
			0.02 mm
6.0	0.016	16	*Medium Silt*
6.5	0.011	11	
7.0	0.008	8	
			0.006 mm
7.5	0.0055	5.5	*Fine Silt*
8.0	0.004	4.0	
8.5	0.00275	2.75	
9.0	0.002	2.0	0.002 mm
9.5	0.00138	1.38	*Clay*
10.0	0.001	1.0	

Appendix B. Pearson's Correlations for Vesleskarvet air and ground temperatures with SAWS weather variables

Table 22. Pearson's Correlations (r) for 2016 monthly averages of ambient air temperature with the SAWS recorded air temperature, humidity, pressure, wind speed and wind direction

	Temperature	*Pressure*	*Humidity*	*Wind Speed*	*Wind Direction*
Jan	0.915	0.708	-0.147	-0.789	-0.124
Feb	0.962	0.293	0.233	-0.005	0.107
Mar	0.980	-0.101	0.214	0.096	-0.370
Apr	0.985	0.302	0.503	0.364	-0.302
May	0.982	-0.323	0.038	0.455	-0.326
Jun	0.962	-0.162	0.225	0.232	0.031
Jul	0.989	-0.138	-0.132	-0.162	-0.103
Aug	0.993	0.406	0.432	0.242	-0.090
Sep	0.991	0.480	-0.058	0.077	0.079
Oct	0.960	-0.051	0.197	-0.139	0.019
Nov	0.965	0.281	-0.196	-0.693	0.424
Dec	0.972	0.581	-0.420	-0.744	0.360
Average	**0.971**	**0.190**	**0.074**	**-0.089**	**-0.024**

Table 23. Pearson's Correlations (r) for 2016 monthly averages of near-surface temperature with the SAWS recorded air temperature, humidity, pressure, wind speed and wind direction

	Temperature	*Pressure*	*Humidity*	*Wind Speed*	*Wind Direction*
Jan	0.909	0.854	-0.462	-0.949	-0.295
Feb	0.736	0.162	0.401	0.188	-0.122
Mar	0.741	-0.028	0.129	0.015	-0.446
Apr	0.821	-0.095	0.707	0.288	-0.296
May	0.874	-0.154	0.246	0.490	-0.508
Jun	0.771	-0.136	0.630	0.050	-0.018
Jul	0.829	-0.043	0.278	-0.139	-0.364
Aug	0.868	0.633	0.417	0.105	-0.083
Sep	0.857	0.529	0.200	0.201	-0.170
Oct	0.807	-0.228	0.156	-0.028	0.009
Nov	0.723	0.023	0.193	-0.438	-0.018
Dec	0.644	0.716	-0.366	-0.631	0.025
Average	**0.798**	**0.186**	**0.211**	**-0.071**	**-0.190**

Table 24. Pearson's Correlations (r) of 2016 monthly averages of 15 cm ground depth temperature with the SAWS recorded air temperature, humidity, pressure, wind speed and wind direction

	Temperature	*Pressure*	*Humidity*	*Wind Speed*	*Wind Direction*
Jan	0.888	0.869	-0.275	-0.910	-0.158
Feb	0.820	0.244	0.471	0.102	-0.059
Mar	0.815	-0.014	0.122	-0.014	-0.432
Apr	0.853	-0.029	0.698	0.258	-0.279
May	0.879	-0.169	0.177	0.417	-0.432
Jun	0.819	-0.121	0.554	0.052	-0.014
Jul	0.892	-0.070	0.158	-0.168	-0.293
Aug	0.880	0.601	0.383	0.068	-0.057
Sep	0.904	0.533	0.114	0.116	-0.087
Oct	0.798	-0.204	0.023	-0.181	0.104
Nov	0.771	0.001	-0.031	-0.660	0.255
Dec	0.815	0.666	-0.461	-0.759	0.202
Average	**0.845**	**0.192**	**0.161**	**-0.140**	**-0.104**

Table 25. Pearson's Correlations (r) of 2016 monthly averages of 30 cm ground depth temperature with the SAWS recorded air temperature, humidity, pressure, wind speed and wind direction

	Temperature	*Pressure*	*Humidity*	*Wind Speed*	*Wind Direction*
Jan	0.847	0.861	-0.360	-0.872	-0.032
Feb	0.672	0.160	0.478	0.158	-0.127
Mar	0.663	0.072	0.004	-0.115	-0.376
Apr	0.725	-0.157	0.651	0.113	-0.166
May	0.735	-0.089	0.176	0.329	-0.403
Jun	0.626	-0.126	0.629	-0.081	0.022
Jul	0.751	-0.009	0.226	-0.196	-0.311
Aug	0.741	0.638	0.267	-0.060	0.033
Sep	0.809	0.560	0.103	0.053	-0.067
Oct	0.685	-0.269	-0.045	-0.172	0.127
Nov	0.618	-0.071	0.021	-0.544	0.156
Dec	0.744	0.687	-0.416	-0.706	0.134
Average	**0.718**	**0.188**	**0.145**	**-0.175**	**-0.084**

Table 26. Pearson's Correlations (r) of 2016 monthly averages of 60 cm ground depth temperature with SAWS recorded air temperature, humidity, pressure, wind speed and wind direction

	Temperature	*Pressure*	*Humidity*	*Wind Speed*	*Wind Direction*
Jan	0.725	0.752	-0.622	-0.720	0.248
Feb	0.433	-0.010	0.438	0.235	-0.220
Mar	0.374	0.216	-0.183	-0.253	-0.264
Apr	0.462	-0.375	0.476	-0.129	0.047
May	0.402	0.081	0.153	0.178	-0.355
Jun	0.276	-0.221	0.602	-0.222	0.108
Jul	0.359	0.120	0.236	-0.255	-0.234
Aug	0.416	0.599	0.039	-0.228	0.193
Sep	0.570	0.601	0.040	-0.074	0.012
Oct	0.525	-0.386	-0.133	-0.144	0.142
Nov	0.415	-0.162	0.111	-0.344	0.015
Dec	0.586	0.676	-0.413	-0.661	0.057
Average	**0.462**	**0.157**	**0.062**	**-0.218**	**-0.021**

Appendix C. Photos showing the lack of organic matter

Figure 35. Photo taken at Slettfjell

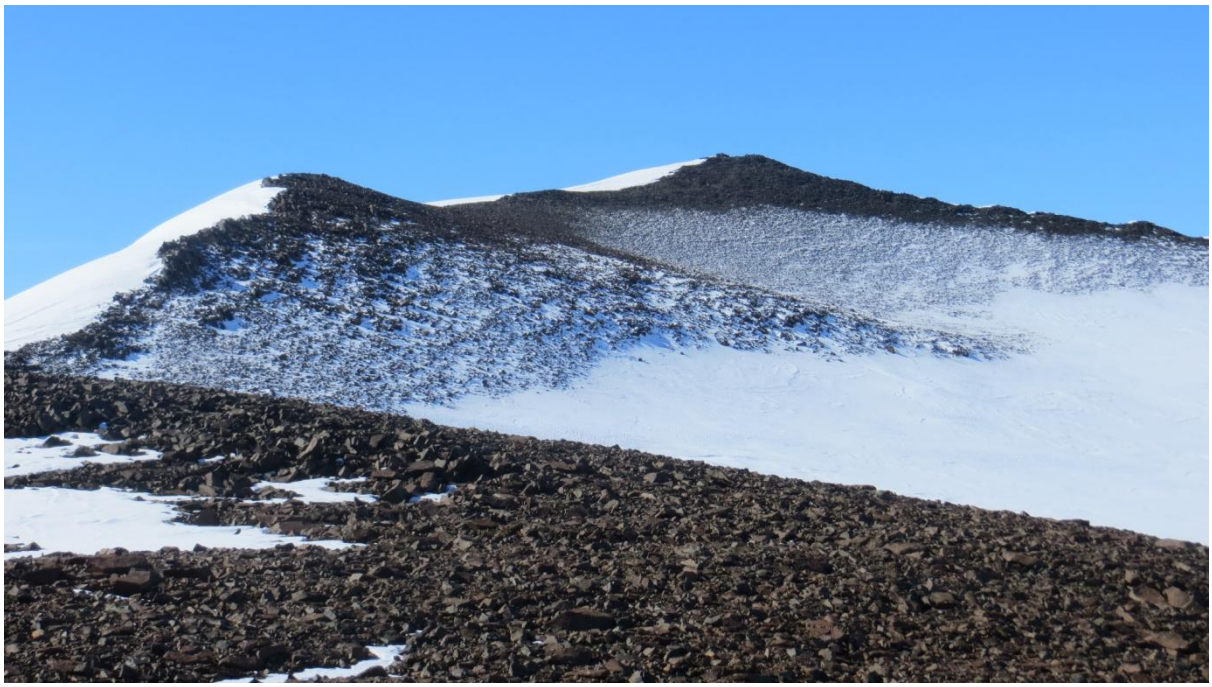

Figure 36. Grunehogna